

**AFRL-ML-WP-TR-2002-4167**

**ROBUST FIBER COATINGS**



**Richard W. Goettler**

**McDermott Technology, Inc.  
Contract Research Division  
1562 Beeson Street  
Alliance, OH 44601**

**AUGUST 2002**

**Final Report for 01 October 1998 – 31 May 2002**

**Approved for public release; distribution is unlimited.**

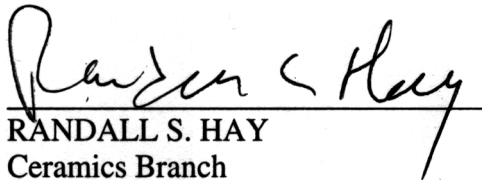
**MATERIALS AND MANUFACTURING DIRECTORATE  
AIR FORCE RESEARCH LABORATORY  
AIR FORCE MATERIEL COMMAND  
WRIGHT-PATTERSON AIR FORCE BASE, OH 45433-7750**

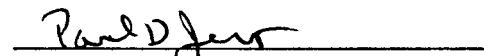
## NOTICE


WHEN GOVERNMENT DRAWINGS, SPECIFICATIONS, OR OTHER DATA ARE USED FOR ANY PURPOSE OTHER THAN IN CONNECTION WITH A DEFINITELY GOVERNMENT-RELATED PROCUREMENT, THE UNITED STATES GOVERNMENT INCURS NO RESPONSIBILITY OR ANY OBLIGATION WHATSOEVER. THE FACT THAT THE GOVERNMENT MAY HAVE FORMULATED OR IN ANY WAY SUPPLIED THE SAID DRAWINGS, SPECIFICATIONS, OR OTHER DATA, IS NOT TO BE REGARDED BY IMPLICATION OR OTHERWISE IN ANY MANNER CONSTRUED, AS LICENSING THE HOLDER OR ANY OTHER PERSON OR CORPORATION, OR AS CONVEYING ANY RIGHTS OR PERMISSION TO MANUFACTURE, USE, OR SELL ANY PATENTED INVENTION THAT MAY IN ANY WAY BE RELATED THERETO.

THIS REPORT IS RELEASABLE TO THE NATIONAL TECHNICAL INFORMATION SERVICE (NTIS). AT NTIS, IT WILL BE AVAILABLE TO THE GENERAL PUBLIC, INCLUDING FOREIGN NATIONS.

THIS TECHNICAL REPORT HAS BEEN REVIEWED AND IS APPROVED FOR PUBLICATION.

  
RANDALL S. HAY  
Ceramics Branch  
Metals, Ceramics & NDE Division

  
PAUL D. JERO, Actg Chief  
Ceramics Branch  
Metals, Ceramics & NDE Division

  
GERALD J. PETRAK, Asst Chief  
Metals, Ceramics & NDE Division  
Materials & Manufacturing Directorate

IF YOUR ADDRESS HAS CHANGED, IF YOU WISH TO BE REMOVED FROM OUR MAILING LIST, OR IF THE ADDRESSEE IS NO LONGER EMPLOYED BY YOUR ORGANIZATION, PLEASE NOTIFY, AFRL/MLLN, WRIGHT-PATTERSON AFB OH 45433-7817 TO HELP US MAINTAIN A CURRENT MAILING LIST.

COPIES OF THIS REPORT SHOULD NOT BE RETURNED UNLESS RETURN IS REQUIRED BY SECURITY CONSIDERATIONS, CONTRACTUAL OBLIGATIONS, OR NOTICE ON A SPECIFIC DOCUMENT.

REPORT DOCUMENTATION PAGE				Form Approved OMB No. 0704-0188	
<p>The public reporting burden for this collection of information is estimated to average 1 hour per response, including the time for reviewing instructions, searching existing data sources, gathering and maintaining the data needed, and completing and reviewing the collection of information. Send comments regarding this burden estimate or any other aspect of this collection of information, including suggestions for reducing this burden, to Department of Defense, Washington Headquarters Services, Directorate for Information Operations and Reports (0704-0188), 1215 Jefferson Davis Highway, Suite 1204, Arlington, VA 22202-4302. Respondents should be aware that notwithstanding any other provision of law, no person shall be subject to any penalty for failing to comply with a collection of information if it does not display a currently valid OMB control number. <b>PLEASE DO NOT RETURN YOUR FORM TO THE ABOVE ADDRESS.</b></p>					
1. REPORT DATE (DD-MM-YY) August 2002		2. REPORT TYPE Final		3. DATES COVERED (From - To) 10/01/1998 – 05/31/2002	
4. TITLE AND SUBTITLE ROBUST FIBER COATINGS				5a. CONTRACT NUMBER F33615-98-C-5219	
				5b. GRANT NUMBER	
				5c. PROGRAM ELEMENT NUMBER 62102F	
6. AUTHOR(S) Richard W. Goettler				5d. PROJECT NUMBER 4347	
				5e. TASK NUMBER 51	
				5f. WORK UNIT NUMBER 20	
7. PERFORMING ORGANIZATION NAME(S) AND ADDRESS(ES) McDermott Technology, Inc. Contract Research Division 1562 Beeson Street Alliance, OH 44601				8. PERFORMING ORGANIZATION REPORT NUMBER  RDD98:43702-400-100-01R	
9. SPONSORING/MONITORING AGENCY NAME(S) AND ADDRESS(ES) Materials and Manufacturing Directorate Air Force Research Laboratory Air Force Materiel Command Wright-Patterson Air Force Base, OH 45433-7750				10. SPONSORING/MONITORING AGENCY ACRONYM(S) AFRL/MLLN	
				11. SPONSORING/MONITORING AGENCY REPORT NUMBER(S) AFRL-ML-WP-TR-2002-4167	
12. DISTRIBUTION/AVAILABILITY STATEMENT Approved for public release; distribution is unlimited.					
13. SUPPLEMENTARY NOTES This report contains color.					
14. ABSTRACT (Maximum 200 Words) <p>Ceramic matrix composites (CMC) were fabricated using scheelite (CaWO<sub>4</sub>) coatings on Nextel 610 alumina fibers. The objective was to demonstrate the ability of such an oxidation-resistant fiber coating to provide fiber-matrix interface debonding and damage tolerance to a CMC that had been processed to a relatively high density. Various precursor routes for the scheelite coatings were investigated to identify coating that would minimize fiber strength degradation (some level of degradation was unavoidable, likely as a result of impurity in the precursors). Likewise, various matrix precursors for use in densifying the CMC by a multiple impregnation process were investigated for minimal degradation to the Nextel 610 fibers. Tensile tests of unidirectional CMCs with uncoated fibers and those containing scheelite coatings in both an alumina and a duplex matrix of alumina plus CeraBlak<sup>TM</sup> (a high temperature stable amorphous phosphate) were performed to elucidate the functionality of the scheelite fiber coating. Comparison of stress-strain curves and stress-strain hysteresis data, along with fracture surface analysis, show that the scheelite fiber coatings provide a weak fiber-matrix interface that imparts the desired stress-strain behavior to the CMC.</p>					
15. SUBJECT TERMS Ceramic Matrix Composites, Fiber Coatings, Scheelite, Alumina Fibers					
16. SECURITY CLASSIFICATION OF:			17. LIMITATION OF ABSTRACT: SAR	18. NUMBER OF PAGES 102	19a. NAME OF RESPONSIBLE PERSON (Monitor) Randall S. Hay 19b. TELEPHONE NUMBER (Include Area Code) (937) 255-9825
a. REPORT Unclassified	b. ABSTRACT Unclassified	c. THIS PAGE Unclassified			

## TABLE OF CONTENTS

<b><u>SECTION</u></b>	<b><u>TITLE</u></b>	<b><u>PAGE</u></b>
<b>1</b>	<b>SUMMARY</b>	<b>1</b>
<b>2</b>	<b>INTRODUCTION</b>	<b>3</b>
<b>3</b>	<b>METHODS, ASSUMPTIONS, AND PROCEDURES</b>	<b>5</b>
<b>4</b>	<b>RESULTS AND DISCUSSIONS</b>	<b>6</b>
	<b>Task 1</b> – Verification of Stability Between Nextel Fiber and CaWO <sub>4</sub> Fiber Coatings	6
	Stability Results with Ammonium Tungstate and EDTA- complexed Calcium Precursor	6
	Stability Results with Ammonium Metatungstate and Calcium Salts	9
	Ammonium Tungstate Based Precursors Revisited; Stabilized with Hydrogen Peroxide	18
	Stability Results with Precursors based on W-metal Digested in Hydrogen Peroxide	21
	Stability Results with ATFI Formulated Scheelite Precursor	24
	Stability Results with Scheelite Slurry Coatings	25
	<b>Task 2</b> – Matrix Precursor Stability	29
	McDermott Alumina Polymer	29
	Alumina Polymer Derived from Al-metal/Formic acid/Hydrogen Peroxide	34
	Alumina Polymer Derived from Al-metal/Formic Acid/Carbonic acid	34
	Mullite Precursor	36
	Silica Precursors	39
	Applied Thin Film's CeraBlak™ Precursor	40
	<b>Task 3</b> – Composite Processing and Properties - First Series of CMC's	41
	First Series of CMCs	41
	<b>Task 3</b> – Composite Processing and Properties - Second Series of CMCs	58
	<b>Task 3</b> – Composite Processing and Properties - Third Series of CMC's	70
	Solution-Based Precursor	70
	Slurry-Based Precursors	71
<b>5</b>	<b>CONCLUSION</b>	<b>86</b>
	<b>ATTACHMENT 1 – REFERENCES</b>	<b>87</b>

## LIST OF FIGURES

<b><u>FIGURE</u></b>	<b><u>TITLE</u></b>	<b><u>PAGE</u></b>
1	Scheelite coatings deposited on Nextel 610 fiber via an ammonium tungstate/Ca-EDTA precursor containing ethanol addition. EDS of position 1 shows alumina whereas EDS of position 2 shows $\text{CaWO}_4$ . Micrograph is of as-deposited coating. (SEM magnification out of calibration at time of sample examination .....	8
2	Weibull plot of scheelite coated fiber heat-treated at $1100^\circ\text{C}/1\text{hr}$ . Coatings deposited from ammonium tungstate/Ca-EDTA based precursor containing ethanol additions .....	9
3	Scheelite coatings deposited on Nextel 610 fiber via a metatungstate/Ca-formate (plus ethanol) precursor. Micrograph is of an as-deposited coating .....	10
4	Weibull plot of scheelite coating Nextel 610 fiber heat-treated at $1100^\circ\text{C}/1$ hour. Coatings deposited from ammonium metatungstate/Ca-formate based precursor.....	11
5	Weibull plot of scheelite coated Nextel 610 fiber heat-treated at $1100^\circ\text{C}/1$ hour. Coatings deposited from an ammonium metatungstate/Ca-nitrate based precursor.....	12
6	Scheelite coating on Nextel 610 following $1100^\circ\text{C}/1$ hour heat-treatment. Coatings derived from ammonium metatungstate/Ca-nitrate precursor (with ethanol) .....	13
7	EDS data of AF231 coating .....	14
8	Weibull plot of Nextel 610 single filaments passed through a hydrogen peroxide/ethanol mix prior to an $1100^\circ\text{C}/1$ hour heat-treatment .....	15
9	Weibull plots of Nextel 610 fibers coated with scheelite precursors formulated from ammonium metatungstate and either calcium nitrate or calcium formate .....	16
10	SEM (a) and EDS (b) results from sample AF238. Point one highlights the low-contact angle grains that appear to be a calcium phosphate phase. Point 2 highlights a high-contact grain that appears to be scheelite based on a bulk scan.....	17
11	Marker 1 indicates the scheelite-Nextel 610 interfacial region of sample AF238 scanned by WDS and that showed the presence of phosphorous.....	18
12	Weibull plots of Nextel 610 fibers coated with ammonium tungstate/Peroxide based precursors and heat-treated at $1100^\circ\text{C}$ for 1 hour.....	20
13	SEM (a) and EDS (b) results of sample AF243 showing both low-and high-contact angle coating grains on Nextel 610. The low-contact angle grains appear to be a calcium phosphate phase .....	21

## LIST OF FIGURES - Continued

<b><u>FIGURE</u></b>	<b><u>TITLE</u></b>	<b><u>PAGE</u></b>
14	Weibull plots for Nextel 610 fibers with different Ca/W ratios an following an 1100°C/ 1 hour heat-treatment. Precursors were based on W-metal/H <sub>2</sub> O <sub>2</sub> plus calcium formate .....	23
15	TGA curves of scheelite precursors made from different calcium salts .....	23
16	X-ray diffraction pattern for AF289. Small peaks at approximately 19 an 22 degrees correspond to Ca <sub>3</sub> WO <sub>6</sub> .....	24
17	X-ray diffraction pattern for AF290. No peaks for Ca <sub>3</sub> WO <sub>6</sub> .....	25
18	SEM photomicrographs of coatings from 5.2 wt. Percent slurry and 650°C coater furnace set point .....	27
19	SEM photomicrographs of coatings from 9 wt. Percent slurry and 815°C coater furnace set point .....	28
20	TGA curves of substituted and unaltered MTI alumina polymers.....	30
21	DTA/TGA of 37.5% alumina polymer/formic acid solution dried at 105°C.....	31
22	DTA/TGA of 37.5% alumina polymer/formic acid solution dried at 150°C.....	32
23	DTA/TGA of 28.1% alumina polymer/formic acid solution dried at 105°C.....	33
24	DTA/TGA of 28.1% alumina polymer/formic acid solution dried at 150°C.....	33
25	TGA curve of powder contained from dried Al-metal/formic Acid/oxalic acid alumina precursor .....	35
26	DTA/TGA curve of powder obtained from dried Al-metal/formic acid/carbonic acid alumina precursor .....	36
27	XRD curves near 26° 2θ for the mullite precursor formed from different levels of decomposed MTI alumina polymers .....	38
28	Strength of Nextel 610 fibers coated with colloidal silica and MTI (25.6% decomposed) alumina polymer precursor and heat-treated at 1000°C And 1100°C .....	39
29	Strength retention for Nextel 610 fibers coated with CeraBlak™ Precursor.....	40
30	X-ray diffraction analysis of NWU scheelite precursor (AF284).....	42
31	X-ray diffraction analysis of MTI scheelite precursor AF279.....	42
32	X-ray diffraction analysis of MTI scheelite precursor AF287.....	43
33	Microstructures of CMCs with CaWO <sub>4</sub> coating AF279 (MTI precursor).....	44
34	Microstructures of CMCs with CaWO <sub>4</sub> coating AF284 (ATFI precursor).....	45

## LIST OF FIGURES - Continued

<b><u>FIGURE</u></b>	<b><u>TITLE</u></b>	<b><u>PAGE</u></b>
35	Microstructures of CMCs with CaWO <sub>4</sub> coating AF287 (MTI precursor).....	46
36	CaWO <sub>4</sub> coating (AF279) from MTI precursor based on W-metal/H <sub>2</sub> O <sub>2</sub> and calcium formate.....	47
37	CaWO <sub>4</sub> coating (AF287) from MTI precursor based on W-metal/H <sub>2</sub> O <sub>2</sub> and calcium formate (formulation based on a slight calcium deficiency) .....	48
38	CaWO <sub>4</sub> coatings (AF282) from ATFI precursor .....	49
39	Stress-strain curves of AF279 CMCs with MTI W-metal/Ca-formate peroxide derived CaWO <sub>4</sub> fiber coatings in an all alumina matrix (top) and alumina-CeraBlak™ duplex matrix (test performed by AFWL) .....	51
40	Stress-strain curves of AF284 CMCs with ATFI alkoxide precursor derived CaWO <sub>4</sub> fiber coatings in an alumina-CeraBlak™ duplex matrix (test performed by AFWL) .....	52
41	Fracture surface of AF279-1 CMC with CaWO <sub>4</sub> coatings from MTI precursor in an all alumina matrix .....	53
42	Fracture surface of AF279-2 CMC with CaWO <sub>4</sub> coatings from MTI precursor in an alumina-CeraBlak™ duplex matrix.....	54
43	Fracture surface of AF279-3 CMC with CaWO <sub>4</sub> coatings from MTI precursor in an alumina duplex matrix from polysiloxane .....	55
44	Fracture surface of AF284-1 CMC with CaWO <sub>4</sub> coatings from ATFI precursor in an all alumina matrix .....	56
45	Fracture surface of AF284-3 with CaWO <sub>4</sub> coatings from ATFI precursor in an alumina-silica duplex matrix from polysiloxane .....	57
46	X-ray diffraction pattern for powder derived from the ATFI coating precursor .....	58
47	XRD result for AF293 scheelite coating from W-metal/calcium formate in peroxide solution .....	61
48	XRD results for AF295 scheelite coating from W-metal/calcium formate in peroxide solution .....	61
49	Strength of coated and uncoated fibers following heat treatment.....	62
50	Comparison of TGA curves for scheelite precursors AF293 and AF295 .....	63
51	Stress-strain curves for unidirectional un-notched CMC in an all alumina matrix (formed using MTI alumina polymer). Coated fiber is lot AF293 – “aged” ....	65

## LIST OF FIGURES - Continued

<b><u>FIGURE</u></b>	<b><u>TITLE</u></b>	<b><u>PAGE</u></b>
52	Microstructure of CMC containing scheelite precursor in an all alumina matrix .....	66
53	Stress-strain curves for unidirectional un-notched CMC with an alumina-CeraBlak™ duplex matrix. Coatings were obtained from the unaltered AF293 scheelite precursor .....	67
54	TGA comparison of CeraBlak™ and MTI alumina polymer .....	67
55	Secondary electron images of fracture surface of CMC with scheelite fiber coatings in an alumina-CeraBlak™ duplex matrix .....	68
56	Backscattered electron images of fracture surface of CMC with scheelite fiber coatings in an alumina-CeraBlak™ duplex matrix .....	69
57	TGA curves for scheelite precursors formed from tungsten metal, hydrogen peroxide and calcium formate .....	71
58	Single filament strengths of coated and uncoated Nextel 610 fibers .....	72
59	Microstructure of a round 3 CMC containing coating uncoated fiber in an alumina-CeraBlak™ duplex matrix .....	74
60	Microstructure of third round of CMC made with solution based (AF298) scheelite fiber coatings in an alumina-CeraBlak™ duplex matrix .....	75
61	CMC with slurry derived fiber coatings processed at 815°C during the coating process .....	76
62	CMC fabricated using slurry derived coatings fired to 1038°C during the fiber coating operation .....	77
63	Room-temperature stress-strain curves for series 3 CMCs. Testing Performed by Virginia Tech.....	78
64	Macroscopic views of CMC fractures: (a) uncoated, 9b) AF298 Solution coatings, © 815°C heated slurry coatings and (d) 1038°C Heated slurry coatings .....	79
65	SEM images of fracture surface of series 3 CMC with uncoated fiber in an alumina-CeraBlak™ duplex matrix .....	80
66	SEM images of fracture surface of series 3 CMC with solution-based AF298 scheelite fiber coatings in an alumina-CeraBlak™ duplex matrix .....	81
67	SEM images of fracture surface of series 3 CMC containing slurry-derived scheelite fiber coatings (815°C condition) in an alumina-CeraBlak™ duplex matrix .....	82
68	SEM images of fracture surface of series 3 CMC containing slurry-derived scheelite coatings (1038°C condition) in an alumina-CeraBlak™ duplex matrix .....	83
69	Hysteresis curves of CMCs with uncoated fibers.....	84



## LIST OF FIGURES - Continued

<b><u>FIGURE</u></b>	<b><u>TITLE</u></b>	<b><u>PAGE</u></b>
70	Hysteresis curves of CMCs with solution-derived scheelite fiber coatings (AF298) .....	84
71	Hysteresis curves of CMCs with slurry-derived scheelite fiber coatings (815°C condition) .....	85
72	Hysteresis curve of CMCs with slurry-derived scheelite fiber coating (1038°C condition) .....	85

## LIST OF TABLES

<u>TABLE</u>	<u>TITLE</u>	<u>PAGE</u>
1	Test Matrix Summarized.....	15
2	Precursors Formulated from Ammonium Tungstate Stabilized with Peroxide.....	19
3	Strengths of Fibers Dip Coated with NWU Scheelite Precursor .....	24
4	Measurements of Single Fiber Filaments Strengths .....	26
5	Precursors studied in the Al-formic acid hydrogen peroxide system .....	34
6	Description of CaWO <sub>4</sub> coated fibers .....	41
7	Description of Series 1 unidirectional CMCs.....	43
8	Summary of notched and un-notched strengths of initial series of CMC samples. Data for individual room temperature tests is shown .....	50
9	Strength of coated and uncoated Nextel 610 fiber (tested at ATFI).....	59
10	Results of phosphorous chemical analysis on scheelite precursor raw materials .....	60
11	Summary of un-notched tensile strengths of second series of CMC samples. Data for individual room temperature tests is shown .....	64
12	Summary on un-notched tensile strengths of the third series of CMC samples. Data for individual room temperature tests is shown .....	73

## **SECTION 1 - SUMMARY**

The highly desired ceramic matrix composite is the one in which the high strength and strain-to-failure is achieved through judicious selection of a fiber coating that can survive the high-temperature oxidizing use environment that is envisioned for these engineered structural materials. Scheelite ( $\text{CaWO}_4$ ) had been identified as a promising oxidation-resistant fiber coating, but its functionality within a CMC having a dense matrix had remained to be proven. The objective of this program was to verify that scheelite coatings provide for high strains-to-failure, nonlinearity in the stress-strain curves and the corresponding fiber pullout expected in CMC fracture. It was important under this program to evaluate CMCs with as high of a matrix density as possible to insure that the fiber coating was duly tested rather than having the fracture behavior being influenced by damage of a weak matrix phase, typical for the porous matrix class of CMCs. Nextel 610 alumina fibers were chosen as the reinforcement because of its higher strength compared to the Nextel 720 mullite-alumina fiber that is also a candidate for scheelite coatings. Unidirectional CMC were fabricated and tested throughout the program to examine the functionality of the scheelite coatings.

The first task was to demonstrate a scheelite precursor that produced suitable fiber coatings and that did not reduce the strength of the Nextel 610 fibers. This task proved difficult as all of the solution-based precursors that were evaluated ended up causing some strength degradation of the fiber. The solution-based coatings typically caused a 20-30 percent strength degradation after  $1100^\circ\text{C}/1$  hour heat treatments and about 15% after  $1000^\circ\text{C}/1$  hour heat treatments. Towards the end of the program, fibers were coated with a scheelite slurry, and those coatings resulted in slightly less fiber strength degradation. Phosphorous contamination was identified as a possible cause for the degradation caused by the solution-based precursors. The cause for the strength degradation observed with the slurry coated fibers was not investigated. These coated fibers were carried forward into composite fabrication even with less than virgin strengths with the thinking that they were still adequate for evaluating the functionality of the scheelite coatings within the CMCs.

A parallel initial task involved the selection of appropriate matrix precursors for use in densifying the CMC panels. The process utilized to densify the composites involved an initial step of pressure casting a unidirectional fiber lay-up with an alumina slurry. That initial step generally deposited a volume fraction of matrix about equal to the volume fraction of Nextel 610 fiber. The slurry-cast CMC was then fired to provide some initial rigidity to the matrix. Subsequent densification of the matrix way is achieved through repeated vacuum/pressure infiltration and drying/firing of the CMC panels using a solution-based or polymeric precursor. It was deemed important that these precursors also not significantly damage the strength of the Nextel 610 fibers at the processing temperatures employed. Various alumina, mullite, silica and CeraBlak<sup>TM</sup> (a substantially amorphous aluminum phosphate material from Applied Thin Films) precursors were examined. An alumina precursor developed by McDermott and the CeraBlak<sup>TM</sup> precursor were used for the bulk of the composite fabrication, however, a polysiloxane silica precursor was also used to densify some panels in the initial round of CMCs. The CeraBlak<sup>TM</sup> precursor exhibited excellent strength retention with the Nextel 610 fiber, whereas the McDermott alumina precursor caused substantial degradation at  $1100^\circ\text{C}/1$  hour and moderate degradation at  $1000^\circ\text{C}$ . Because of the concern with fiber strength degradation caused by both

the scheelite coatings and the matrix precursors, the processing temperatures during CMC panel fabrication were limited to 1000°C or below for all three rounds of CMC panels that were produced during the program.

Throughout the program, the fracture surfaces of the tensile tested unidirectional CMC showed a substantial amount of fiber-matrix interfacial debonding along the scheelite coatings. The strengths of the composites tested with scheelite coatings routinely exhibited lower strengths than control composites with uncoated fibers. However, for the composites with the all alumina matrix, the specimens containing the scheelite coatings exhibited non-linearity in the stress-strain curve, whereas those without scheelite coatings were linear to failure.

The comparison of data in composites with the duplex matrix of alumina and CeraBlak™ was not as straight forward. The stress-strain curves of composites with uncoated fiber showed some minor amount of non-linearity, however a greater degree of nonlinearity was observed for those specimens that contained scheelite fiber coatings. In addition, hysteresis testing of alumina-CeraBlak™ matrix CMCs revealed much broader hysteresis loops for specimens containing scheelite fiber coatings. It appears that the CeraBlak™ phase of the matrix does not bond strongly to the Nextel 610 fibers. The high strengths observed with the CeraBlak™ matrix and uncoated fibers (~600 MPa at  $V_f \sim 40\%$ ) in a CMC with only 10% total residual porosity is a promising result in itself that warrants additional investigations. The ability of the CeraBlak™ matrix to not substantially reduce the strength of the fibers is a promising result related to matrix processing technology for CMCs. Additional work will be required to demonstrate a scheelite coating that does not damage the strength of the fibers before dense CMCs can be fabricated with fully realized strength properties up to 1200°C.

## **SECTION 2 - INTRODUCTION**

It is well recognized that a weakly bonded fiber-matrix interface is required to provide toughness to a dense, structural ceramic matrix composite (CMC). This fiber-matrix interface control is typically accomplished through incorporation of a fiber coating interphase within the CMC. Early developments in the field emphasized fiber coatings based on carbon and boron nitride. As the CMC field has matured, there has been greater research emphasis on oxide based fiber coatings in order to retain control of the desired interface properties during composite use in high temperature and oxidizing environments. The lack of a functional fiber coating that is stable over a wide temperature range (up to 1200°C) has been a major barrier to the deployment of CMCs for a range of defense and commercial applications. Researchers are attempting to extend the life of carbon and boron nitride fiber coatings, i.e., keeping oxygen from ingressing to the coatings, by means of providing SiC overcoats, multilayering with SiC, doping the coating with silicon and adding inhibitors to the matrices. These approaches have been met with reasonable success. The life of these CMCs using these approaches are quite limited once the matrix cracking stress is exceeded. A more oxidatively robust fiber coating would increase the chances for commercialization of CMCs. CMCs utilizing robust oxide fiber coatings offer the opportunity to improve the reliability of CMCs in service, and hence, to extend the opportunities for their use in key Air Force applications.

Oxide fiber coatings are generally considered for use within oxide fiber and oxide matrix CMC systems. If the oxide coatings are desired because of their thermodynamic stability to the use environment, then in order to have the full CMC exhibit stability as well, oxide fibers and oxide matrices become the best combination with oxide fiber coatings. Because of the high diffusion rate of oxygen through ionic oxide compounds [1], oxide fiber coatings on SiC fibers do a poor job of protecting the fibers from oxidation induced strength degradation.

It should be acknowledged that a competing oxide-based CMC approach being pursued by many researchers involves using an oxide fiber, without a fiber coating, which reinforces a rather porous oxide matrix. The advantage of these systems is their rather low cost since no separate fiber coating steps are required and the matrix is processed/densified in a single step using fabrication approaches similar to that used for polymer matrix composites. These type of composites show satisfactory in-plane strength properties and strains-to-failure of greater than 0.3%. The damage tolerance of these materials comes not from fiber-matrix interface debonding and sliding, but instead from accumulated and globally distributed matrix damage. The robustness of these composite systems is in doubt because the porous matrix translates into composites with poor interlaminar mechanical properties, poor thermal conductivity and poor erosion/abrasion resistance. The main limitation of these composites to 1200°C applications arises from the lack of fiber-matrix interface control. Use of these composites is limited in their time-temperature exposure so as not to promote reactivity and/or sintering between the fibers and the matrix which can lead to strength degradation of the composite. These porous matrix composites have served well to raise the interest level in oxide-oxide CMCs and will undoubtedly find use in applications having less severe structural and environmental (time, temperature and chemical) requirements. A dense oxide based CMC relying on an oxide fiber coating to impart toughness to the composite will provide higher design allowables because of

greater interlaminar mechanical properties, and with a carefully selected interface, will likely provide more stable properties over time at service temperatures approaching 1200°C.

Under this program, McDermott Technology investigated a CMC system comprised of Nextel 610 alumina fiber containing scheelite ( $\text{CaWO}_4$ ) in a matrix comprised of primarily alumina, but in some instances incorporating a second bonding phase. Scheelite was selected by MTI as a potential fiber coating following the initial identification by Morgan and Marshall that certain nonlayered oxide compounds such as monazite and xenotime families of rare earth phosphates ( $\text{Re}^{3+}\text{PO}_4$ ) exhibit easy debonding from alumina and aluminosilicate based fibers [2]. Scheelite, being an  $\text{ABO}_4$  compound with similar crystal chemistry as the phosphates, but with a tungstate tetrahedron rather than a phosphate making up the crystal lattice, appears to debond from candidate Nextel oxide fibers as well [3]. Why these  $\text{ABO}_4$  compounds are weakly bonded to alumina and aluminosilicate fibers remains to be fully explained.

This report first summarizes the initial technical work performed to obtain scheelite fiber coatings for Nextel 610 that did not cause fiber strength degradation. Early program activities were also focused on the development of matrix precursors that would allow for fabrication of CMC with low (less than 10 percent) residual porosity levels and that did not adversely effect the fiber strength. The processing and mechanical properties of three series of CMC specimens that were fabricated at various stages of development and understanding of the coating and matrix precursors are presented.

### **SECTION 3 – METHODS, ASSUMPTIONS, AND PROCEDURES**

The approach taken to produce high strength CMCs was to focus on retention of the fiber strength throughout all stages of composite processing. The concern was that high strength fibers within the CMC would be required to achieve the stress levels and strains during composite testing to activate the fiber-matrix interfacial debonding/sliding mechanisms. If the fiber strength was severely compromised, then low strength composites showing little or no fiber pullout would be obtained, and there would be no advantages shown between composite systems with fiber coatings and those without. We were hopeful that the strength retention issue with regards to the scheelite coatings would not be a major issue since excellent strength retention had been observed between scheelite coatings and Nextel 720 fibers in prior work. In reality, coating-fiber stability proved to be a significant challenge under this program.

Prior to the start of this program, the challenges in being able produce a relatively dense CMC without damaging the fibers were well appreciated. McDermott had a wealth of information that the candidate precursors for use in achieving final densification of initial pressure cast CMC preforms tended to cause fiber strength degradation. Fortunately, McDermott and Applied Thin Films had preliminary results on promising precursor routes for alumina and novel aluminum phosphate phases that had potential to be less damaging to the fibers. McDermott's matrix processing technology involving an initial pressure casting step followed by repeated vacuum/pressure infiltrations and dry/firing cycles to reduce the residual porosity was well established. The only concern was the ability not to damage the fibers during the matrix infiltration steps.

Prior to coating fibers, the degree of strength degradation of the candidate precursors was evaluated by performing single fiber tensile tests on fiber coating by a dip coating process. Large batches of coating precursors were then formulated for coating fibers in McDermott's fiber coater that relied on the immiscible liquid displacement technique developed by Hay [4]. The strength of those coated fibers was then determined prior to proceeding to the fabrication of CMC panels so that composite strength properties could be correlated to the strength of the coated fibers. Likewise, the various matrix precursors used for the infiltration steps were screened for their ability to not damage the strength of the fibers.

The ultimate processing temperatures used for CMC panels were selected based on the relationship between the strength of fibers coated with the scheelite and matrix precursors as a function of temperature. That guideline actually caused relatively low processing temperatures (<1000°C) to be used for the composites processed under this program so as to insure that adequate strength CMC would be produced for effectively assessing the performance of the scheelite coatings. Control CMC panels that did not contain scheelite fiber coatings were co-processed with the CMC panels that contained scheelite coatings in order more effectively evaluate the functionality of the scheelite coatings. The functionality of the scheelite coatings were determined by examining the degree of non-linearity in room temperature stress-strain curves and the presence and the size of hysteresis loops in tensile loading/unloading tests. In addition, scanning electron microscopy was utilized to examine the fracture surface of the tensile samples to determine whether fiber-matrix debonding had occurred at the Scheelite coating.

## **SECTION 4 - RESULTS AND DISCUSSIONS**

### **Task 1 – Verification of Stability Between Nextel Fiber and CaWO<sub>4</sub> Fiber Coatings**

The proposed objective of this task was to show that scheelite did not degrade the strength of Nextel 720 fiber. During the program kick-off meeting, the Air Force program management recommended utilizing Nextel 610 fiber in the program rather than Nextel 720. This recommendation was adopted and the stability of scheelite with Nextel 610 fiber became the main focus of this task.

As has been shown by the Air Force Wright Lab on work with monazite fiber coatings, the precursor selection has a strong effect on the retained strength of the coated fiber [5]. Tungstate chemistry does not provide as many options for solutions-based scheelite precursors as are available for monazite precursors through the broader phosphate chemistry. The following precursor chemistries had been identified for scheelite:

1. Ammonium tungstate, (NH<sub>4</sub>)<sub>2</sub>WO<sub>4</sub>, plus calcium nitrate salt complexed with ethylenediaminetetraacetate (EDTA) (1Ca:1EDTA)
2. Ammonium metatungstate, (NH<sub>4</sub>)<sub>6</sub>H<sub>2</sub>W<sub>12</sub>O<sub>40</sub>, plus calcium formate or calcium nitrate salt, in a hydrogen peroxide, H<sub>2</sub>O<sub>2</sub>, containing aqueous solution
3. Tungsten metal digested in a hydrogen peroxide solution and mixed with a calcium formate salt solution

### **Stability Results with Ammonium Tungstate and EDTA-complexed Calcium Precursor**

Stock source solutions for the tungstate (WO<sub>4</sub><sup>2-</sup>) anion, derived from ammonium tungstate, and of the Ca<sup>2+</sup> cation, derived from calcium nitrate, were prepared for use in formulating scheelite precursors. The stock solution for Ca<sup>2+</sup> was prepared by dissolving calcium nitrate (Ca(NO<sub>3</sub>)<sub>2</sub>·4H<sub>2</sub>O, Aldrich Chemical Co.) and EDTA in demineralized water. It is necessary to increase the pH of the solution to a value of approximately 10 through ammonium hydroxide additions in order to achieve complete complexation of the calcium cation by EDTA. The stock solution for tungstate was prepared by dissolving ammonium tungstate (Aldrich Chemical Co.) in demineralized water at a concentration of less than 5 weight percent (this low solubility limits the yield that can ultimately be achieved for the scheelite precursor). The pH of the ammonium tungstate solution is increased to 10 through ammonium hydroxide addition. These separate solutions were stable over time.

A determination of the oxide yield of the starting salts, calcium nitrate and ammonium tungstate, was performed prior to formulating the stock solutions. This was performed by bulk thermal gravimetric analysis. The WO<sub>3</sub> yield of the ammonium tungstate powder was found to be 80.33% versus a theoretical yield of 81.66%. The lower than theoretical yield could be caused by residual ammonia in the powder and moisture absorption. The CaO yield of the calcium nitrate powder was found to be 23.46% versus a theoretical yield of 23.75%. The lower yield implies that the water of hydration associated with the salt is likely less than the theoretical value of four. The alumina crucible containing the decomposed calcium nitrate was measured while still hot (greater than 150°C) and immediately upon cool down to prevent the absorption of



carbon dioxide, a common problem with CaO, and moisture. In fact, weighing the crucible 24 hours later resulted in a higher calculated yield of 23.92%, thus highlighting the need to take special precautions in the yield analysis. A similar procedure was used for measuring the residual WO<sub>3</sub> resulting from the decomposition of the ammonium tungstate.

By knowing the actual oxide yields of the salts used to form the salt solutions, and by taking extreme care in the formulation of the solutions, the yields of the stock solutions are known to a reasonable accuracy. By mixing these solutions in the appropriate ratios based on their yields, one has the best chance for achieving a stoichiometric scheelite precursor. However, there is undoubtedly some error in these yield measurements, and even this “best effort” formulation may result in an actual Ca/W ratio not equal to one. It is assumed that the best fiber strength retention would be obtained with as close to a stoichiometric precursor as possible. The hypothesis followed was that several scheelite precursors in which the Ca/W ratio was varied above and below 1 should be prepared to insure that actual stoichiometric scheelite formulation would be bracketed in the test matrix.

Initially, a “best effort” stoichiometric scheelite precursor was formulated having a yield of approximately 4% by weight. This scheelite precursor was used to coat Nextel 610 fiber by a dip-coating process. Because of the low scheelite yield, 24 dips (or passes) through the precursor were performed to deposit a coating of suitable thickness. These coated fibers, as well as uncoated Nextel 610 fibers were fired in air at 10°C/min to 1100°C and held for one hour. Some precipitation from this scheelite precursor began to occur within a relatively short time (less than 2 hours). The entire batch of fibers were coated before any significant precipitation had occurred. Past results have shown this precipitate to be scheelite, so the coating composition/stoichiometry should not be adversely effected by the occurrence of precipitation within the precursor. SEM evaluation of the fiber did not show any scheelite coating. It was concluded that the lack of coating was caused by the poor wetting of the fiber by the aqueous-based precursor.

A second scheelite precursor based on ammonium tungstate and EDTA-complexed calcium cations was formulated to which ethanol was added to serve as a wetting aid (~9 w/o ethanol in solution). SEM evaluation showed the presence of a thin scheelite coating (**Figure 1**), although somewhat spotty. There was adequate coverage to proceed with heat-treatment and tensile testing studies to assess fiber strength retention. The Weibull plots for this batch of scheelite coated fiber is shown in **Figure 2**. The coated fiber showed significant strength reduction. It is interesting that a slightly higher strength was obtained for the uncoated heat-treated Nextel 610 versus a desized (825°C) Nextel 610 as demonstrated by the position of the Weibull plots in **Figure 2**.

The level of strength degradation observed with this initial batch of coated fiber was considered to be unacceptable. Some precipitation had started to occur within the precursor about half way through the dip-coating of the batch of fiber (about 22 fibers). The precipitate was believed to be scheelite based on previous studies, but this precipitate was not analyzed.

The instability that was observed with the ammonium tungstate/Ca-EDTA (plus ethanol) precursor forced the decision to examine other precursor routes for scheelite fiber coatings. A stable precursor that would allow for the continuous coating of fibers over a few days period was required.

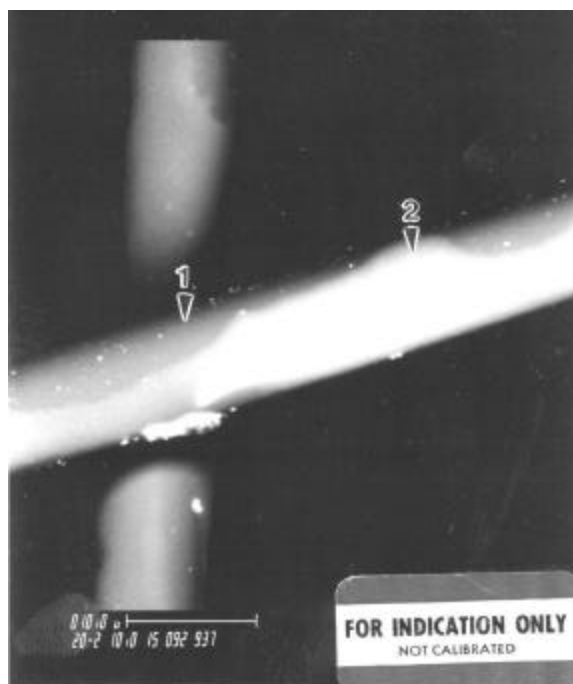


**Figure 1.** Scheelite coatings deposited on Nextel 610 fiber via an ammonium tungstate/Ca-EDTA precursor containing ethanol addition. EDS of position 1 shows alumina whereas EDS of position 2 shows  $\text{CaWO}_4$ . Micrograph is of as-deposited coating. (SEM magnification out of calibration at time of sample examination)

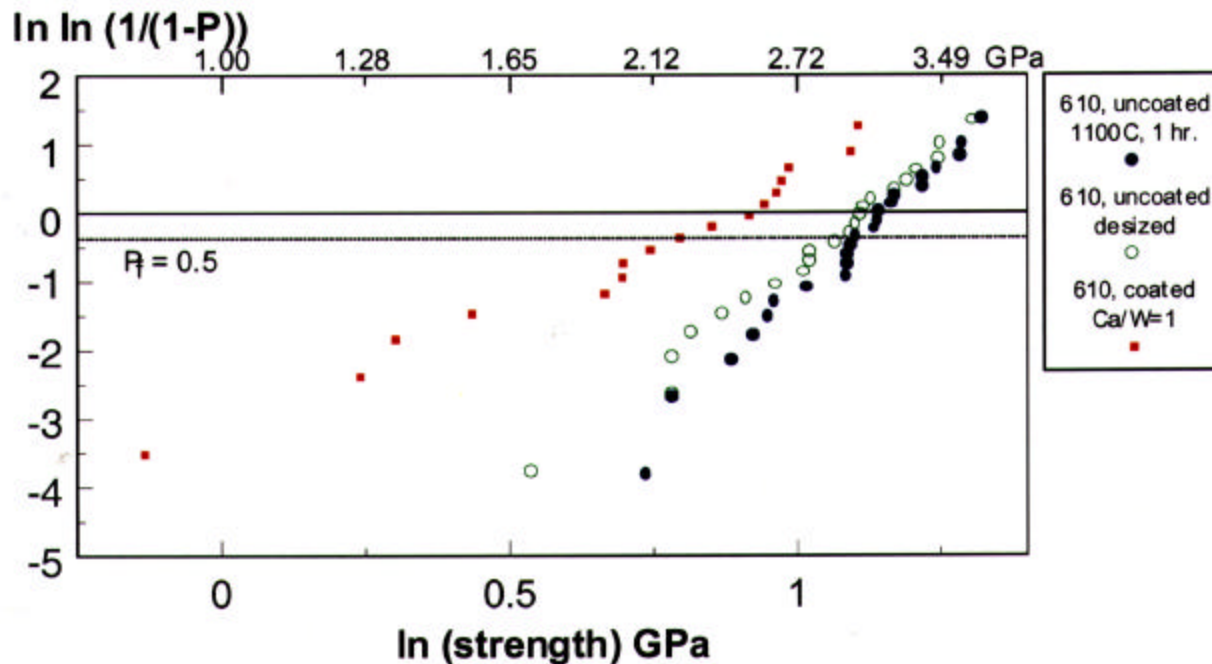


**Figure 2.** Weibull plot of scheelite coated fiber heat-treated at 1100°C/1 hr. Coatings deposited from ammonium tungstate/Ca-EDTA based precursor containing ethanol additions.

### **Stability Results with Ammonium Metatungstate and Calcium Salts**

Ammonium metatungstate was chosen as a raw material for its high solubility in water. Calcium formate (Gelest, Inc.) was chosen as the initial source for calcia. Stock solutions of calcium formate in hydrogen peroxide (30% in water) and ammonium metatungstate in hydrogen peroxide were prepared, and the oxide yield was determined. From the start, a slight amount of ethanol was added to all of the metatungstate based scheelite precursor solutions to improve the wetting characteristics to the Nextel 610 fiber during the dip coating process. MTI attempted to fabricate precursor solutions with Ca/W ratios of 0.98, 0.99, 0.995, 1.0, 1.005, 1.01, and 1.02. Unfortunately, an error was made in the CaO yield of the calcium formate used in the formulation and, as a result, the actual Ca/W ratios formulated were 0.905, 0.914, 0.919, 0.924, 0.928, 0.933, and 0.942. These precursors were more concentrated than those based on ammonium tungstate/Ca-EDTA because of the greater solubility of ammonium metatungstate relative to ammonium tungstate. As a result, only 14 dips were used for each fiber rather than the 24 previously used. The coatings that were obtained were still rather thin and spotty as shown in **Figure 3**. The Weibull plots for Nextel 610 coated with these precursors and heat-treated to 1100°C for one hour are shown in **Figure 4**. All of the precursors yielded very similar amounts strength degradation, especially in the mid- to high-strength ranges. There was

variation in the data between the different precursors and Ca/W ratios at the lower strength levels. All the batches of fiber, regardless of the Ca/W ratio exhibited substantially lower strengths than the control, similarly heat-treated uncoated fibers.

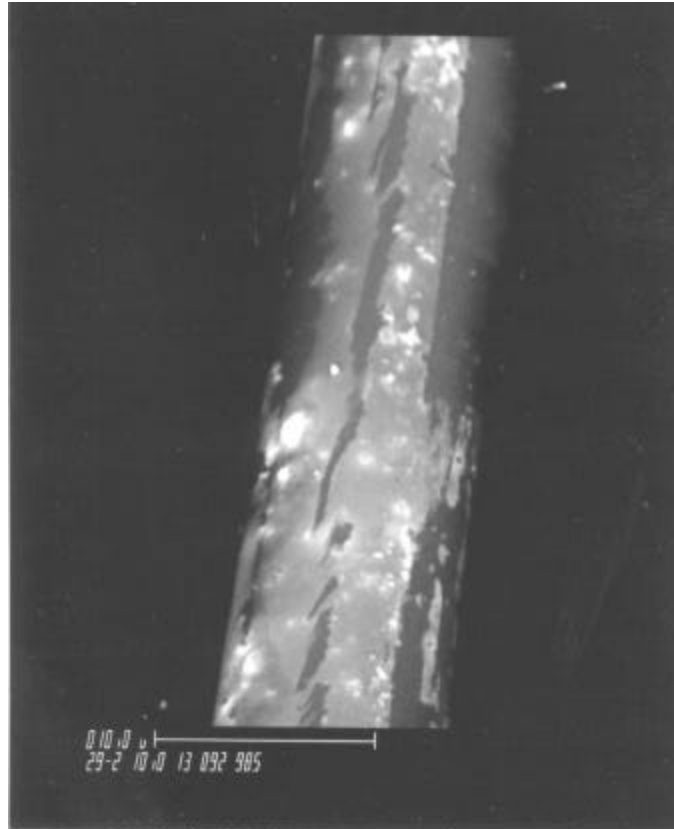


**Figure 3.** Scheelite coatings deposited on Nextel 610 fiber via a metatungstate/Ca-formate (plus ethanol) precursor. Micrograph is of an as-deposited coating.

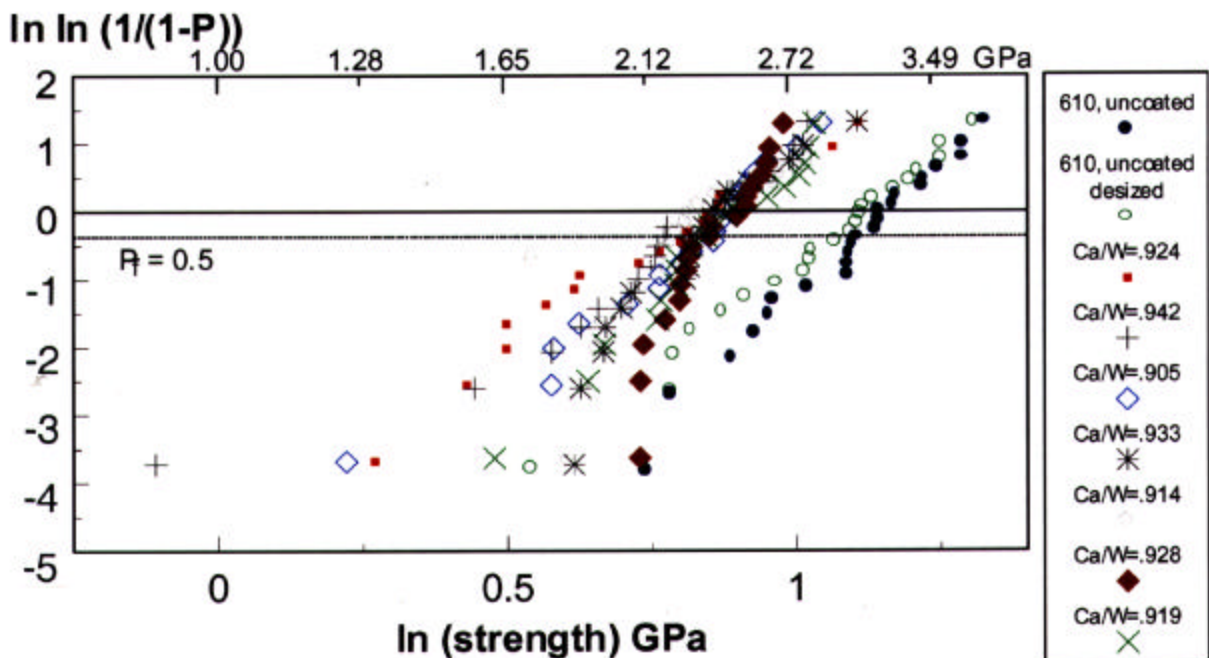


**Figure 4.** Weibull plot of scheelite coated Nextel 610 fiber heat-treated at 1100°C/1 hour. Coatings deposited from ammonium metatungstate/Ca-formate based precursor .

The precursors based on ammonium metatungstate and calcium formate were not as stable as desired. It was observed that within one to three days a precipitate would form (in precursors with and without the ethanol addition). In some instances, the precursor would actually bubble over. Based on the limited shelf life that could be expected from such a precursor, we decided to investigate additional fiber coating precursors that may have a longer shelf life. It was desired to obtain the scheelite-Nextel 610 stability data under this task with a precursor chemistry that can be used for depositing continuous fiber coatings.

Rather than using calcium formate, which may have inherent instabilities in the presence of the peroxide, calcium nitrate was investigated. A stock aqueous solution of  $\text{Ca}(\text{NO}_3)_2 \cdot x\text{H}_2\text{O}$  was prepared. The same stock solution of  $(\text{NH}_4)_6\text{H}_2\text{W}_{12}\text{O}_{40}$  in  $\text{H}_2\text{O}_2$  used for the previous series of scheelite precursors was used to prepare solutions with varying Ca/W ratios. Precursors were made with Ca/W ratios of 0.995, 0.9975, 1.0, 1.0025, and 1.005. **Figure 5** shows the Weibull plots obtained for the coated and heat-treated Nextel 610. The amount of strength degradation seen in this series of samples was surprising given the closer true stoichiometry than the samples tested and reported in **Figure 4**. SEM/EDS analysis of the heat-treated coated fiber revealed possible causes for the severe strength degradation. As shown by the SEM photomicrograph in **Figure 6**, two types of coating grains are present on the surface of the Nextel 610 fiber – high

angle and low angle contact (labeled 1 in photo). The high angle contact grains are scheelite, and the low angle contact grains most likely have phosphorous impurities (based on the EDS data presented in *Figure 7*). Other regions of analysis showed possible sodium and zinc impurities. This SEM analysis was performed on samples from  $\text{Ca/W} = 1.0025$ .

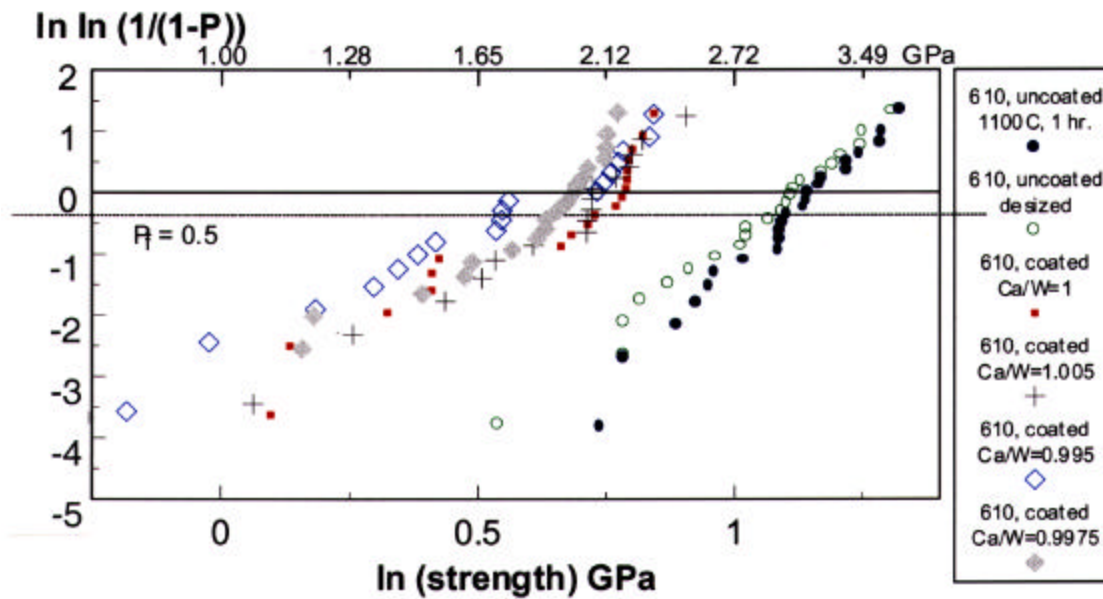


**Figure 5.** Weibull plot of scheelite coated Nextel 610 fiber heat-treated at 1100°C/1 hour. Coatings deposited from an ammonium metatungstate/Ca-nitrate based precursor.

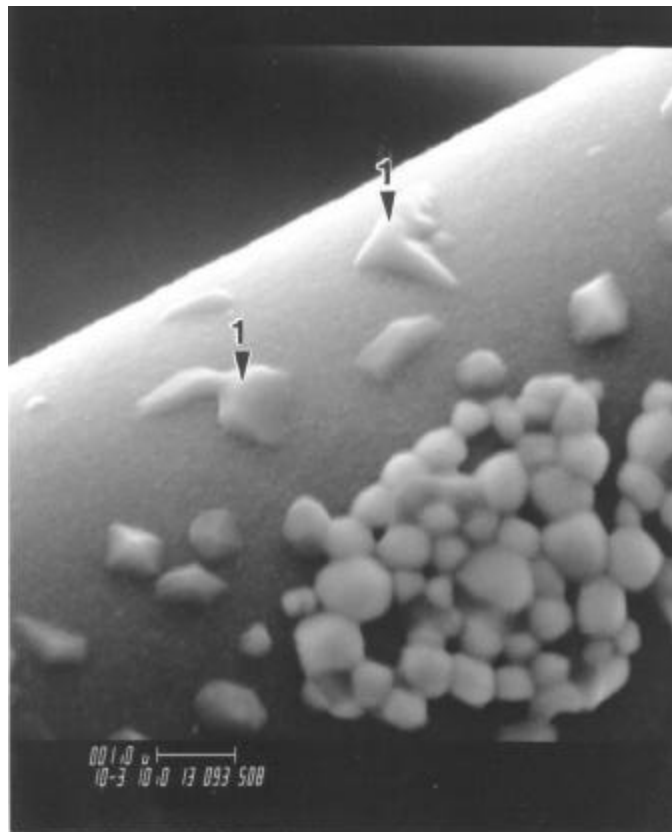


**Figure 6.** Scheelite coating on Nextel 610 following 1100°C/1 hour heat-treatment. Coatings derived from ammonium metatungstate/Ca-nitrate precursor (with ethanol).

An ACS grade of calcium nitrate was used for these ammonium metatungstate/Ca-nitrate based precursors. That level of purity had provided some initial encouraging fiber strength results for scheelite coatings and Nextel fibers in the past on a U.S. Dept. of Energy program. Based on the findings here, it was decided to use a more pure calcium nitrate. A 98% assay calcium nitrate powder with a 99.98% purity (on a metals basis) was purchased for use in additional precursor formulations. The ACS grade calcium nitrate that had been used is listed as 99.0-103.0% assay with a magnesium and alkali content of  $\leq 0.2\%$ , an order of magnitude less pure, on a metals basis. The specifications given for these powders do not mention phosphorous or phosphate impurities.

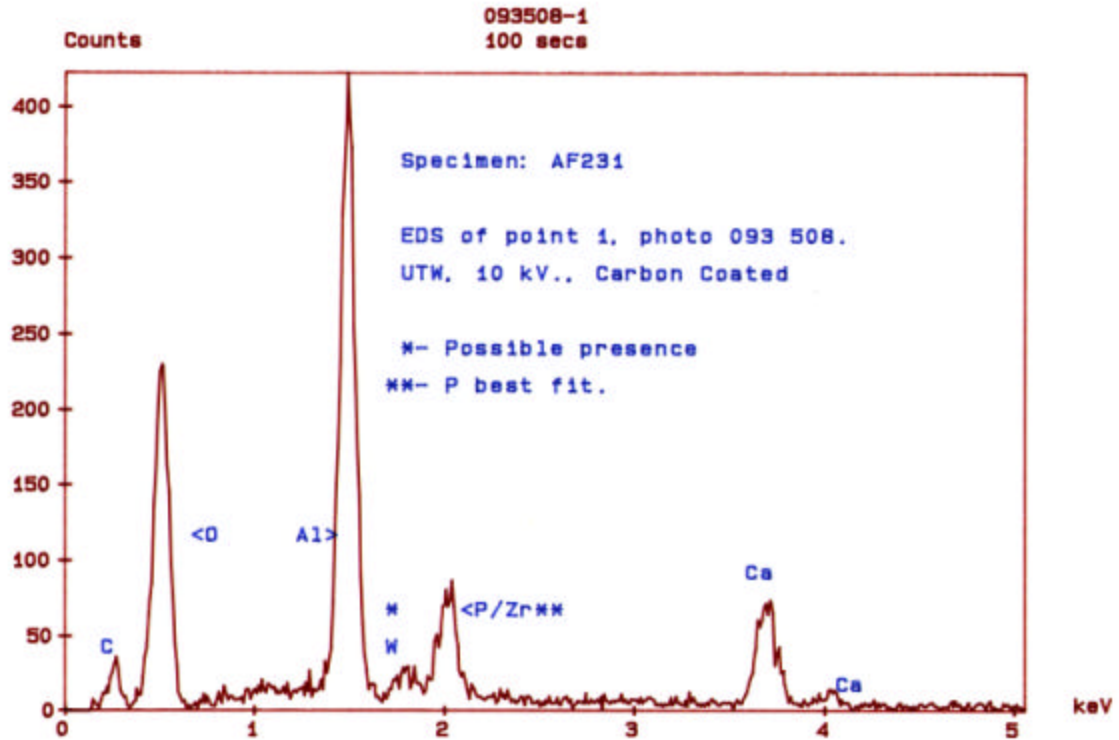


*Figure 7.* EDS data of AF231 coating

A concern was raised that the hydrogen peroxide solution with ethanol additions used for these scheelite precursors could perhaps be causing the strength degradation. To investigate this, Nextel 610 fibers were dip coated in a hydrogen peroxide/ethanol mix using an identical procedure as is used to deposit scheelite coatings single fiber. The fibers were heated to 1100°C for 1 hour. **Figure 8** shows the resulting Weibull strength distribution for these fibers. The peroxide/ethanol exposed fibers show a slightly lower strength than the control Nextel 610 fibers, but not significant enough to explain the low coated strengths.



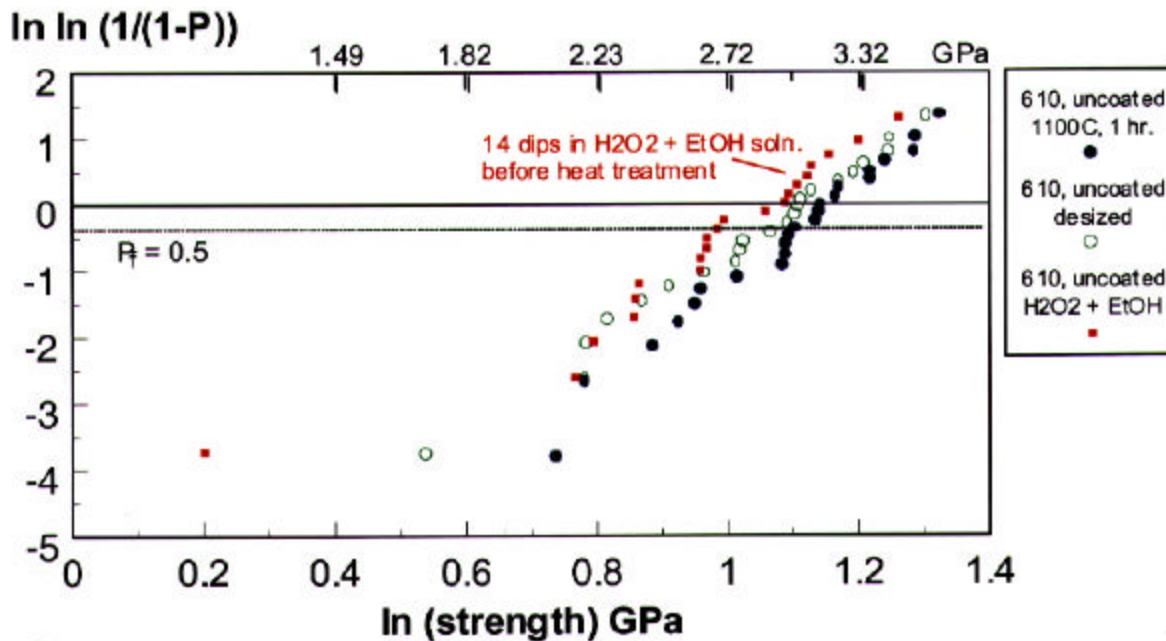


**Figure 8.** Weibull plot of Nextel 610 single filaments passed through a hydrogen peroxide/ethanol mix prior to an 1100°C/1 hour heat-treatment.

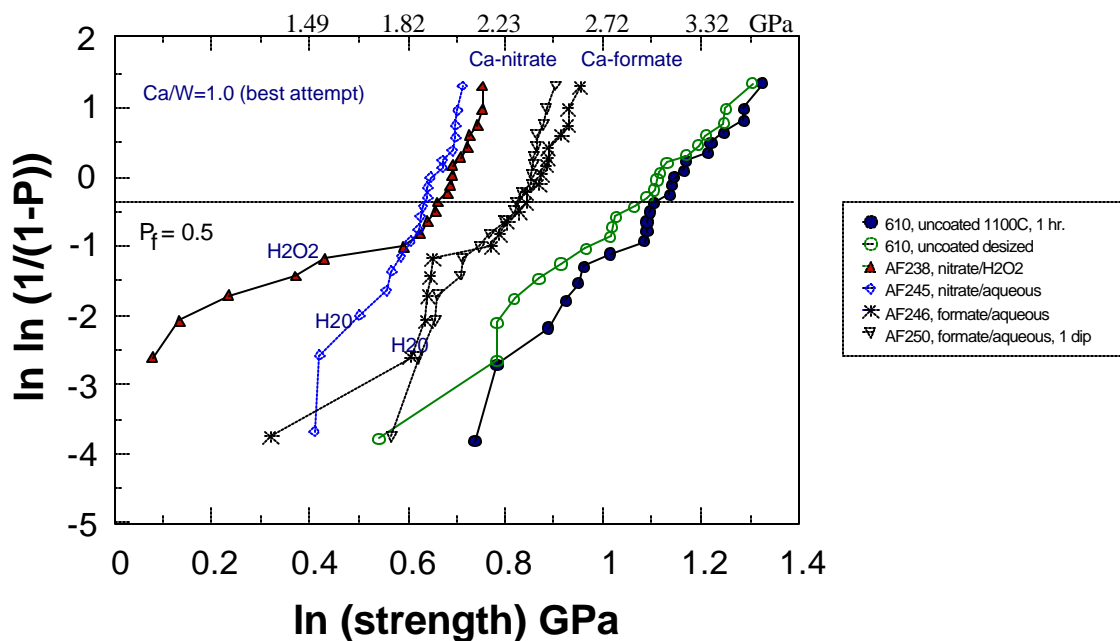
An additional series of experiments were performed to further examine and to reconfirm the fiber strength retention results obtained using precursors derived from ammonium metatungstate. The test matrix examined is summarized in *Table 1*.

Table 1. Test Matrix Summarized					
Precursor ID	WO <sub>4</sub> <sup>2-</sup> source	WO <sub>4</sub> <sup>2-</sup> stock soln. solvent	Ca <sup>2+</sup> source	Ca <sup>2+</sup> stock soln. solvent	Wetting Aid
AF238	metatungstate	H <sub>2</sub> O <sub>2</sub>	99.98% Ca-nitrate	demin. water	ethanol
AF245	metatungstate	demin. water	99.98% Ca-nitrate	demin. water	ethanol
AF246	metatungstate	demin. water	Ca-formate	demin. water	ethanol
AF250	metatungstate	methanol + demin. water	Ca-formate	demin. water	methanol

Ammonium metatungstate from GFS Chemical  
Calcium formate from Gelest, Inc.

The precursor AF250 listed above was a higher concentrated precursor (14% by weight scheelite yield) that was formulated so that a single dip coating process could be used rather than the multiple dip costing process that was the baseline procedure adopted to insure adequate scheelite deposition. It was thought that the process involved in performing the dip coatings could possibly cause cumulative damage to the fiber in some way. The Weibull plots of **Figure 9** summarize the single fiber strengths following coating and heat-treatment at 1100°C for 1 hour. Three trends were observed:

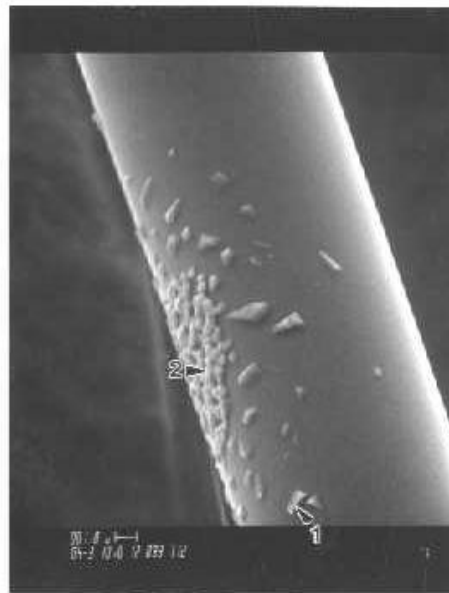
- (1) the retained fiber strengths with the metatungstate/Ca-nitrate precursors appears to be independent of whether hydrogen peroxide or water is used as the solvent,
- (2) scheelite precursors made from calcium formate rather than calcium nitrate produce less strength degradation of the Nextel 610 fiber, and
- (3) the number of dips used to deposit the scheelite coatings does not appear to be a factor in the amount of strength degradation observed.



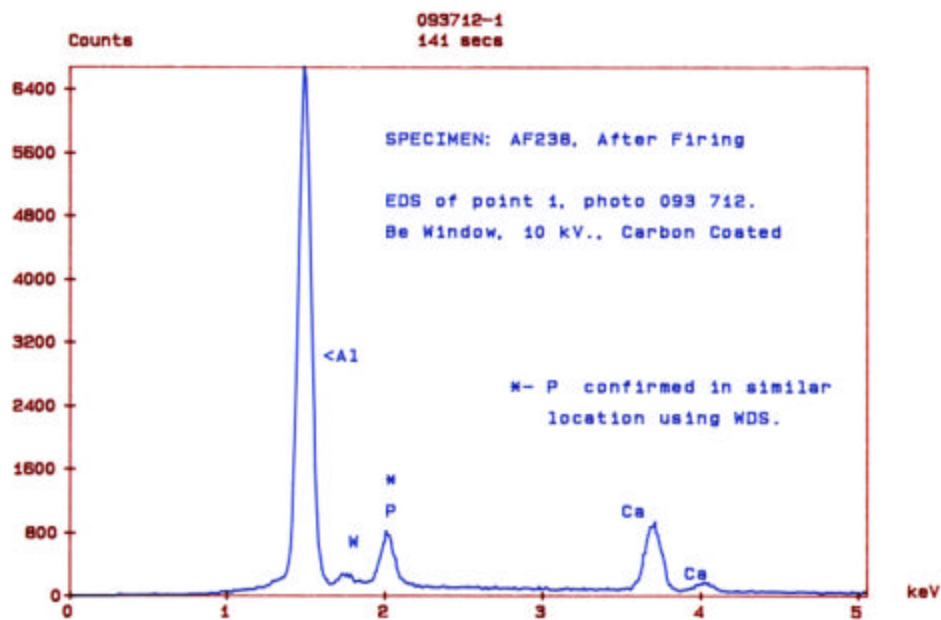
**Figure 9.** Weibull plots of Nextel 610 fibers coated with scheelite precursors formulated from ammonium metatungstate and either calcium nitrate or calcium formate.

SEM evaluation of coated fibers from lot AF238 (described in Table 1) revealed a spotty coating with coating grains of both a high- and low-contact angle with the fiber. The low-contact angle grains show a substantial phosphorous content by both EDS and WDS analysis (see the scan of grain 1 in **Figure 10**). Once again, these low-contact angle grains appear to be a

calcium phosphate phase. The high-contact angle grains (grain 2 of Figure 2) show only W and Ca, at least at the grain surface. **Figure 11** shows an interfacial region between a high-contact angle grain and the Nextel 610 fiber. Some phosphorous was detected at the interface by WDS.



(a)



(b)

**Figure 10.** SEM (a) and EDS (b) results from sample AF238. Point one highlights the low-contact angle grains that appear to be a calcium phosphate phase. Point 2 highlights a high-contact grain that appears to be scheelite based on a bulk scan.

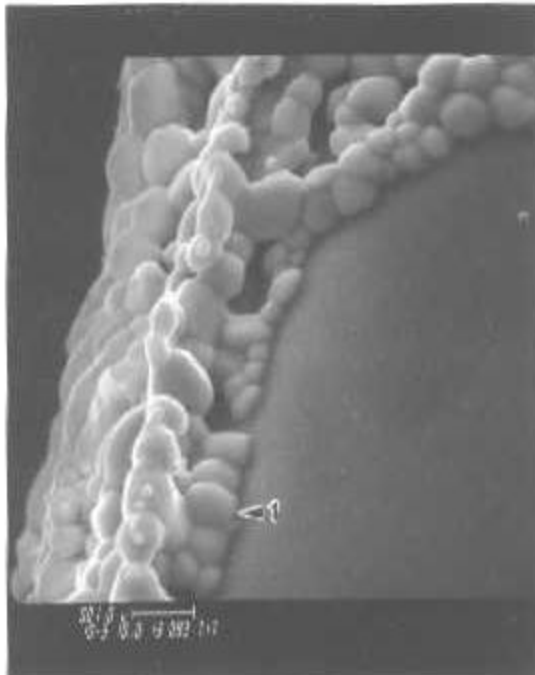


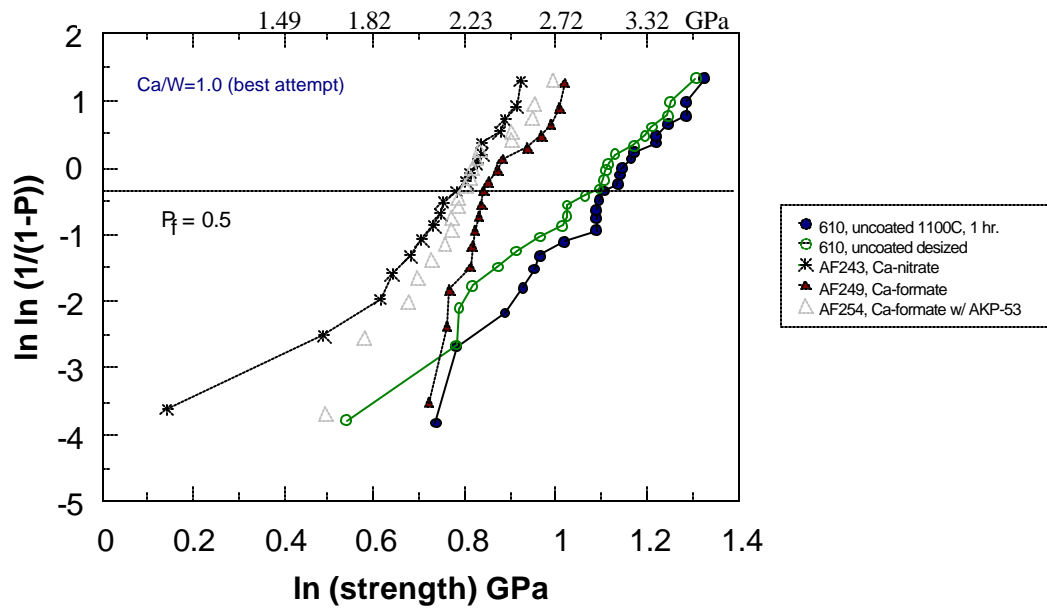
**Figure 11.** Marker 1 indicates the scheelite-Nextel 610 interfacial region of sample AF238 scanned by WDS and that showed the presence of phosphorous.

#### **Ammonium Tungstate Based Precursors Revisited; Stabilized with Hydrogen Peroxide**

Given the problems encountered with phosphorous contamination observed with the ammonium metatungstate based precursors, MTI investigated alternate precursors based on ammonium tungstate. MTI discovered that stable aqueous ammonium tungstate solutions could be formulated if a small amount of hydrogen peroxide was added. Without hydrogen peroxide additions, only tungstate solutions of low concentration could be formulated because of the low solubility of ammonium tungstate. In addition, if an ammonium tungstate solution (without peroxide) were to be added to a calcium salt solution, scheelite would immediately precipitate out from solution. The peroxide addition allows the formation of a stable (over a reasonable time scale for use in coating fiber) scheelite precursor upon mixing with calcium salt solutions. **Table 2** summarizes the precursors formulated from ammonium tungstate solutions containing peroxide.

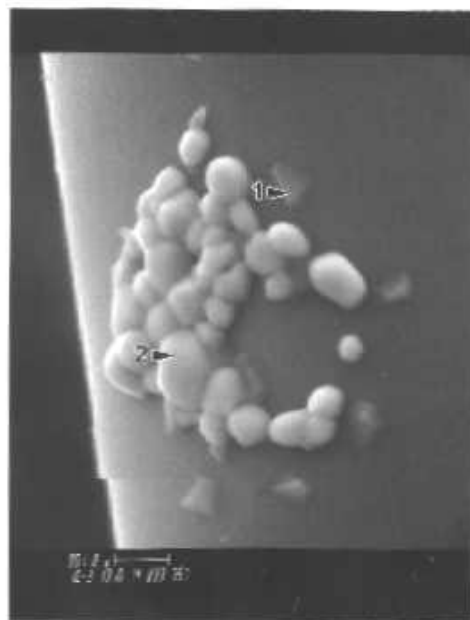
<b>Table 2. Precursors Formulated from Ammonium Tungstate Stabilized with Peroxide</b>					
<b>ID</b>	<b>W Source</b>	<b>solvent</b>	<b>Ca Source</b>	<b>solvent</b>	<b>Wetting Aid</b>
AF243	Aldrich ammonium tungstate	H <sub>2</sub> O <sub>2</sub> /water	99.98% Ca-nitrate	demin. water	methanol
AF249	Aldrich ammonium tungstate	H <sub>2</sub> O <sub>2</sub> /water	Gelest Ca-formate	demin. water	methanol
AF254	Aldrich ammonium tungstate	H <sub>2</sub> O <sub>2</sub> /water + AKP-53 alumina	Gelest Ca-formate	demin. water	methanol

Sample AF254 included Sumitomo AKP-53 alumina powder that had been classified to yield a small particle size distribution. The alumina powder was added to possibly react with any phosphorous impurities that may be present. Nextel 610 single fibers were dip coated with these precursors, heat-treated at 1100°C for 1 hour and tensile tested. The Weibull plots of **Figure 12** summarize the retained strength of these coated fibers. This series of samples also shows that there is better strength retention when using calcium formate rather than calcium nitrate. The addition of the Sumitomo AKP-53 alumina powder does not have a beneficial effect. SEM evaluation of coated fibers from lot AF243 also revealed a spotty coating with coating grains of both a high- and low-contact angle with the fiber. Once again, the low-contact angle grains show the presence of phosphorous by EDS analysis (see **Figure 13**).



**Figure 12.** Weibull plots of Nextel 610 fibers coated with ammonium tungstate/peroxide based precursors and heat-treated at 1100°C for 1 hour.

(a)



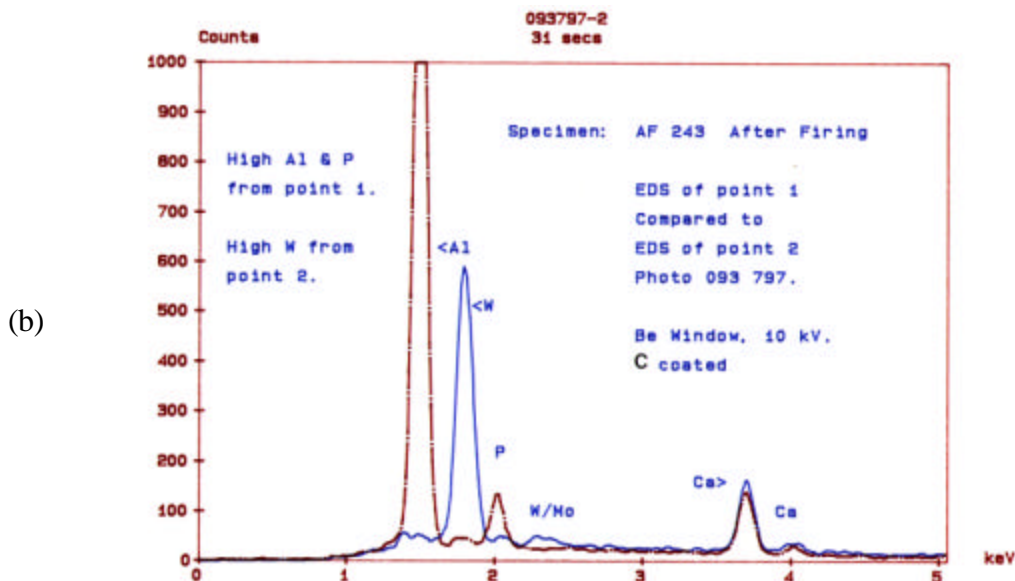


**Figure 13.** SEM (a) and EDS (b) results of sample AF243 showing both low- and high-contact angle coating grains on Nextel 610. The low-contact angle grains appear to be a calcium phosphate phase.

### **Stability Results with Precursors based on W-metal Digested in Hydrogen Peroxide**

The initial tungsten sources (ammonium metatungstate and ammonium tungstate) chosen for the scheelite precursors seemed to contain phosphorous impurities that could be a source for the degradation observed in the fiber strengths following 1100°C/1 hour heat-treatments (usually at least 20% reduction). The fault was placed on the tungstate sources since ICP analysis performed at Northwestern University revealed no phosphorous in the 30% hydrogen peroxide solution, the ethanol, nor the ACS grade calcium nitrate (analyzed as a aqueous solution formed with in-house demineralized water). Unfortunately, accurate phosphorous analysis could not be performed on the tungstate based raw materials (the raw materials were supplied as water or hydrogen peroxide solutions). In the samples based on a hydrogen peroxide solvent, the peroxide creates a noisy background that swamps the phosphorous signal. In addition, the phosphorous peaks overlap the tungsten peaks, causing the phosphorous peaks to appear as small shoulders on the tungsten peaks. The conclusion reached was that the best means for potentially achieving a scheelite precursor without phosphorous contamination would be to utilize precursors formulated using tungsten metal dissolved in hydrogen peroxide.

Nextel 610 fibers were dip coated with a scheelite precursor formulated from W-metal in hydrogen peroxide plus calcium formate in water (precursor no. AF263). The coated fibers were heated for one hour at 1100°C and 1200°C in air. The 1100°C heated fibers exhibited an average residual tensile strength of 2.09 GPa while the 1200°C samples had an residual strength of 1.7

GPa. These are quite poor residual strengths. The results are no better than that achieved with ammonium metatungstate and calcium nitrate.

Since the purity of the calcium formate was not known at the time that the precursor was formulated, additional precursors were formulated using calcium acetate of a known purity level (99.9965% metals basis). Three precursors were formulated at what is estimated to be Ca/W ratios of 0.99, 1.00 and 1.01. The dip-coated fibers were heated at 1100°C for one hour in air. The resulting Weibull plots of the retained tensile strengths are shown in *Figure 14*. Regardless of the Ca/W ratio tested, there was significant departure from the control uncoated fibers (2.21, 2.09, and 2.30 GPa average strengths, respectively versus a control value of 3.01 GPa).

Continued difficulty had been experienced throughout this task in achieving a 1100°C strength retention for coated fibers in excess of 80 percent. It was decided to proceed to composite fabrication activities (Task 3) utilizing the coating precursor routes based on W-metal dissolved in hydrogen peroxide. It is desirable to use the W-metal routes because of lower cost compared to ammonium tungstate and to possibly avoid the phosphorous contamination problem that was observed using the ammonium metatungstate. The tungsten metal based precursors also showed good stability as long as they were kept refrigerated and kept cool (via an ice bath) during continuous fiber coating. We also found that TGA runs of scheelite powders based on ammonium metatungstate resulted in powders with various shades of yellow/green indicating the presence of multi phases. We also compared W-metal based scheelite precursors formed using different calcium salts by TGA. The results for precursors formed from calcium formate, acetate and propionate are shown in *Figure 15*. It is most desirable to use a coating precursors that exhibits the least amount of decomposition products in order to minimize any deleterious effects that the volatile species may have on the fiber strength. On this basis, a precursor based on calcium formate is preferred. We can not explain why the acetate shows a larger weight loss than the propionate.



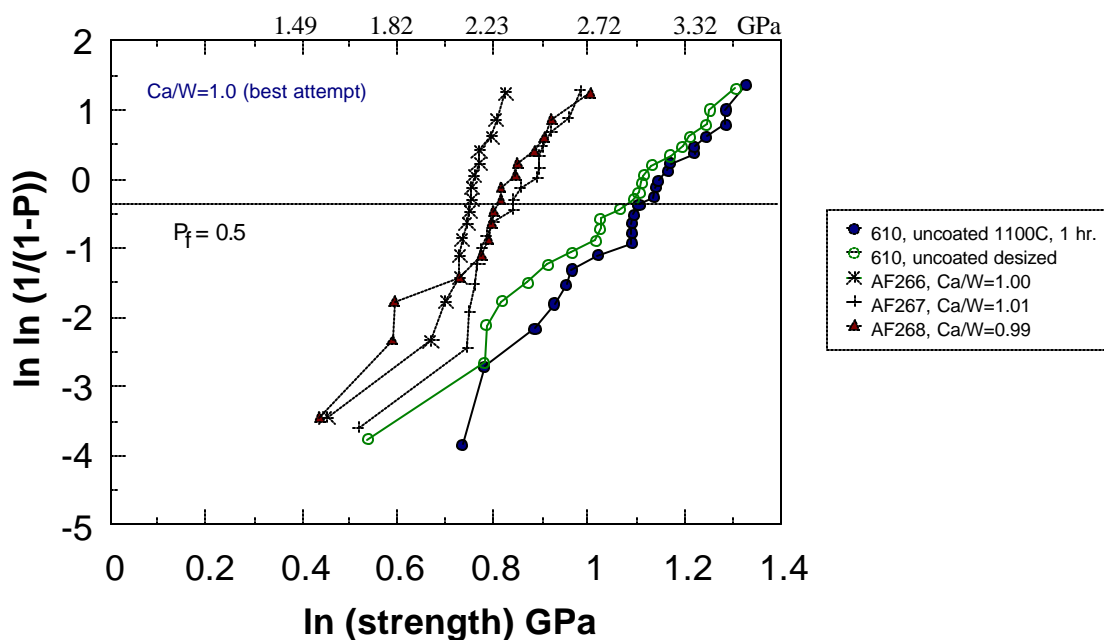


**Figure 14.** Weibull plots for Nextel 610 fibers with different Ca/W ratios and following an 1100°C/ 1 hour heat-treatment. Precursors were based on W-metal/H<sub>2</sub>O<sub>2</sub> plus calcium formate.

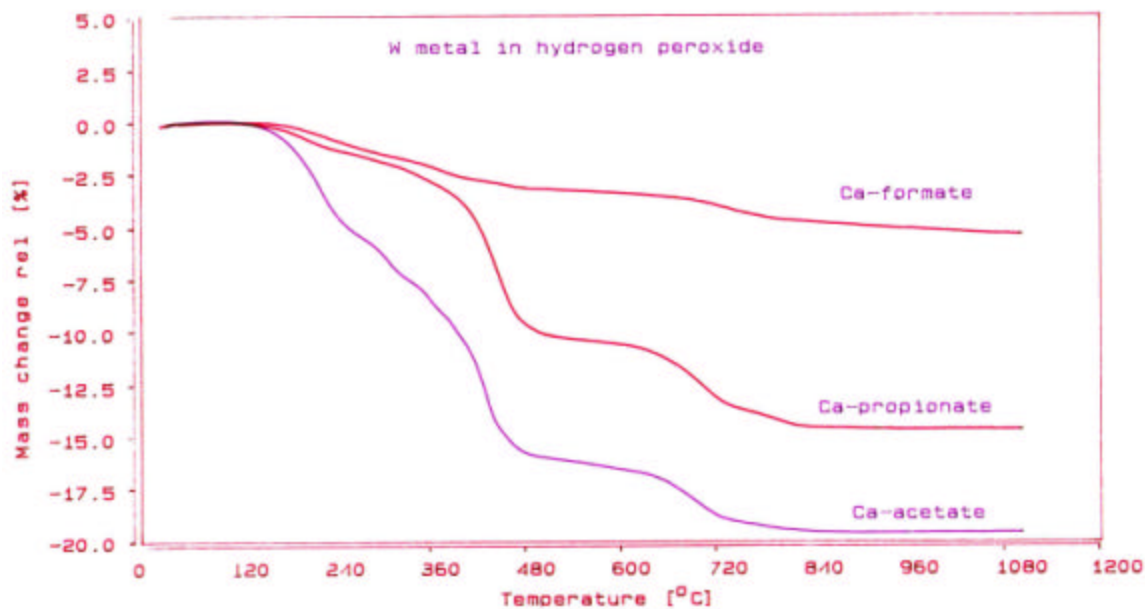


**Figure 15.** TGA curves of scheelite precursors made from different calcium salts.

### **Stability Results with ATFI Formulated Scheelite Precursor**

ATFI developed a scheelite precursor based on tungsten alkoxide and calcium nitrate in ethanol. A proprietary complexing agent was utilized to stabilize the tungsten species present in solution. Two precursors were supplied to MTI for dip coating of fiber and strength retention experiments. One of the batches (AF289) contained a small  $\text{Ca}_3\text{WO}_6$  peak as shown by the x-ray diffraction pattern of **Figure 16**. The other batch showed no presence of  $\text{Ca}_3\text{WO}_6$  (see the **Figure 17**). Single fibers were dip coated and the fibers were heat treated at 1000°C and 1100°C for one hour. A batch of uncoated fibers was also heat treated. The resulting retained tensile strength of the fibers is given in **Table 3**. The strengths of the fibers coated with the precursor that was closer to  $\text{CaWO}_4$  stoichiometry showed slightly higher strengths following the 1000°C heat treatment. The strength degradation of fibers containing the more stoichiometric precursor was still quite substantial after 1100°C/1 hour heat-treatment.

<b>Table 3. Strengths of Fibers Dip Coated with NWU Scheelite Precursor</b>			
<b>Coating</b>	<b>Stoichiometry</b>	<b>Heat-Treatment Temp. (C°)</b>	<b>Tensile Strength (GPa)</b>
Uncoated	NA	1000	2.76
AF289	Slight $\text{Ca}_3\text{WO}_6$	1000	2.33
AF290	No $\text{Ca}_3\text{WO}_6$	1000	2.49
AF290	No $\text{Ca}_3\text{WO}_6$	1100	2.03

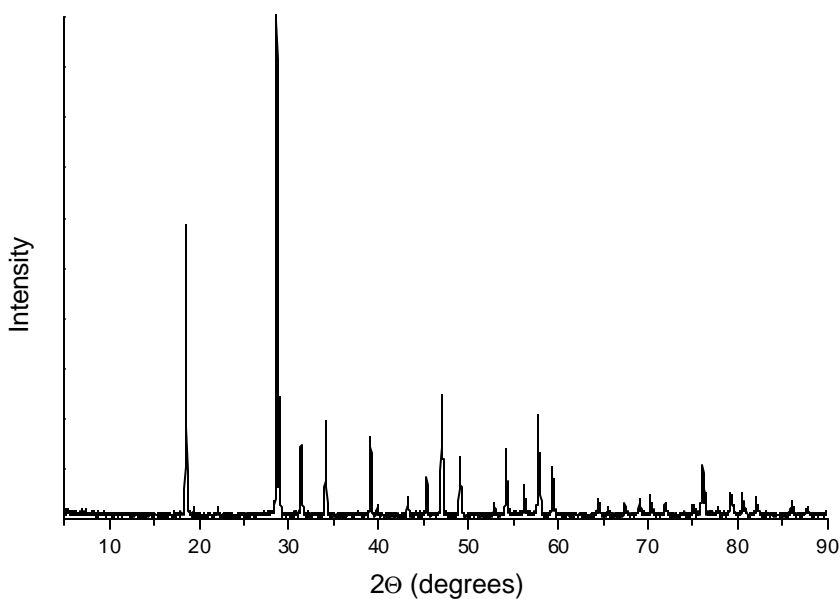


**Figure 16.** X-ray diffraction pattern for AF289. Small peaks at approximately 19° ( $I_{45}$  peak) and 22° ( $I_{60}$  peak) correspond to  $\text{Ca}_3\text{WO}_6$ . The  $I_{100}$  peak for  $\text{Ca}_3\text{WO}_6$  overlaps scheelite peak at 31.4°

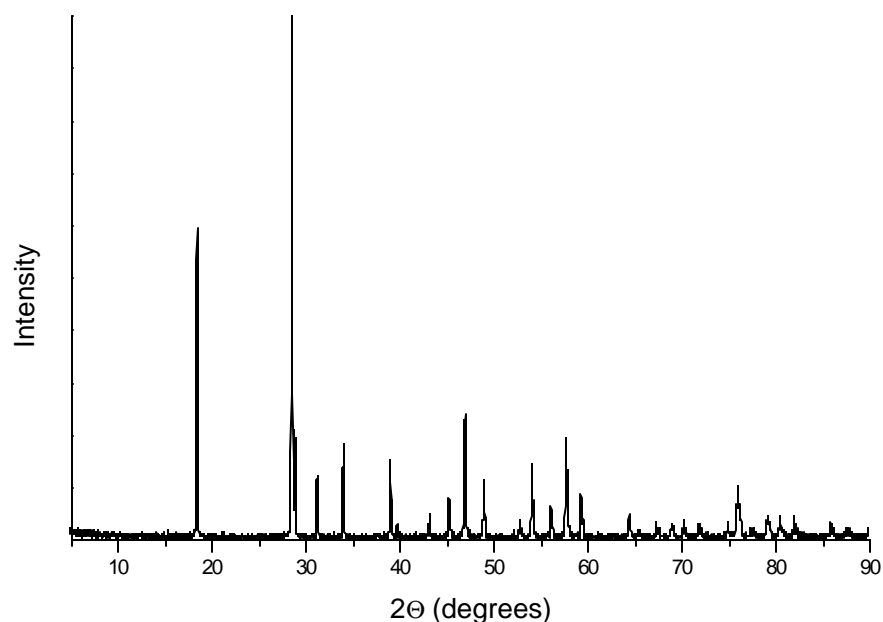


**Figure 17.** X-ray diffraction pattern for AF290. No peaks for  $\text{Ca}_3\text{WO}_6$ .

### **Stability Results with Scheelite Slurry Coatings**

Under a prior government supported program, fiber strength retention experiments were performed with Nextel 720 and  $\text{LaPO}_4$  coatings where the coatings were deposited from washed precipitated rhabdophane slurries [6]. The fibers showed excellent strength retention. The excellent strength retention was attributed to good stoichiometry control, a neutral pH, and the absence of residual cationic and anionic species from the lanthanum salts and phosphoric acid used in the formulations. Similar results were obtained by the Air Force Wright Laboratory [7]. Based on these results, MTI proceeded to investigate whether a precursor based on a scheelite slurry could also be formulated to give good fiber strength retention and yield morphologically good coatings.

Scheelite precipitates directly from salt solutions whereas with  $\text{LaPO}_4$ , the hexagonal hydrated rhabdophane phase is precipitated. The rhabdophane powder must be thermally treated to convert it to the monoclinic monazite phase. The rhabdophane crystals are small, generally under 0.3 microns with an elongated geometry. The scheelite precipitates tend to be a few microns in size and the slurries would require milling to reduce the particle size to an appropriate range for coating of 10-12 micron diameter fibers. Rather than formulate a scheelite slurry for particle size reduction, MTI choose to concentrate on the particle size reduction of a commercial 99.9% purity scheelite powder (Aldrich Chemical, cat. no. 24,866-5). The powder was attrition milled using an alumina-lined container and yttria stabilized zirconia shaft and milling media.

Throughout the milling process, Darvan C dispersant (ammonium polymethacrylate) was added to reduce the viscosity of the slurry and allow for efficient milling. The slurry was milled for a total of 19 hours during which time the median particle size was reduced from 8.95 to 0.181 microns. Two batches of coated fibers were prepared with the slurry precursor:

1. 5.2 wt. percent slurry, 650°C furnace temperature, ~40 inch/min through coater
2. 9 wt. percent slurry, 815°C furnace temperature, ~40 inch/min through coater

Uncoated fiber tows and fiber tows with coatings derived from a standard W-metal/peroxide solution precursor and slurry based precursors were heat treated at 1050°C for one hour. Single fiber filament strengths were measured for the coated and uncoated fibers. The results are shown in **Table 4**. The slurry coatings appear to cause less strength degradation to the Nextel 610 fibers during heat-treatment than the solution based scheelite precursors.

<b>Table 4. Measurements of Single Fiber Filaments Strengths</b>	
<b>Coating</b>	<b>Strength after 1050° C/1 hr. (GPa)</b>
Uncoated – baseline	2.87
AF298 solution	2.03
5.2 w/o slurry 650°C max. coater temp.	2.57
9 w/o slurry 815°C max. coater temp.	2.31

The cause for the strength degradation associated with the slurry-based coatings is unknown. One cause may be the presence of sodium in the Darvan C. The manufacturer's specification for sodium is less than 70 ppm. We also believe that the observed strength degradation may be influenced by the non-uniformity of the coatings. Slightly higher strengths were observed for the slurry coatings deposited from the 5.2 weight percent precursor than from the 9 weight percent precursor. **Figures 18 and 19** show the nature of the coatings obtained from the two slurry precursors following heat treatment at 1050°C. The coatings obtained using the higher concentration slurry appear to be thicker in the “crusty” regions. These thick coating regions may present regions of stress intensity on the fibers causing somewhat lower stress values. No investigations were performed to determine if there was any phosphorous contamination associated with these slurry based coatings.

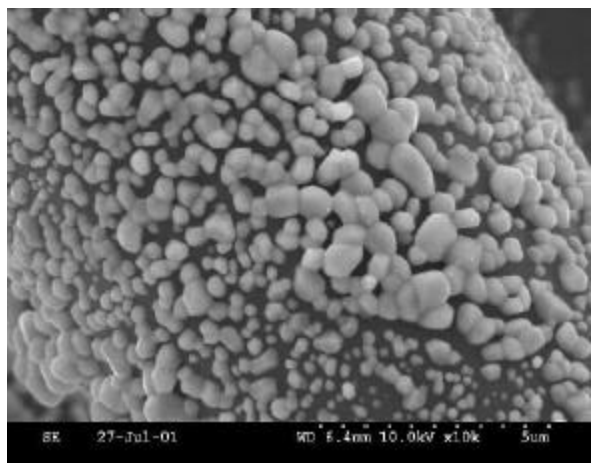
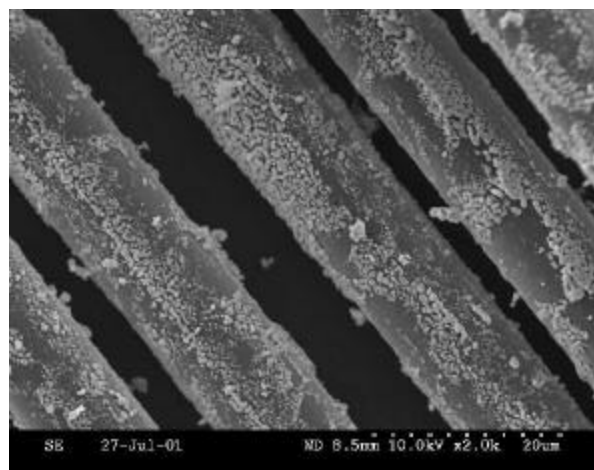
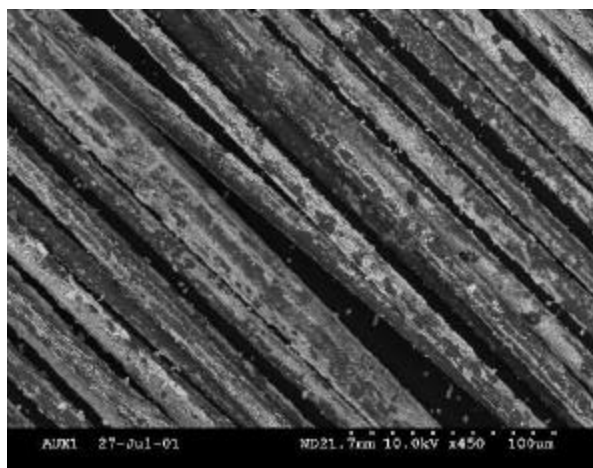


**Figure 18.** SEM photomicrographs of coatings from 5.2 wt. percent slurry and 650°C coater furnace set point.

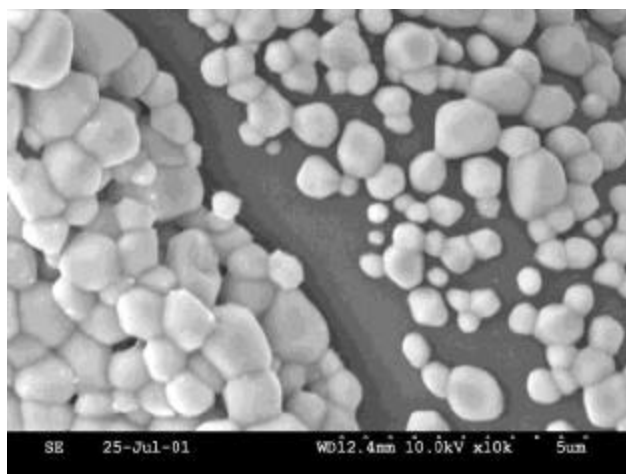
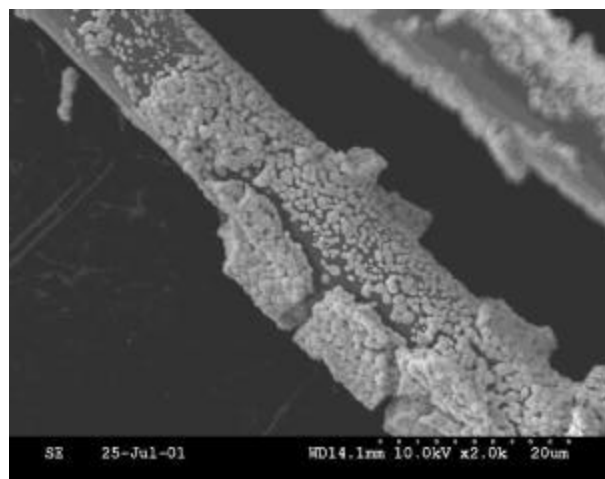
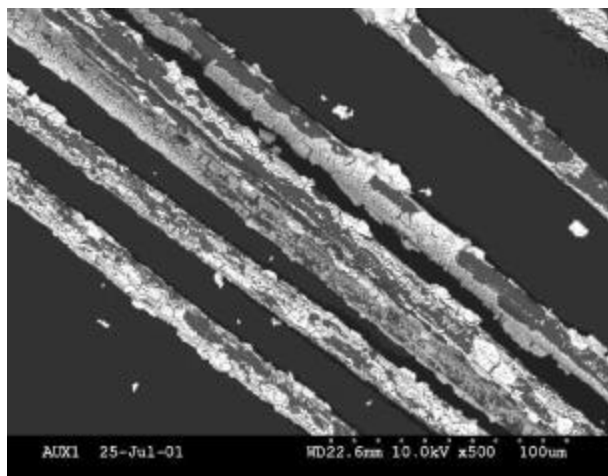


**Figure 19.** SEM photomicrographs of coatings from 9 wt. percent slurry and 815°C coater furnace set point.

## **Task 2 – Matrix Precursor Stability**

The objective of this task was to identify matrix precursors that would not promote strength degradation of the Nextel fibers during composite processing and which, through multiple infiltration of the CMCs, permit processing to a total residual composite porosity of under 10 percent. These matrix precursors are used to provide final densification of the composites. The initial densification of the composites is accomplished by performing a pressure infiltration/casting of the fiber preform using an alumina slurry. The slurry pressure casting typically deposits alumina matrix of about the same volume fraction of the Nextel fiber. The bulk of the remaining residual porosity is filled through multiple infiltrations with a chosen matrix precursor.

The initial selection of a matrix precursor was limited to alumina and mullite precursors. This list was expanded to include a unique amorphous aluminum phosphate precursor from ATFI known as CeraBlak<sup>TM</sup> and a silica polysiloxane precursor (this at the suggestion of the Air Force Wright Lab project manager). MTI attempted to develop precursors that exhibit as low an amount of volatile species during decomposition as possible, and which evolve the volatile species at as low of a temperature as possible with as minimal of a weight loss “tail” at high temperatures as possible. The thinking here is to avoid, or at least minimize, the evolution of acidic decomposition gases that could be a possible cause for fiber strength degradation. The evolution of such gases during processing heat treatment cycles, where the exit path from the CMC is torturous (especially once higher matrix densities are achieved) could cause these decomposition species to “stew” around in the bulk of the composites giving the opportunity to cause fiber strength damage. The following sections summarize the work performed on the candidate matrix precursor systems.

### **McDermott Alumina Polymer**

MTI developed an alumina polymer (US Patent 5,670,103) prior to this program that is formulated by partially decomposing aluminum nitrate nonahydrate at approximately 150°C until it has lost from between 70 to 72 percent of its original weight. The resulting powder is then redissolved in water to give a clear alumina precursor solution. The alumina polymer still contains a fair amount of nitrates. It is hypothesized that the NO<sub>x</sub> species are not completely evolved until possibly quite high temperatures, greater than 750°C, and it is these species that may cause fiber strength degradation. One approach that was evaluated was to try to substitute the nitrate groups with organic ligands that may decompose to more benign species at the higher temperatures. We have tried to replace the nitrates with oxalic acid, ethylene glycol or formic acid. Oxalic acid, ethylene glycol or formic acid was simply added to the alumina polymer solution and refluxed.

*Figure 20* shows the results of these substitutions on the thermal decomposition of the alumina precursors (the refluxed solutions were dried at ~150°C to yield a powder) as revealed by TGA. It should be noted that the ethylene glycol substituted polymer remained black even at high temperature, the oxalic acid substituted polymer was white after about 300°C, and the formic

acid substituted polymer was a very light brown to about 800°C. The relative weight losses shown in **Figure 20** scale are very closely to the ratios of the molecular weights of the substituted ligands ( $\text{OCOCO}_2\text{H}$ ,  $\text{OCH}_2\text{CH}_2\text{OH}$  and  $\text{OCOH}$ ) and  $\text{NO}_3^-$ . The powder color observation can be explained by the fact that oxalic acid has more oxygen within its structure, and hence there is more rapid and complete burn out of the carbon. Without enough oxygen within the organic ligands, such as with ethylene glycol, high temperature oxidation of the residue is controlled by solid state diffusion of oxygen into the resulting alumina powder and the powder ends up remaining dark in color owing to the residual carbon until higher temperatures are reached. **Figure 20** indicates that the polymer substituted with oxalic acid exhibits a much earlier degradation of the precursor (nearly complete by 360°C) than the unaltered or ethylene glycol substituted polymer (most of the decomposition not occurring until 400°C to 480°C). These results point out how fairly minor changes to the matrix precursor can significantly impact the nature of the volatile species and the temperature at which they are evolved during decomposition.

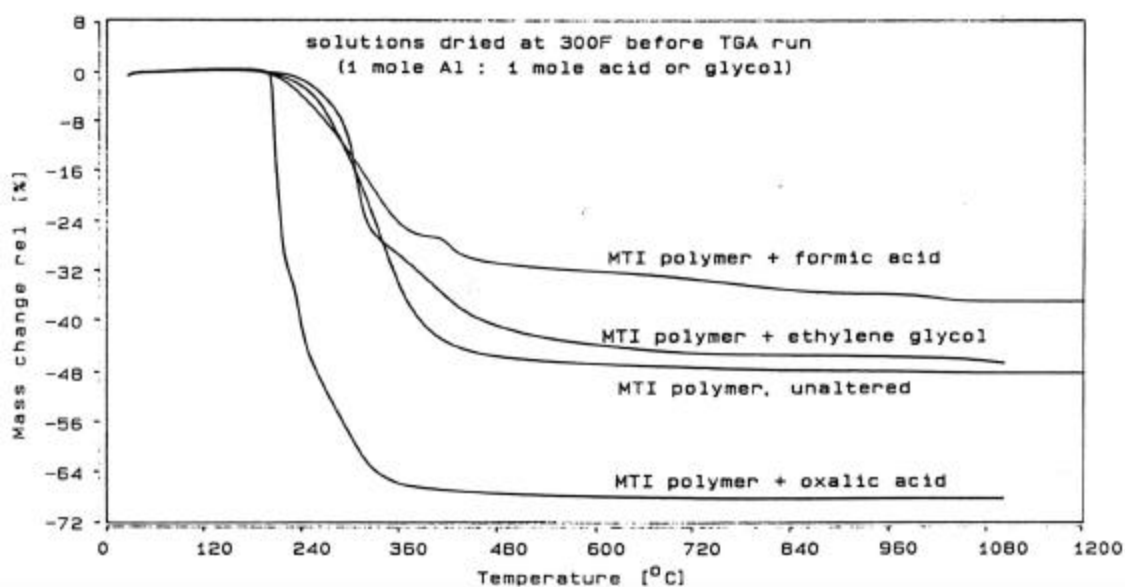


**Figure 20.** TGA curves of substituted and unaltered MTI alumina polymers

The challenge under this program has been to create a liquid precursor in which the organic for nitrate substitution is complete. It appears that the precursors must be dried to some degree to promote the substitution. If the drying operation is taken too far, then the redissolution of the powder is difficult and undissolved powder may remain. When the nitrate and organic



species remain in the solution, a rather severe exotherm is observed upon heating of the resulting dried powders. **Figure 21** shows the TGA/DTA scan for a MTI alumina polymer formed from aluminum nitrate that had been decomposed to 37.5% of its original weight. Formic acid was added at a ratio of 3 moles formic acid to 1 mole of  $\text{Al}_2\text{O}_3$ . The resulting formic acid-alumina polymer solution was refluxed for 5 hours and the solution was then dried at 105°C for about 2 hours. The resulting powder was soluble in water. A sharp exothermic reaction exists near 130°C that is associated with the oxidation of the organic groups by the nitrate ions that remain. The solution formed upon redissolving the 105°C dried powder was then dried at a higher temperature (~150°C) in an attempt to drive off additional nitrate groups. The resulting powder was redissolved in water, although a slight amount of the powder did not redissolve. DTA/TGA analysis of dried powder from that solution (**Figure 22**) showed the absence of the low temperature exotherm. The powder dried at the higher temperature (150°C versus 105°C) was much more difficult to redissolve in order to form a workable alumina precursor.

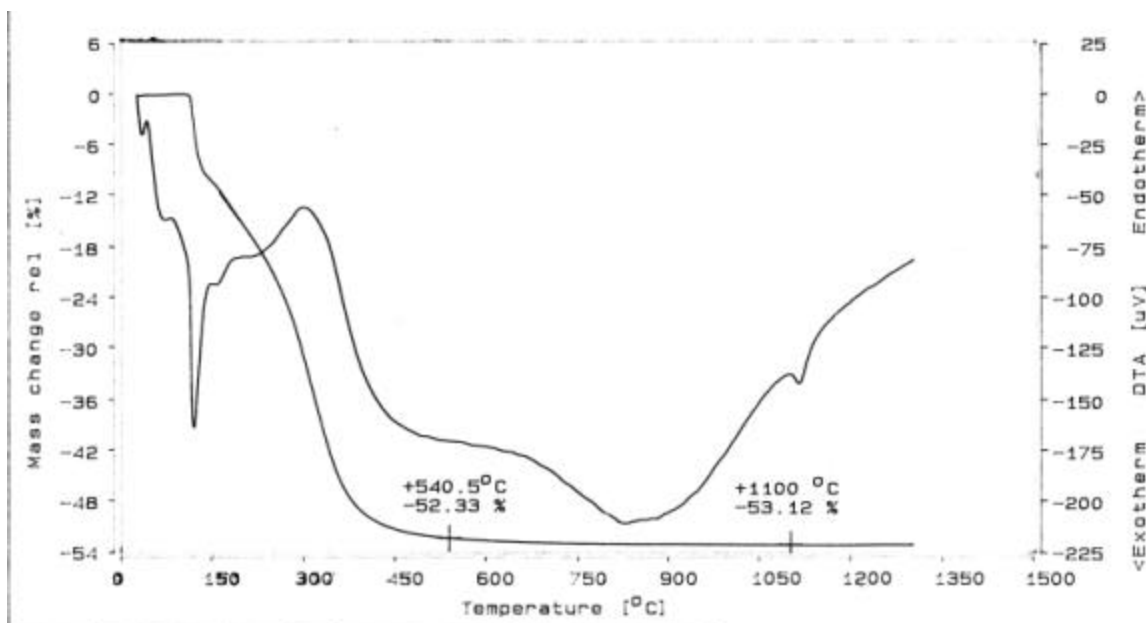


**Figure 21.** DTA/TGA of 37.5% alumina polymer/formic acid solution dried at 105°C

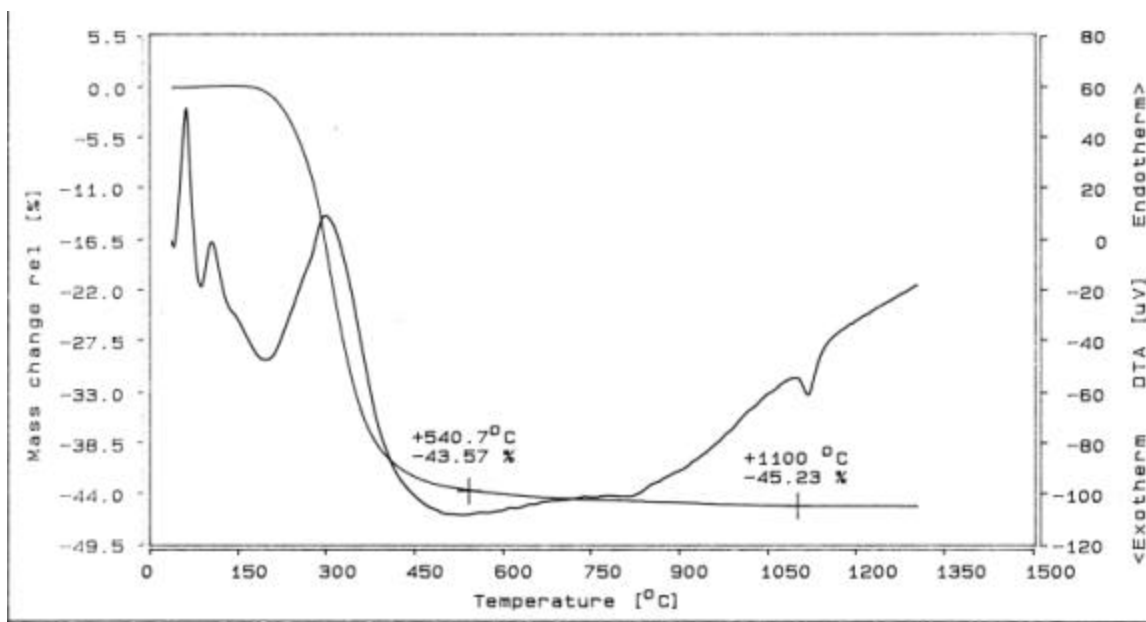


**Figure 22.** DTA/TGA of 37.5% alumina polymer/formic acid solution dried at 150°C

Similar results were obtained with a MTI alumina polymer that had been formed by decomposing aluminum nitrate to 28.1% of its original weight. DTA/TGA curves shown in *Figures 23 and 24* show that higher drying temperatures are required to eliminate the low temperature exotherm. Because of the difficulty (especially with scaling-up of the process) in achieving complete substitution for the nitrate counter-ions, while retaining the ability to redissolve the polymer, it was decided to no longer pursue this matrix precursor route. Rather than attempt to substitute for the nitrate counterion, MTI alumina polymer precursors were formulated using aluminum nitrate decomposed to the furthest extent possible, while still being able to redissolve the polymer in demineralized water. The aluminum nitrate powder was able to be decomposed to as little as 25.6% residual and still be dissolved. These precursors were used to densify series one and two CMC fabricated under Task 3 for mechanical property evaluation. Based on single fiber strength data of alumina polymer coated fibers, the processing temperature needed to be kept at or below 1000°C to prevent substantial strength degradation of the Nextel 610 fiber (see Weibull data presented later in *Figure 27* along with data for colloidal silica coated fiber).

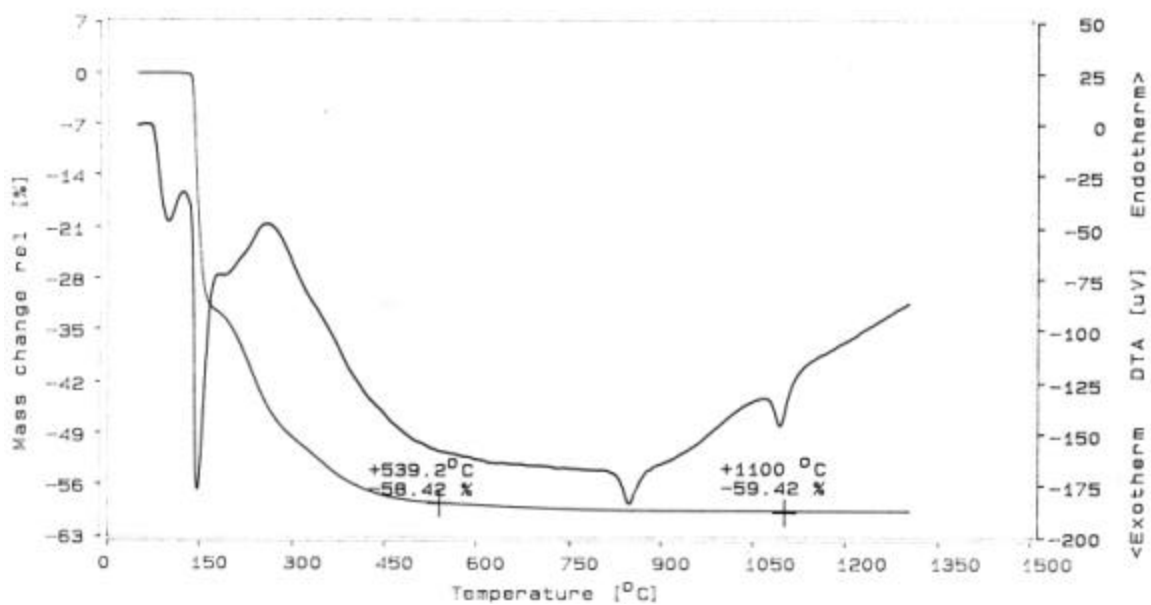


**Figure 23.** DTA/TGA of 28.1% alumina polymer/formic acid solution dried at 105°C.

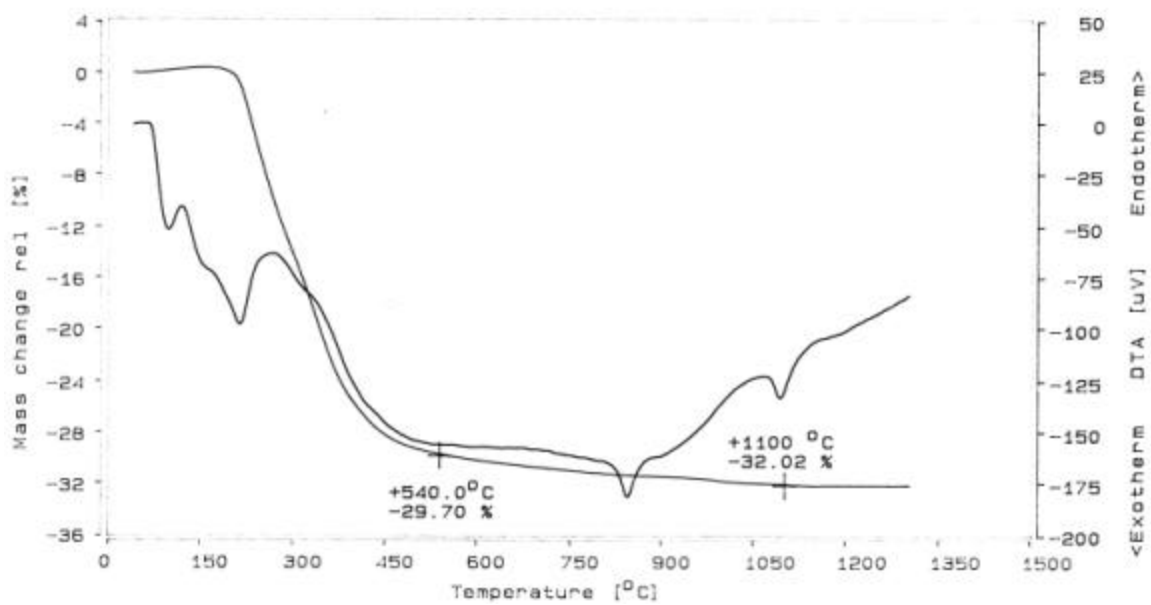


**Figure 24.** DTA/TGA of 28.1% alumina polymer/formic acid solution dried at 150°C.

### **Alumina Polymer Derived from Al-metal/Formic acid/Hydrogen Peroxide**

Work was performed on a precursor that was derived from aluminum metal, formic acid and hydrogen peroxide. The objective was to investigate precursors without nitrate counter-ions and rely on purely organic species for polymerization and stabilization in solution. It was found that refluxing aluminum metal with formic acid and an oxidizer such as hydrogen peroxide yielded such a precursor. Precursors with various ratios of formic acid and hydrogen peroxide to aluminum were studied (see *Table 5*)

**Table 5.** Precursors studied in the Al-formic acid-hydrogen peroxide system.

Sample No.	Al (moles)	Formic Acid (moles)	H <sub>2</sub> O <sub>2</sub> (moles)	Comments
AF110	1	1.76	1	Much white precipitate after prolonged refluxing
AF111	1	1.76	0.75	Fairly complete digestion of Al
AF113	1	1.5	0.75	Fairly complete digestion of Al
AF114	1	1.5	0.5	~90% digestion of Al

Precursors AF111 and AF113 yielded fairly clear solutions. The aluminum metal exhibited nearly complete digestion after refluxing for less than 16 hours. AF114 precursor did not fully digest the aluminum metal with 24 hours of refluxing. The undissolved metal was filtered off. The pH of the fairly dilute precursor solutions was in the range of 3.5 to 4. Unfortunately, upon concentration and/or after sitting for over a day, these three precursors began to exhibit a white, gelatinous precipitate. Precursor AF110 exhibited a large amount of white precipitate after refluxing continuously over a weekend. That precursor was not observed at intermediate refluxing times, but it is assumed that the aluminum metal was fully digested at some point during the refluxing time since only a white precipitate was observed (similar to what was observed for AF111 and AF113 after setting for 1-3 days). Because of the instability of the precursors over only a very short time, they were deemed to be unsuitable for use in final densification of CMC panels under this program.

### **Alumina Polymer Derived from Al-metal/Formic Acid/Carbonic acid**

Prior to this project, some work had been performed on a precursor derived from digesting aluminum metal in formic plus oxalic acid. By controlling the ratios of mono- and bi-functional carboxylates, the aluminum metal could be successfully digested to yield a stable alumina precursor. The ratios of raw materials generally used were from 1.0 to 1.26 moles of aluminum: 1.76 moles formic acid:1.0 mole oxalic acid. A typical TGA curve for a dried

powder obtained from this precursor is shown in **Figure 25**. The precursor exhibited a low volatilization weight loss between 540°C and 1100°C of 0.42% of the original powder weight (or 1.23% normalized to final amount of alumina powder).

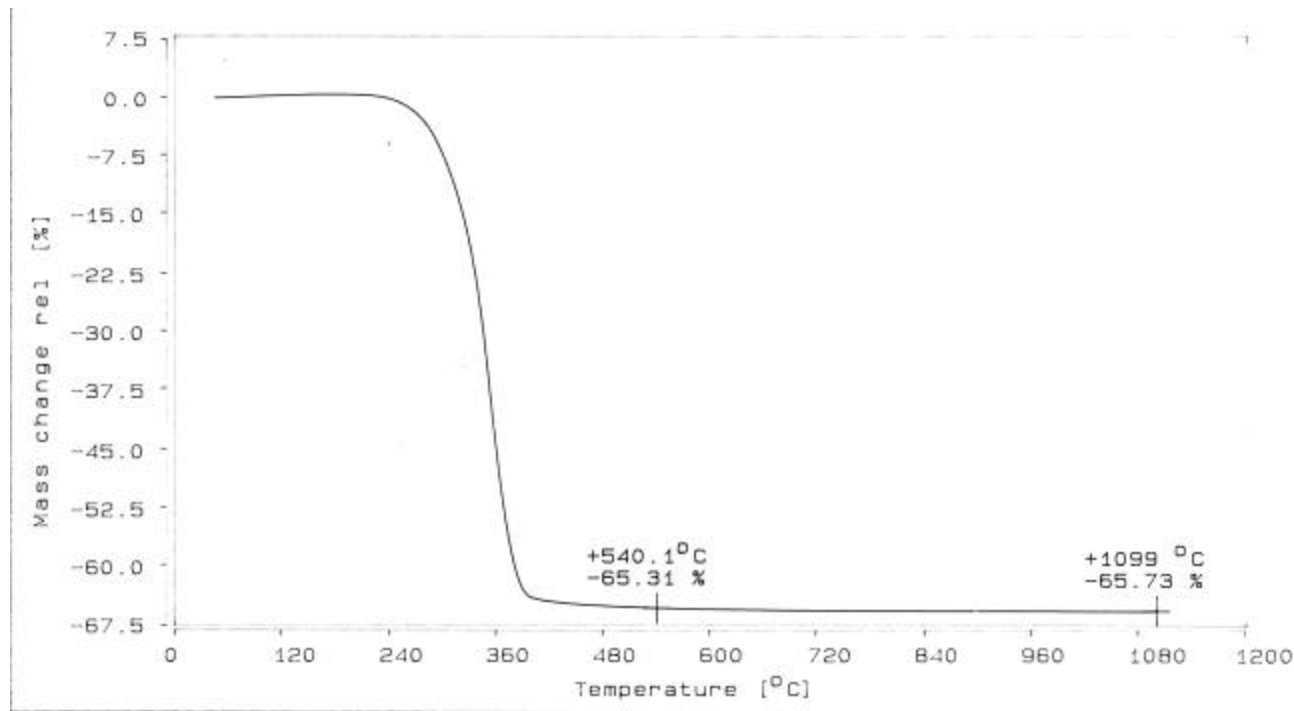


**Figure 25.** TGA curve of powder contained from dried Al-metal/formic acid/oxalic acid alumina precursor

Rather than utilizing the bifunctional oxalic acid, studies were performed with the lower molecular weight bifunctional carbonic acid. Carbon dioxide was continuously bubbled through an aqueous solution that contained 1 mole of aluminum metal to 1.76 moles of formic acid and that was heated under refluxing conditions. It would generally take a couple days for the aluminum metal to be fully digested. There would often be some minor amount of residual precipitate and undigested aluminum that was filter from the precursor solution. DTA/TGA of powder obtained from drying of the precursor solution is shown in **Figure 26**. The carbonic acid based precursor also exhibited a low volatilization weight loss between 540°C and 1100°C of 0.78% of the original powder weight (1.69% normalized to the resultant alumina powder weight). This alumina precursor exhibited some stability problems that would have made it difficult to use for CMC fabrication, given the shelf life required for such a use.

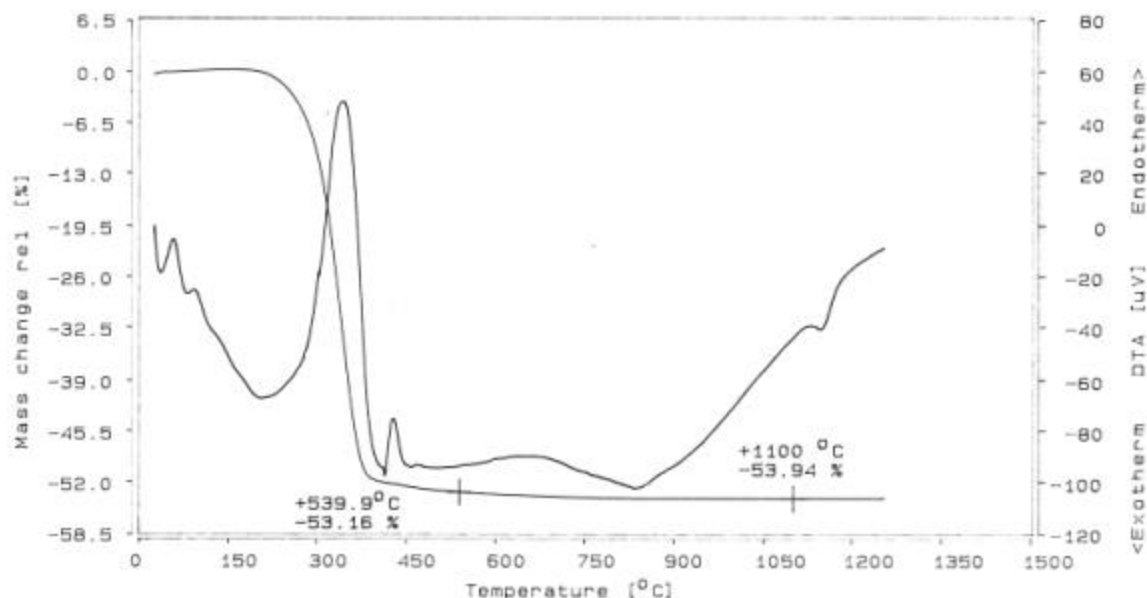


**Figure 26.** DTA/TGA curve of powder obtained from dried Al-metal/formic acid/carbonic acid alumina precursor.

### **Mullite Precursor**

The main objective of this work was to evaluate solution precursor chemistries for mullite matrix formation. The key properties desired for the mullite precursor are a) low temperature formation of 3/2 mullite upon pyrolysis, b) high yield precursor, and c) compatibility with Nextel fibers (minimal strength degradation).

Mullite ( $3\text{Al}_2\text{O}_3 \cdot 2\text{SiO}_2$ ) synthesis has been done using various chemical routes and the subject has been investigated extensively [8]. The precursor chemistries used thus far can be broadly classified into two categories. One approach involves the synthesis of suitable precursors that promote intimate mixing of aluminum and silicon at the molecular level, which allows for mullite crystallization at temperatures as low as 980°C. The second approach involves the use of solid state reaction between alumina and silica particles or admixtures of sols or colloidal solutions where the level of atomic mixing is rather inadequate, resulting in mullite formation at much higher temperatures. In exploring the first approach further, Huling and Messing were the first to point out that the crystallization observed at 980°C was actually indicative of phase separation resulting in formation of "alumina" rich mullite with the excess silica being consumed at later stages to form the 3/2 mullite [9]. This was supported by evidence of a sharp and intense exotherm at 980°C and a very small exotherm on the DTA around 1250°C. However, more recently, E. Tkalcic and coworkers prepared gels using ethanolic solutions of aluminum nitrate and tetraethoxy silane (TEOS) which upon decomposition formed

the 3/2 mullite at 980°C [10]. Thus it appears that precise control of precursor chemistry is required to form stoichiometric 3/2 mullite. The objective of this investigation was to determine whether high-yield containing precursor solutions that are stable and clear could be synthesized to yield mullite at low temperatures.

MTI's proprietary alumina polymer derived from controlled decomposition of aluminum nitrate nanohydrate possesses interesting properties for use as starting material along with TEOS for the mullite precursor. During the decomposition of aluminum nitrate at 135°C, progressive hydrolysis occurs which results in the formation of Al-containing polymeric species. Under a DOE-funded program, MTI and NWU had performed a systematic study of the decomposition kinetics of aluminum nitrate as a function of time of pyrolysis. Characterization of aluminum coordination in the polymeric species by  $^{27}\text{Al}$  NMR showed the presence of varying amounts of 4- and 6-coordinated aluminum. With increasing degree of hydrolysis or decomposition of aluminum nitrate, the intensity of the tetrahedral aluminum peak in the NMR increased. Typically, no tetrahedrally coordinated aluminum was found for polymer residues corresponding to 37 weight percent of the initial amount. The 4-fold coordinated aluminum was present in the form of the Al-13 Keggin ion (three 4-fold tetramers coordinated to one central octahedrally coordinated aluminum atom) and most of the 6-fold coordinated aluminum was present as monomeric species. The ratio of 4- to 6-fold coordinated aluminum species depended on the extent of the hydrolysis/decomposition. Since the mullite structure incorporates both the 4- and 6-fold coordinated aluminum atoms, it was considered useful to explore the influence of Al-coordination in the precursor on mullite formation.

MTI prepared alumina polymer precursors by decomposing the aluminum nitrate by 70% (4 and 6 fold aluminum), 74.1% (intermediate polymer) and 61.6% (only 6-fold aluminum) weight loss. These residual powders were redissolved in DI water and stoichiometric amounts of TEOS and methanol were added to form a homogeneous miscible solution. The mixture was then decomposed further to promote Al-Si mixing.

For all the mullite precursors, the DTA showed a sharp exotherm around 970°C. X-ray diffraction analysis was used to explore whether this exotherm corresponded to aluminum-rich mullite or the desired 3/2 mullite. The main difference in the X-ray diffraction pattern lies with the peak near 26 deg ( $\text{CuK}\alpha_1$  radiation). In aluminum-rich mullite, there is one single peak, and with 3/2 mullite, the peak is split, as the crystalline symmetry decreases from tetragonal to orthorhombic. Two heat treatments were run for each precursor: 975°C for 1 hour, and 1100°C for 1 hour. After anneal at 975°C for 1 hour, the precursor formed by 70% decomposition has a single peak, while for the 61.6% decomposed precursor, the peak appears to be splitting. After 1100°C, 1h anneal, the splitting of the peaks is more dramatic (**Figure 27**). The 70% decomposed precursor shows a single peak, while the peak for the 61.6% precursor shows a greater degree of splitting, indicating a greater degree of transformation to 3/2 orthorhombic mullite. These results were opposite of what we had expected given the difference in aluminum coordination for the two MTI alumina polymer precursors that were used for these mullite precursors. However, there is a significant difference between the results obtained here

compared to a recently reported study where aluminum nitrate and TEOS were decomposed together which resulted in a diphasic precursor yielding 3/2 mullite only at 1300°C [11]. Thus the formation of alumina polymer prior to mixing with TEOS appears to be an important intermediate step, but formation of Keggin ion does not appear to promote the formation of the 3/2 mullite.

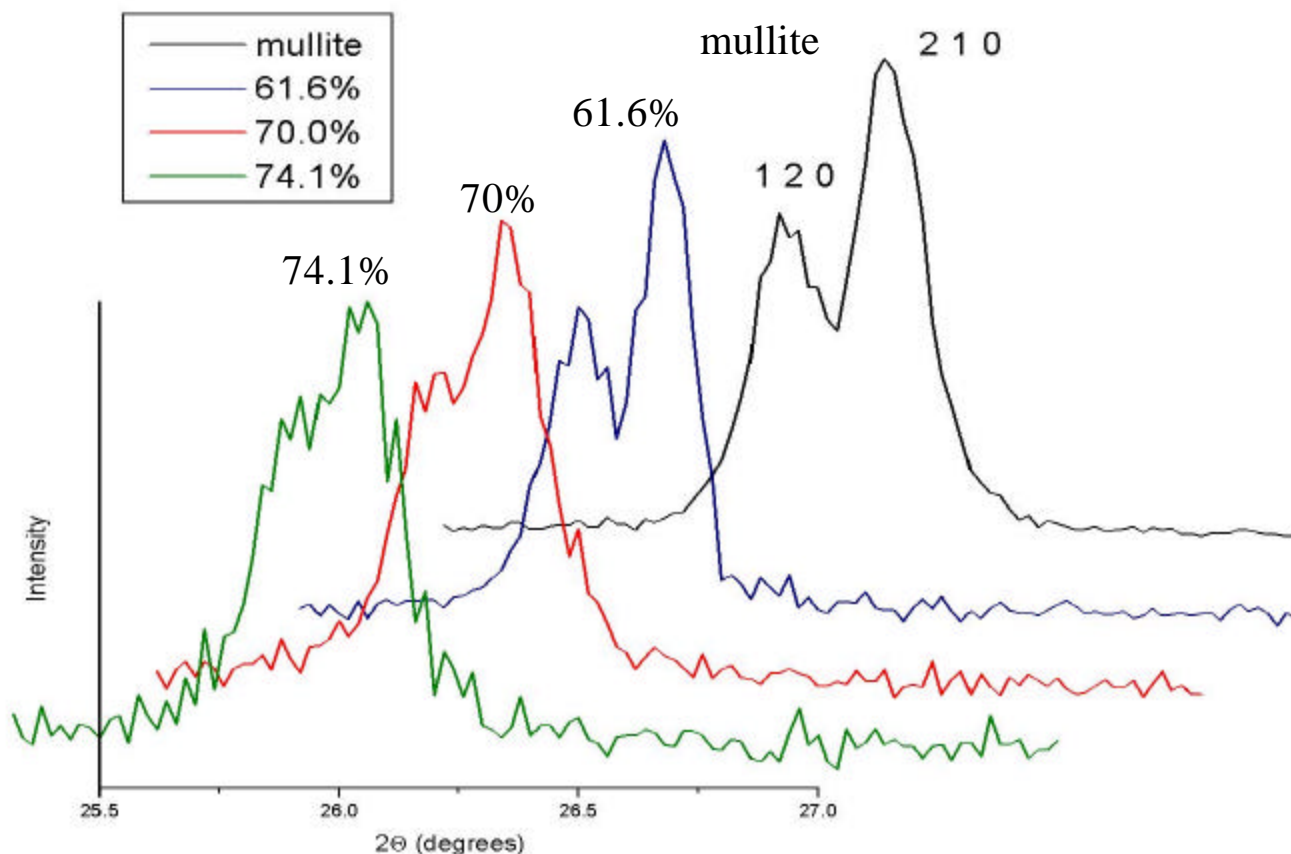


**Figure 27.** XRD curves near  $26^\circ 2\theta$  for the mullite precursor formed from different levels of decomposed MTI alumina polymers.

Single fibers were dip coated with a mullite precursor and heated to 1000°C and 1100°C for one hour. The mullite precursor severely degraded the strength of the Nextel 610 fibers; the fibers were essentially too weak to test. Based on these fiber strength results, this mullite precursor was not considered for use in densifying CMCs under this program.



### Silica Precursors

McDermott investigated the use of a colloidal silica to densify the CMCs. A colloidal silica from Aldrich Chemical, SM-30 Ludox was chosen. SM-30 is 30 weight percent silica with a pH of 10 and it contains a sodium stabilizing counterion. The coated fibers were heat-treated to 1000°C and 1100°C for one hour. The resulting Weibull plots of the fiber strengths are shown in **Figure 28**. The strength retention of fibers coated with colloidal silica is very good up to 1000°C, but drops substantially after 1100°C heat-treatment. An attempt was made to use the colloidal silica to further densify a CMC that had been pressure cast with alumina. It proved to be a poor infiltrant for CMC processing because of a tendency to gel on the outside of the CMC. Very poor weight gain was observed for repeated infiltration attempts with the colloidal silica.

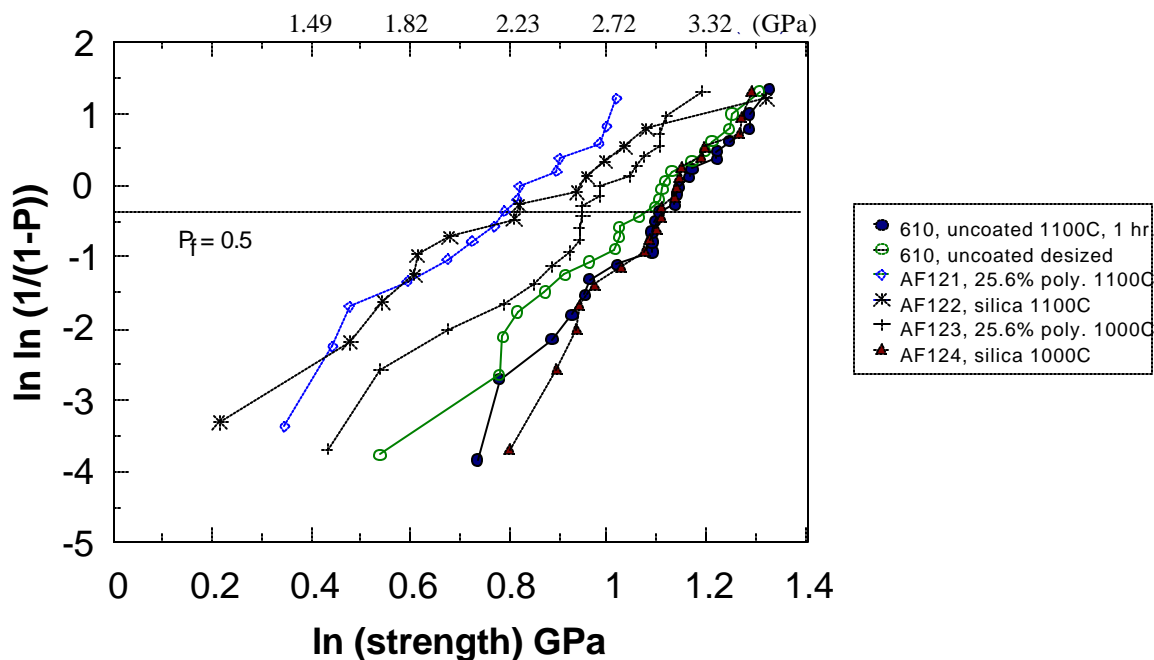


**Figure 28.** Strength of Nextel 610 fibers coated with colloidal silica and MTI (25.6% decomposed) alumina polymer precursor and heat-treated at 1000°C and 1100°C.

Additional work was performed to select an appropriate silicon based polymer for use in densifying the CMCs following the initial pressure casting operation with alumina powder. It was expected that the silicon-based polymers would not have difficulty infiltrating the preform, as did the colloidal silica. A polysiloxane polymer was chosen. A vinyl cure system was chosen using polymethylhydrosiloxane (Gelest cat. No. HMS-991) and vinylmethoxysiloxane (Gelest cat. No. VMM-010) with a platinum catalyst (Gelest cat. No. SIP6830.0). The siloxanes were mixed in a ratio of 1.5:1 polymethylhydrosiloxane to vinylmethoxysiloxane with a loading of

0.07 parts catalyst to 100 parts vinylmethoxysiloxane). The siloxanes were chosen to minimize the amount of carbon in the polymer and to maximize the amount of oxygen. This polymer had a silica yield of 81 weight percent and approximately 37 volume percent yield. This formulation was used to successfully densify the first round CMCs fabricated under this program for mechanical property evaluation (further described under Task 3).

### **Applied Thin Film's CeraBlak™ Precursor**

ATFI has developed an aluminum-phosphate based precursor that yields a substantially amorphous material upon thermal decomposition. The material remains amorphous at temperatures up to 1300°C. The precursor can be either alcohol or aqueous based and can be formulated to yield a high volume fraction yield of solids. The precursor was shown to exhibit the best strength retention for Nextel 610 fibers of any of the precursor evaluated under this program (see *Figure 29*).

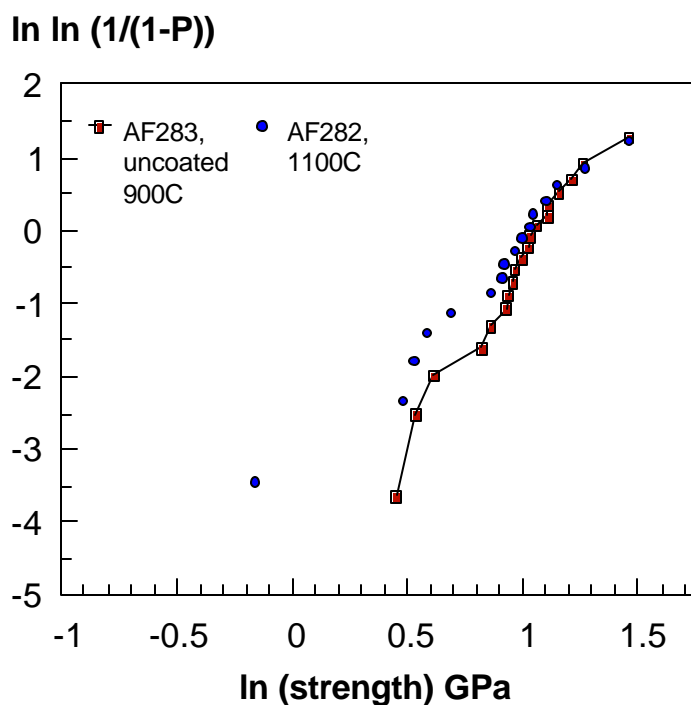


*Figure 29.* Strength retention for Nextel 610 fibers coated with CeraBlak™ precursor.

### **Task 3 – Composite Processing and Properties – First Series of CMCs**

Three series of CMC panels were fabricated during the program at various stages of scheelite and matrix precursor development. A description of the composites fabricated and the resulting mechanical properties is described in the following sections. All of the composites were unidirectionally reinforced with Nextel 610 fiber and the initial matrix densification was achieved by pressure casting an alumina slurry. Subsequent matrix densification was achieved by vacuum/pressure infiltration using various matrix precursors.

#### **First Series of CMCs**

CMCs were fabricated using fibers from three different coating runs and were densified with three different matrix precursors. The coatings were deposited using two different batches of MTI precursor formulated from W-metal in  $H_2O_2$  plus calcium formate and one batch of scheelite precursor from Applied Thin Films that is based on tungsten ethoxide and calcium nitrate in ethanol. The strength of the fibers was measured at various heat treatments in order to determine a suitable heat treatment temperature for the composite while avoiding severe degradation of the fiber strength. A summary of the coated fibers used in this series of CMCs and their strength retention is presented in **Table 6**. The diffraction patterns are shown in **Figures 30 through 32**. All of the precursors showed a slight calcium-rich nonstoichiometry as indicated by the  $I_{60}$  peak for  $Ca_3WO_6$  located at about  $22^\circ 2\theta$ . It is unknown whether any of the precursor contained any phosphorous impurities as had been observed in the past with MTI precursor based on ammonium tungstate and ammonium metatungstate.

**Table 6.** Description of  $CaWO_4$  coated fibers.

<b>Fiber Coating Identification</b>	<b>Description</b>	<b>Strength Retention Avg. strength (GPa)/Temp. (C°)</b>
AF279	MTI, W-metal/ $H_2O_2$ + Ca-formate	As-coated/3.45 900°C/3.42 1000°C/2.34 1100°C/1.06
AF282	NWU, W-ethoxide/EtOH + Ca-nitrate	900°C/2.76 1000°C/2.44 1100°C/1.61
AF287	MTI, W-metal/ $H_2O_2$ + Ca-formate (formulated as Ca-deficient)	900°C/2.49 1000°C/2.03 1100°C/0.95

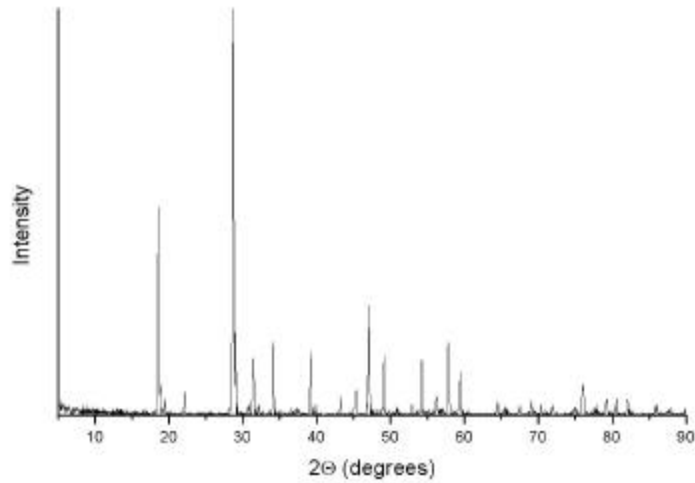


**Figure 30.** X-ray diffraction analysis of NWU scheelite precursor (AF284)

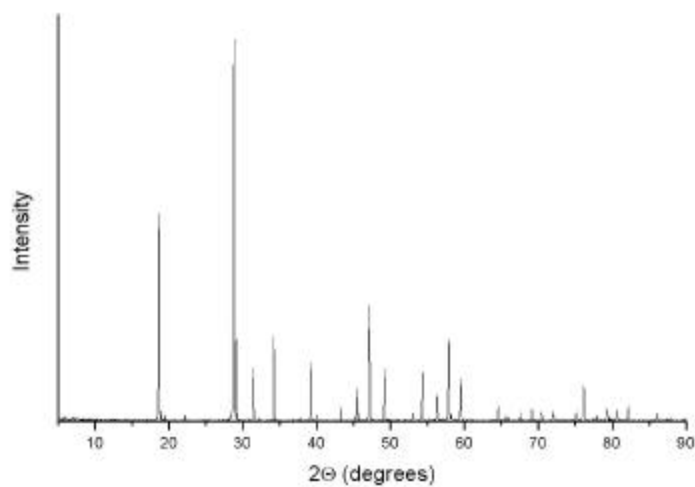


**Figure 31.** X-ray diffraction analysis of MTI scheelite precursor AF279.

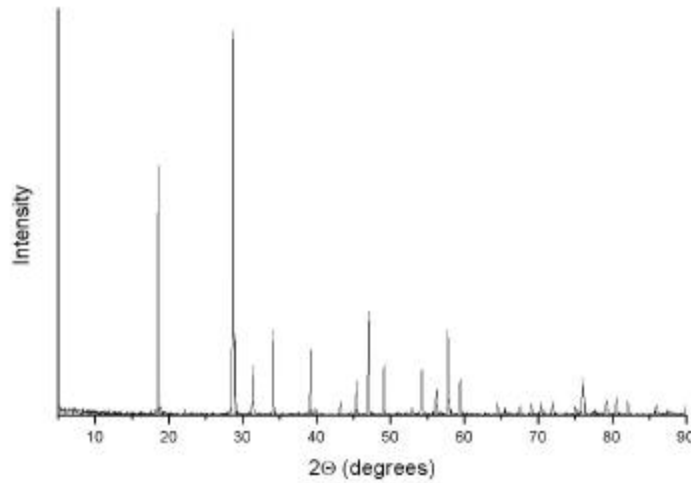


**Figure 32.** X-ray diffraction analysis of MTI scheelite precursor AF287.

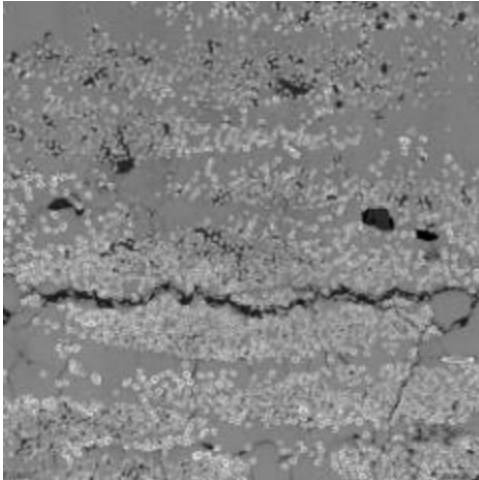
A description of the unidirectional composites fabricated from the three batches of scheelite coated fiber is given in **Table 7**. The fiber volume fraction of the composites has not been measured. Because of inconsistency in the compression of the fiber preform during the alumina pressure casting step, there was significant differences in the fiber volume fraction of the composites. A qualitative assessment of the fiber volume fraction for each composite is given in the table.

**Table 7.** Description of Series 1 unidirectional CMCs

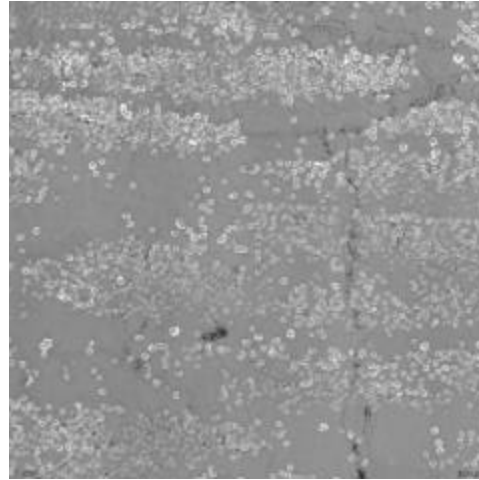
<b>Fiber Coating – Sample ID</b>	<b>Sol-gel Matrix</b>	<b>CMC Residual Porosity (%)</b>	<b>Fiber Volume Fraction</b>
AF279-1	MTI alumina	20.1	Medium
AF279-2	NWU proprietary	20.0	Medium
AF279-3	Polysiloxane	14.8	Medium
AF284-1	MTI alumina	17.9	High
AF284-2	NWU proprietary	17.7	High
AF284-3	Polysiloxane	9.6	High
AF287-1	MTI alumina	21.8	Low
AF287-2	NWU proprietary	20.2	Low
AF287-3	Polysiloxane	13.7	Low

The resulting microstructures for the three CMCs made from each batch of coated fiber are shown in **Figures 33 through 35**. **Figure 36 through 38** are at higher magnification and show the quality of the scheelite fiber coatings. The coatings derived from the MTI precursors

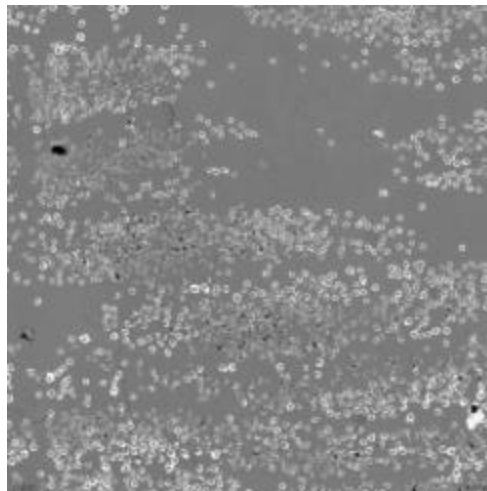
are thicker and appear to have better coverage of the fibers than the coatings obtained with the NWU precursor. The MTI precursor was a higher yielding precursor, which may explain the difference in the coating quality.



Alumina Polymer Matrix, 20% CMC porosity

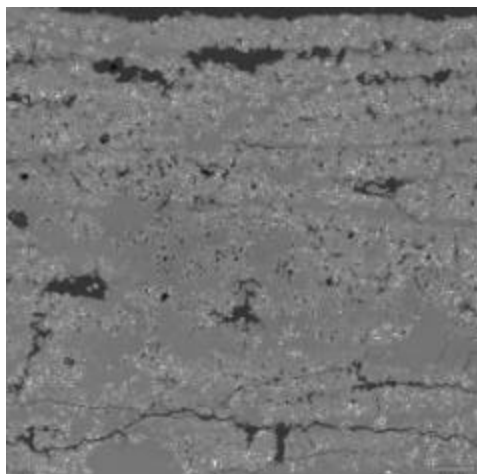


AIPON Matrix, 20% CMC porosity

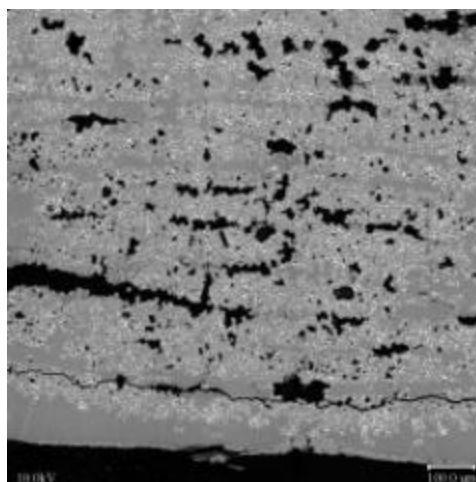


Silica Matrix, 14.8% CMC porosity

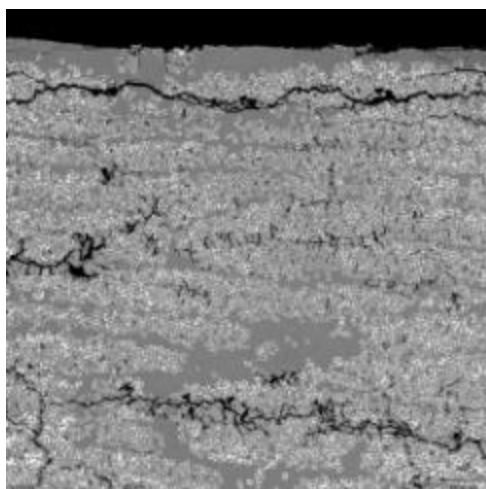
**Figure 33.** Microstructures of CMCs with  $\text{CaWO}_4$  coating AF279 (MTI precursor)



Alumina Polymer Matrix,  
17.9% CMC porosity

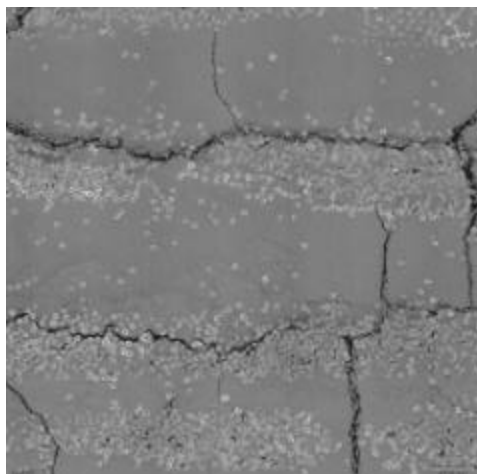


AIPON Matrix, 17.7% CMC porosity

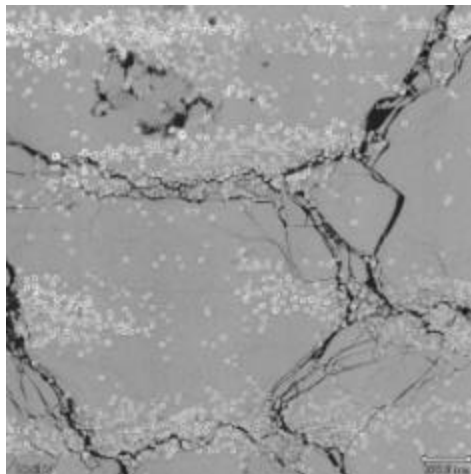


Silica Matrix, 9.6% CMC porosity

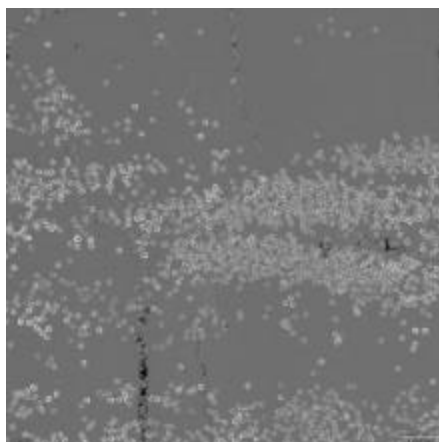
**Figure 34.** Microstructures of CMCs with  $\text{CaWO}_4$  coating AF284 (ATFI precursor)



Alumina polymer matrix, 21.8% CMC porosity



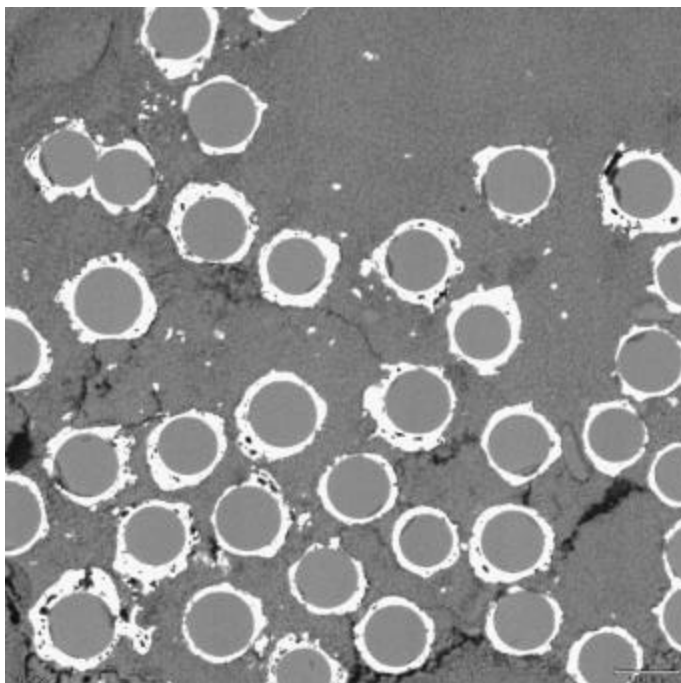
AIPON Matrix, 20.2% CMC porosity



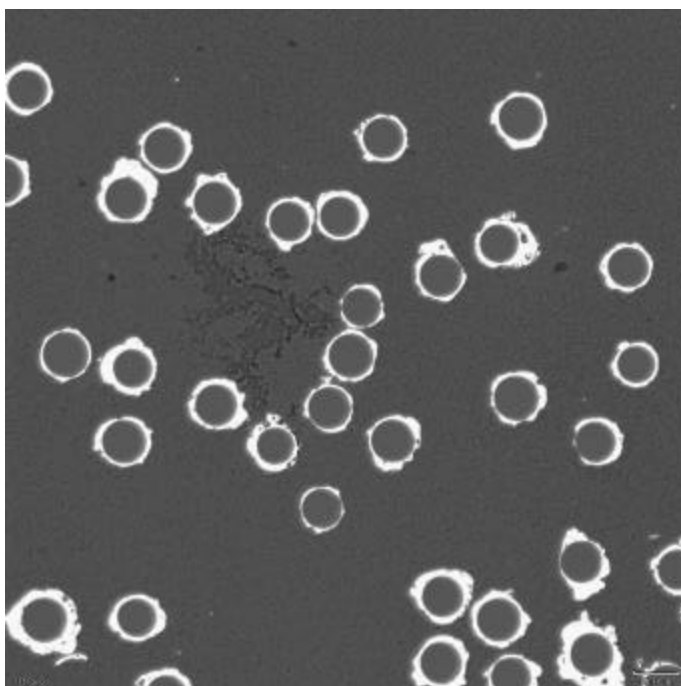
Silica Matrix, 13.7% CMC porosity

**Figure 35.** Microstructure of CMCs with  $\text{CaWO}_4$  coating AF287 (MTI precursor)



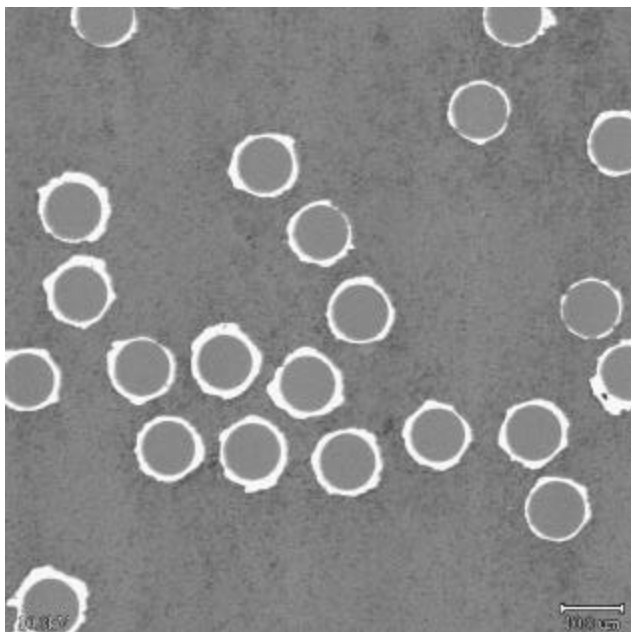


Alumina polymer matrix, 20.1%  
CMC residual porosity

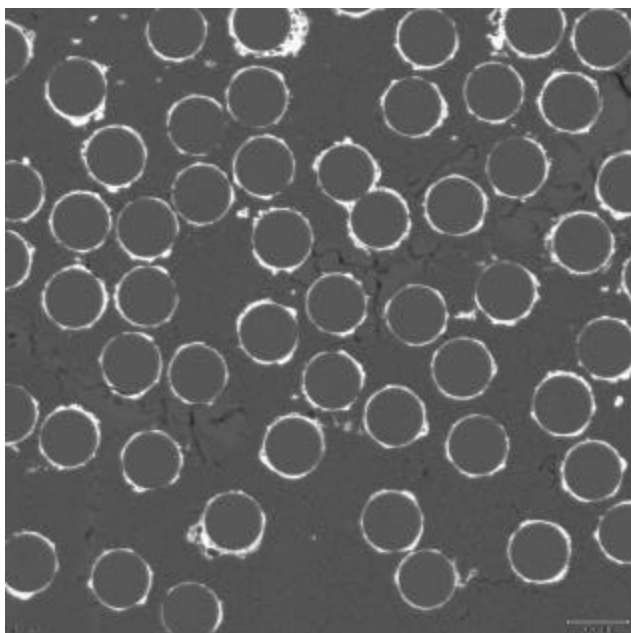


Silica Matrix, 14.8% CMC  
residual porosity

**Figure 36.**  $\text{CaWO}_4$  coatings (AF279) from MTI precursor based on W-metal/ $\text{H}_2\text{O}_2$  and calcium formate.

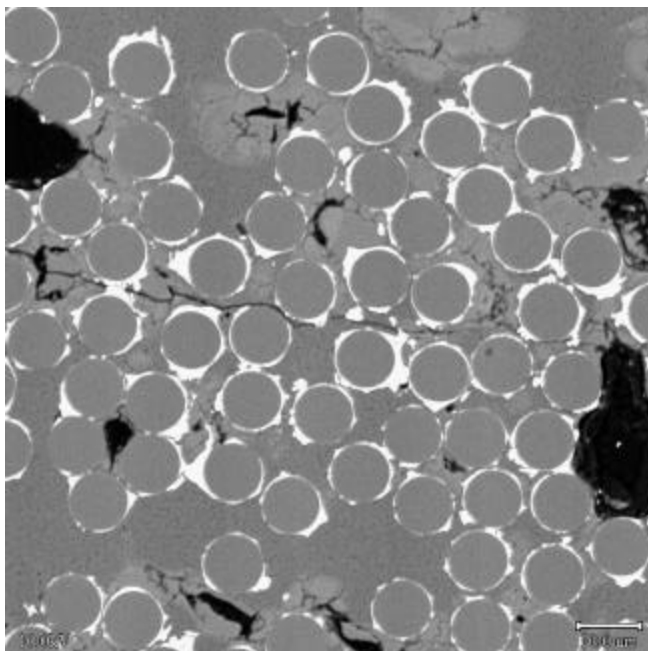


AIPON Matrix, 20.2%  
CMC residual porosity

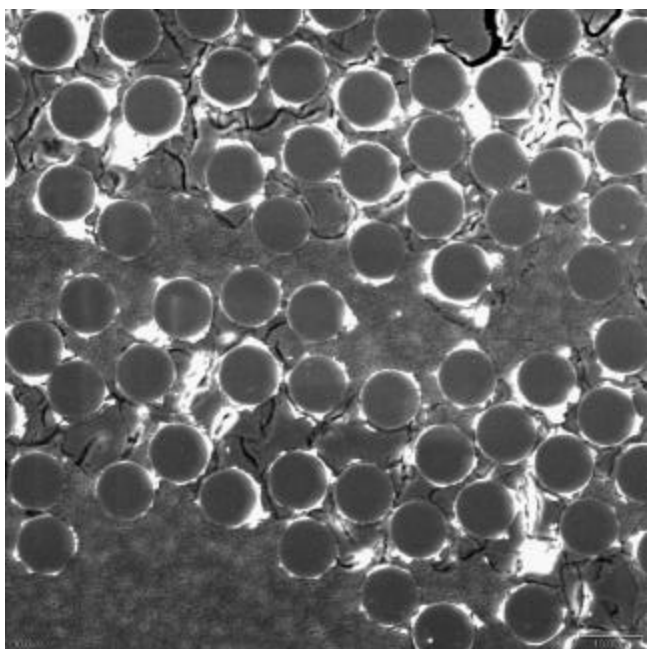


Silica Matrix, 13.7% CMC  
residual porosity

**Figure 37.**  $\text{CaWO}_4$  coatings (AF287) from MTI precursor based on W-metal/ $\text{H}_2\text{O}_2$  and calcium formate (formulation based on a slight calcium deficiency)



AIPON Matrix, 17.7% CMC  
residual porosity



Silica Matrix, 9.6% CMC  
residual porosity

**Figure 38.**  $\text{CaWO}_4$  coatings (AF282) from ATFI precursor

CMC specimens were initially tested in an edge notched configuration (a/W ratio of about 0.25) to try to insure gage failures. Testing of the notched specimens was performed at McDermott and Virginia Tech. Some un-notched specimens were also tested at Virginia Tech and at the Air Force Wright Labs. *Table 8* summarizes the mechanical test results. Testing at

MTI was performed under displacement control at 0.008 mm/sec. Testing at Virginia Tech was performed under load control at 178 N/sec. Testing at Air Force Wright Labs was performed under displacement control at 0.05 mm/sec.

**Table 8.** Summary of notched and un-notched strengths of initial series of CMC samples. Data for individual room temperature tests is shown.

Sample	Coating Precursor	Sol-Gel Matrix	Fiber Volume	Residual Porosity	MTI Tested Strength/Strain notched, MPa	Virginia Tech. Strength/Strain notched, MPa	AFWL Tested Strength/Strain unnotched, MPa	Virginia Tech. Strength/Strain unnotched, MPa
AF279-1	W-metal/Ca-formate	alumina	medium	20.10%	167 0.26%	162 0.26% 93 0.14% 77 0.21%	288 0.44% 247 0.41%	
-2		ATFI CeraBlak	medium	20.00%	226 0.29%	183 0.20% 185 0.17% 99 0.08%	254 0.40% 277 0.36%	
-3		silica	medium	14.80%	157 0.11%	148 0.18% 147 0.09% 71 0.07%	274 0.37% 274 0.35%	
AF284-1	W-ethoxide/Ca-nitrate	alumina	high	17.90%	177 0.12%		358 0.21% 376 0.23% 473 0.29% 428 0.25%	315 0.19% 361 0.23% 491 0.29% 500 0.29%
-2		ATFI CeraBlak	high	17.70%	226 0.24%			445 0.27%
-3		silica	high	9.60%	114 0.13%		276 0.21% 216 0.17%	
AF287-1	W-metal/Ca-formate	alumina	low	21.80%	105 0.20%			
-2	(Ca deficient)	ATFI CeraBlak	low	20.20%	70.3 0.10%			
-3		silica	low	13.70%	63.4 0.04%			

The notched strengths were generally significantly lower than the un-notched strengths. The composites densified with the polysiloxane generally seemed to show somewhat lower strengths. The most interesting data to compare are the AF279 and AF284 un-notched data tested at AFWL and Virginia Tech. Greater strain-to-failure was observed for the CMC having the scheelite coatings that were deposited using MTI's W-metal/Ca-formate peroxide based precursor (AF279 series) regardless of which final matrix precursor was utilized for final composite densification. The strength and the modulus of the CMC's with the ATFI alkoxide based precursor were higher. The modulus of the AF284 (ATFI scheelite coating) series was approximately 162 GPa versus 97.1 GPa for the AF279 (MTI scheelite coating) series, owing primarily to the obvious higher volume fraction of Nextel 610 fibers of the AF284 series (compare **Figures 39 and 40**). Representative stress-strain curves of the un-notched AF279 series are shown in **Figure 39**. A representative stress-strain curve of an un-notched AF284 CMC with the alumina-CeraBlak<sup>TM</sup> duplex matrix is shown in **Figure 40**. A possible cause for the more linear stress-strain curve of the AF284/alumina-CeraBlak<sup>TM</sup> CMC compared to the AF279/alumina-CeraBlak<sup>TM</sup> CMC may be that the scheelite coatings deposited from the ATFI alkoxide based precursor were not as thick nor as continuous in coverage as those obtained from the MTI precursor. As a result, the AF284 series of CMCs may behave a bit more like a CMC without fiber coatings. The thinner and less uniform nature of the ASF284 coatings was confirmed through TEM analysis by the AFRL. Both the AF279 and AF284 scheelite coatings were not hermetic and some matrix had infiltrated the coating pore space.

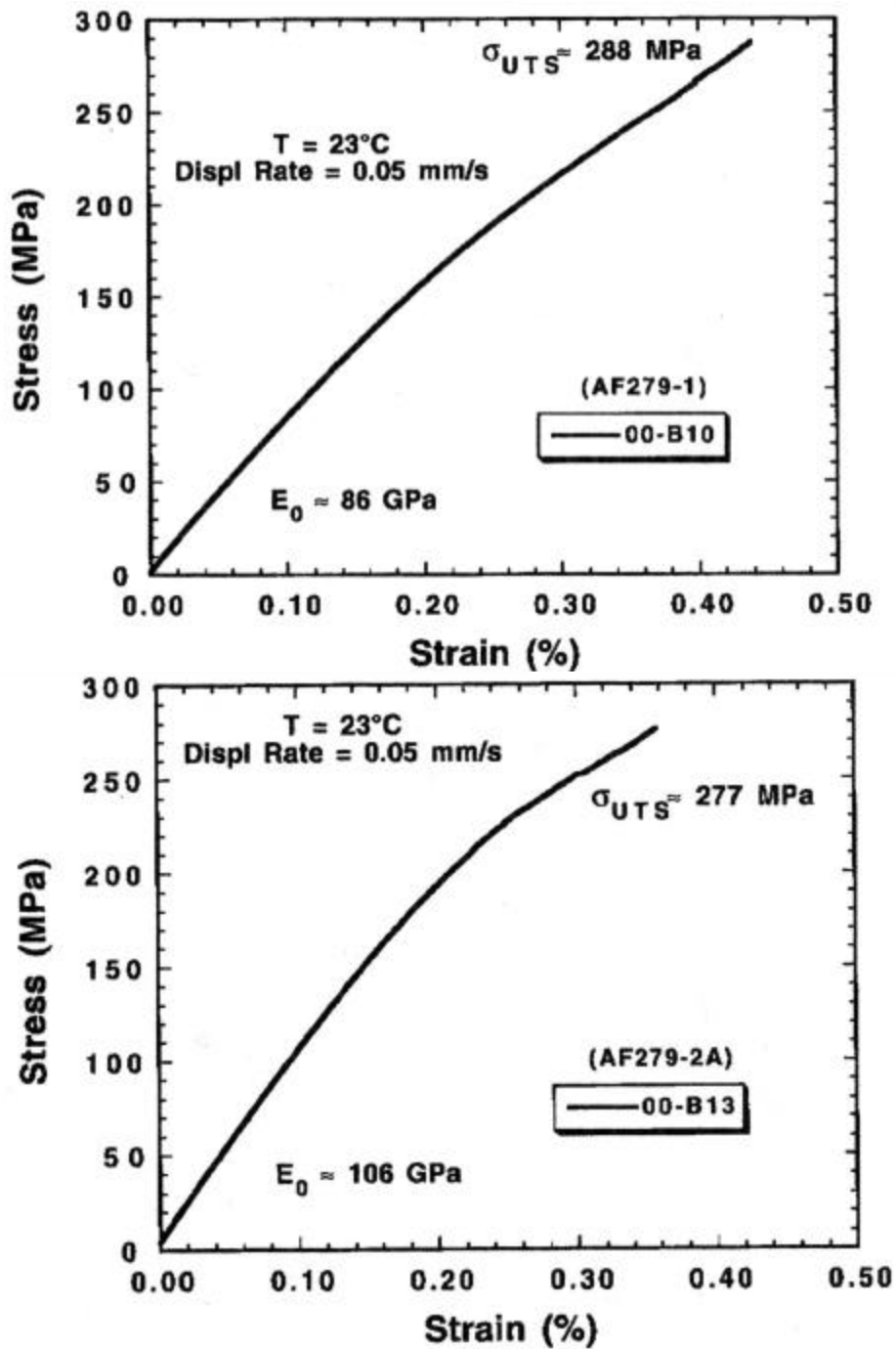


**Figure 39.** Stress-strain curves of AF279 CMCs with MTI W-metal/Ca-formate peroxide derived  $\text{CaWO}_4$  fiber coatings in an all alumina matrix (top) and alumina-CeraBlak<sup>TM</sup> duplex matrix (test performed by AFWL).

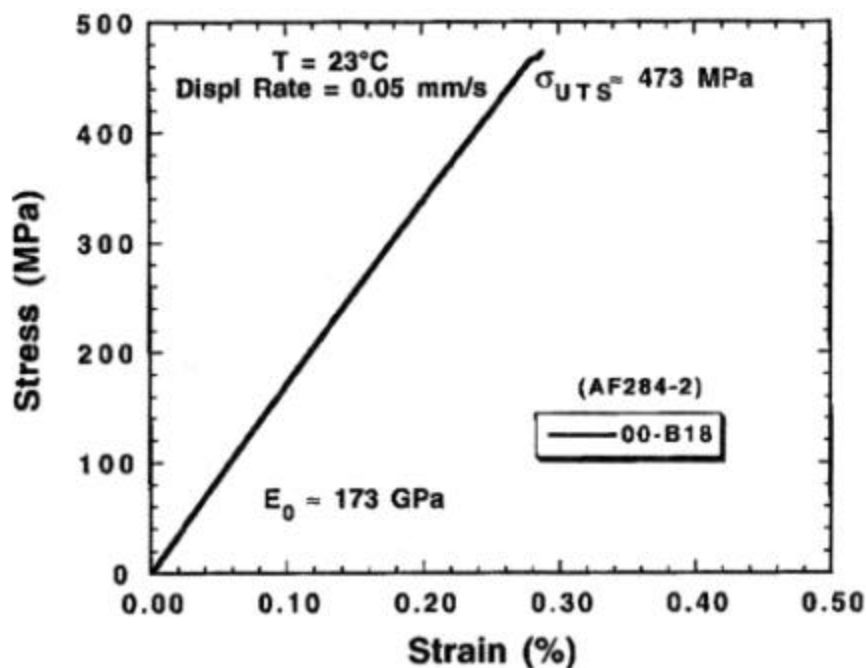


**Figure 40.** Stress-strain curves of AF284 CMCs with ATFI alkoxide precursor derived  $\text{CaWO}_4$  fiber coatings in an alumina-CeraBlak<sup>TM</sup> duplex matrix (test performed by AFWL).

SEM examination was performed of the fracture surfaces of the following samples:

- AF279-1/MTI scheelite coating/all alumina matrix
- AF279-2/MTI scheelite coating/alumina-CeraBlak<sup>TM</sup> duplex matrix
- AF279-3/MTI scheelite coating/alumina-silica duplex matrix from polysiloxane
  
- AF284-1/ATFI scheelite coating/all alumina matrix
- AF284-3/ATFI scheelite coating/alumina-silica duplex matrix from polysiloxane

The fracture surfaces are shown in the following figures. All of the samples show a large amount of debonding along the scheelite fiber coating indicating the desired functionality of the scheelite coating. The non-linear nature of the stress-strain curves for the AF279 series of CMCs also suggests the desired functioning of the scheelite coating. This first series of CMCs was missing a control CMC with uncoated fiber, but co-processed with CMCs containing the various scheelite coatings. As a result, it was impossible to draw firm conclusions about the functioning of the fiber coating. Such baseline control CMC specimens were included in additional rounds of CMCs fabricated under this program.

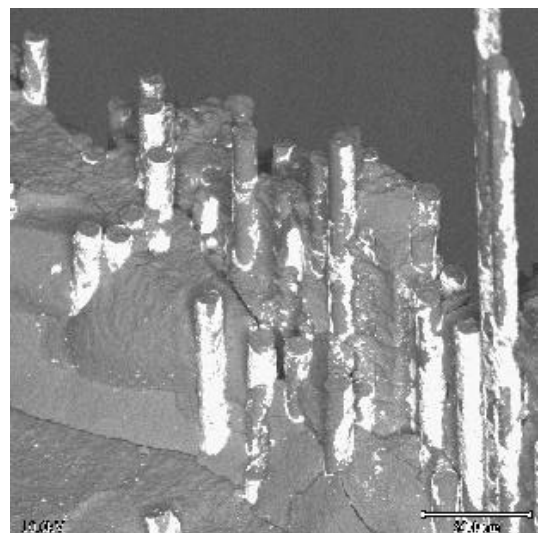
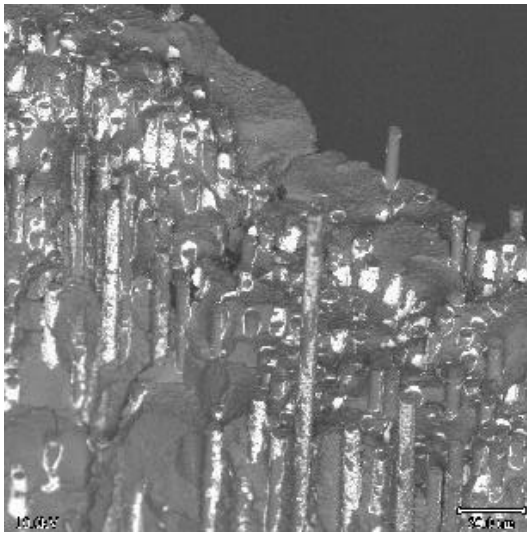
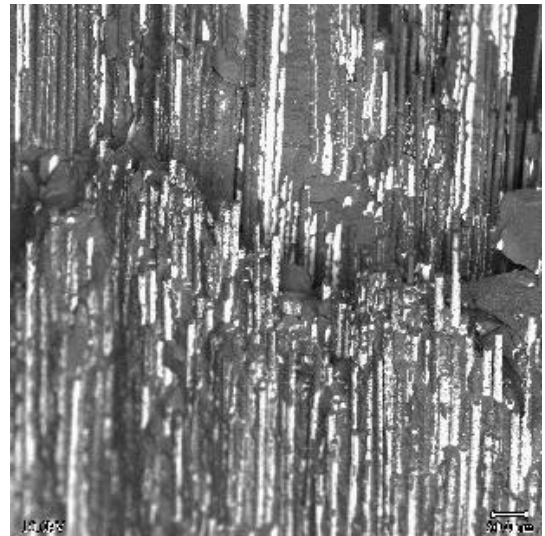
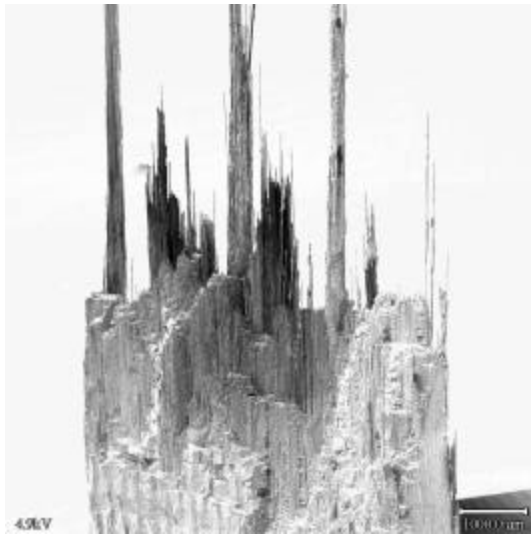


**Figure 41.** Fracture surface of AF279-1 CMC with  $\text{CaWO}_4$  coatings from MTI precursor in an all alumina matrix

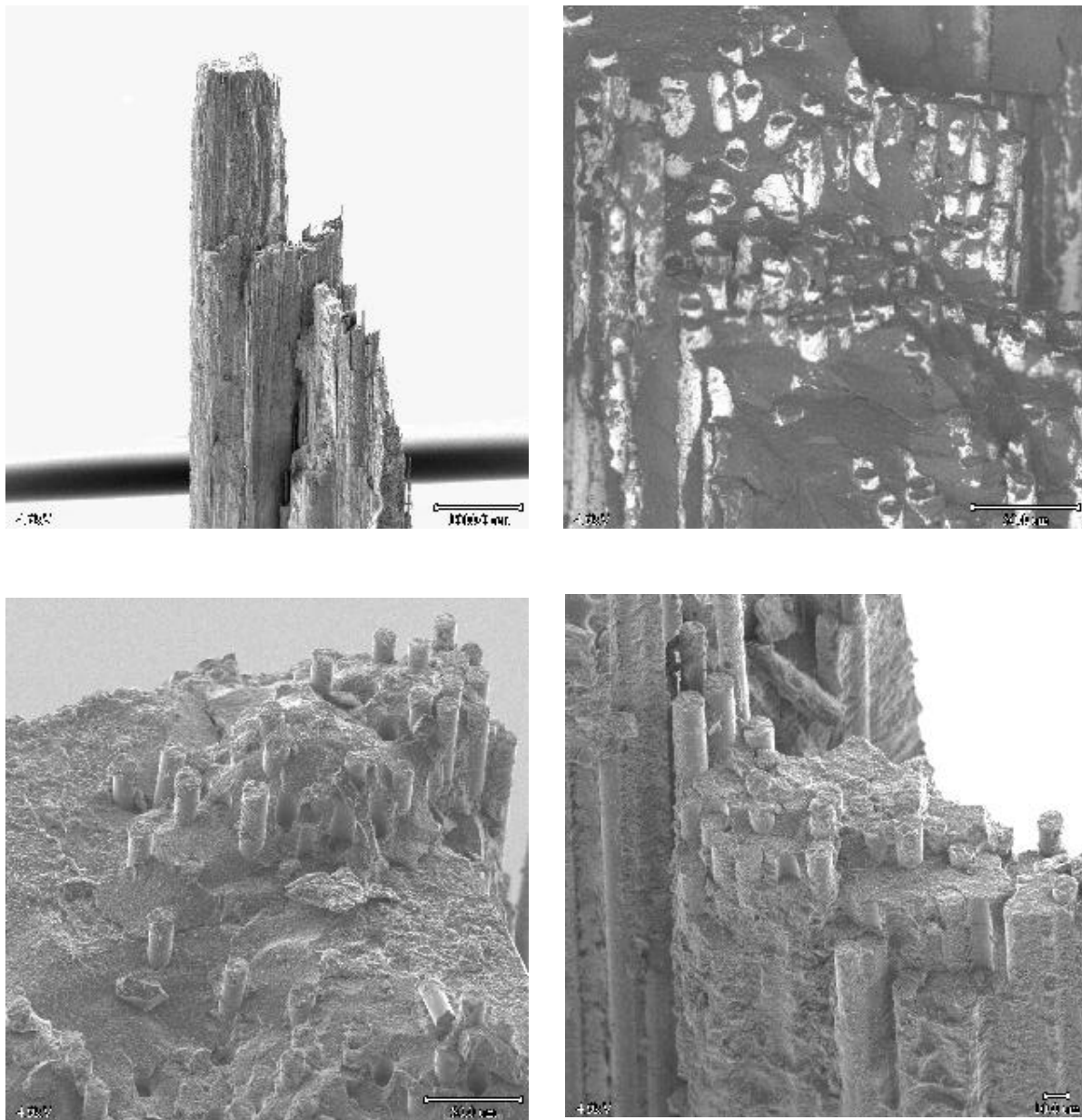


**Figure 42.** Fracture surface of AF279-2 CMC with  $\text{CaWO}_4$  coatings from MTI precursor in an alumina-CeraBlak<sup>TM</sup> duplex matrix.



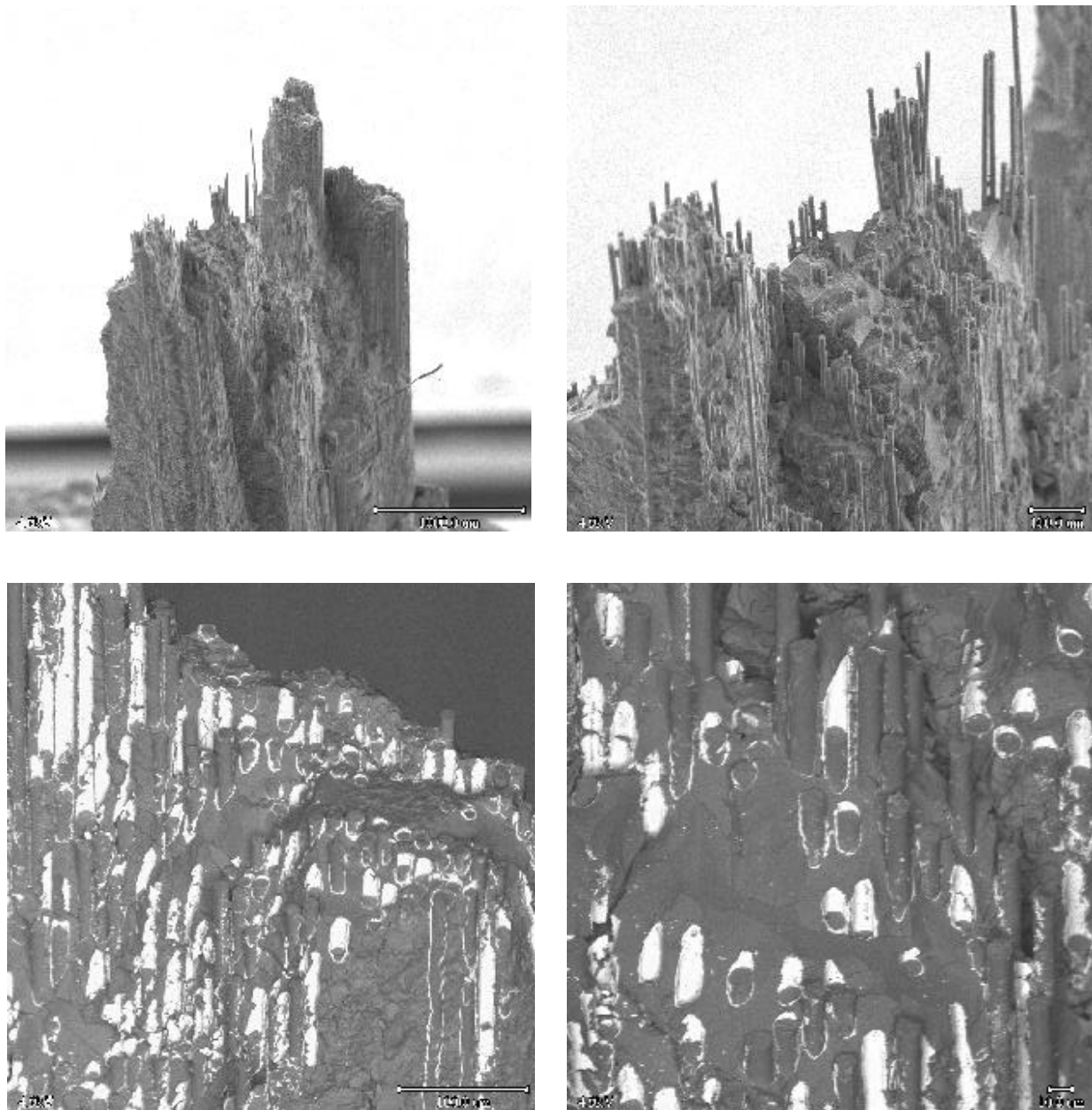


**Figure 43.** Fracture surface of AF279-3 CMC with  $\text{CaWO}_4$  coatings from MTI precursor in an alumina-silica duplex matrix from polysiloxane.

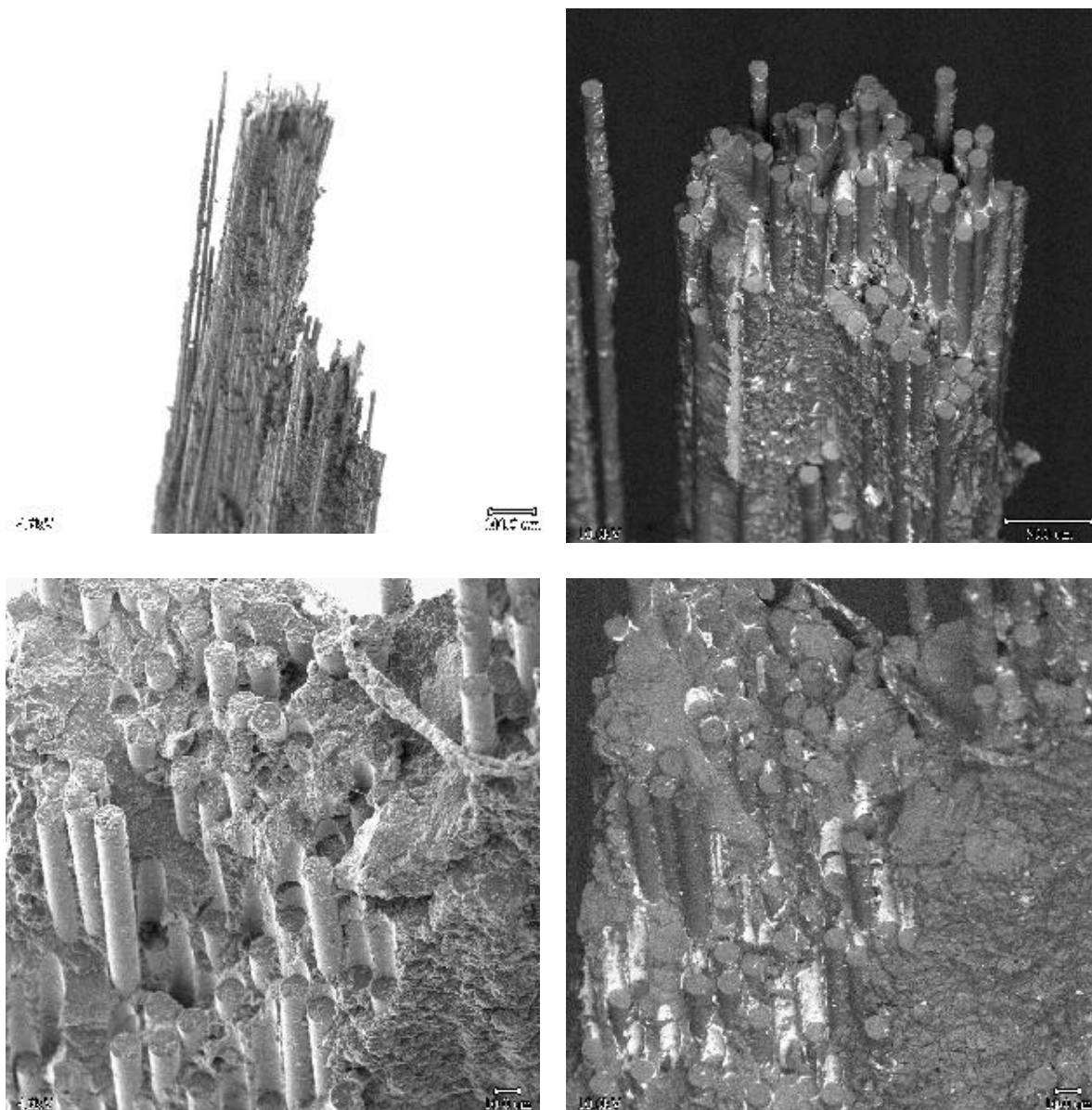


**Figure 44.** Fracture surface of AF284-1 CMC with  $\text{CaWO}_4$  coatings from ATFI precursor in an all alumina matrix.

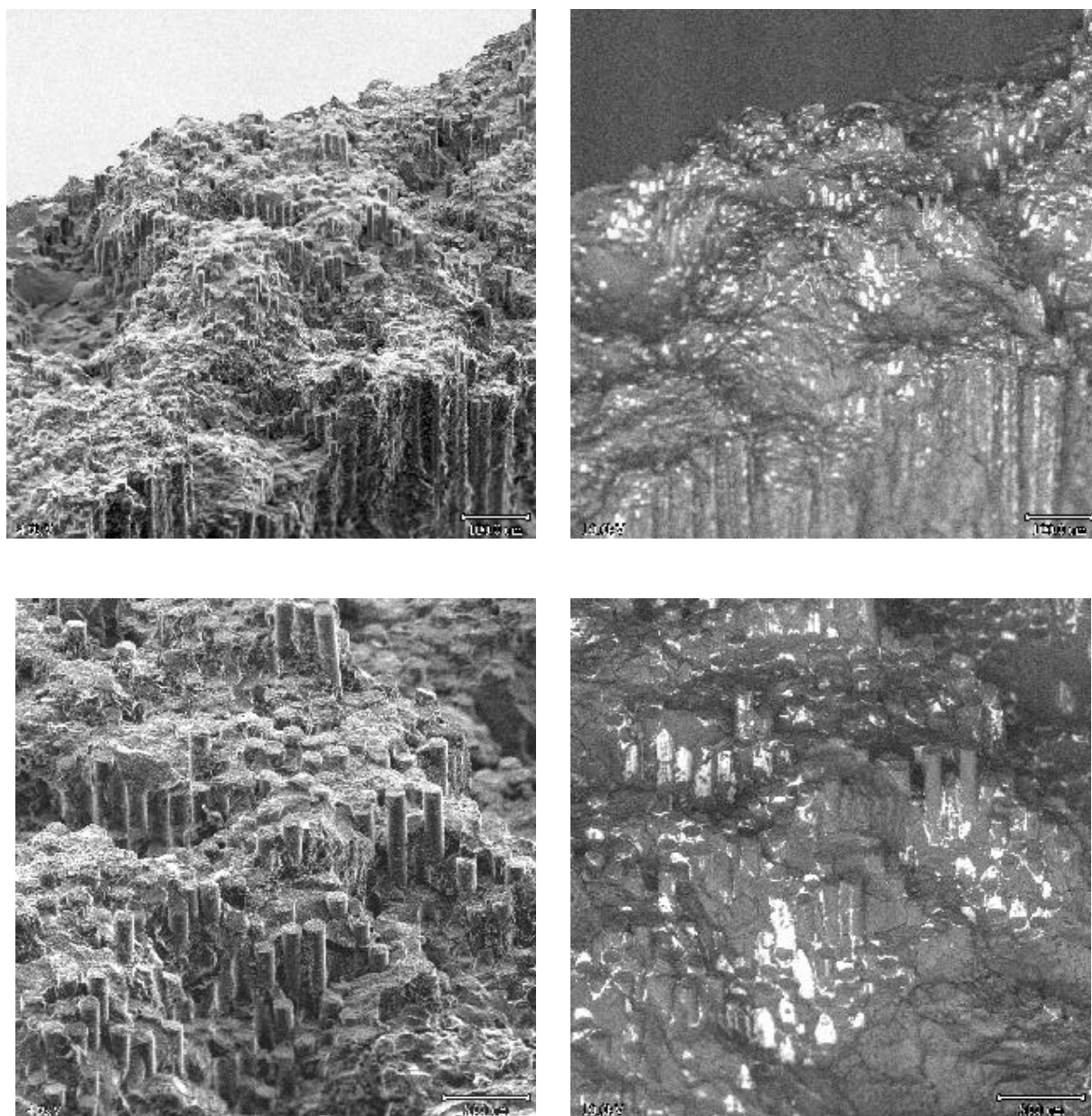


**Figure 45.** Fracture surface of AF284-3 CMC with  $\text{CaWO}_4$  coatings from ATFI precursor in an alumina-silica duplex matrix from polysiloxane.

### **Task 3 – Composite Processing and Properties - Second Series of CMCs**

Based on the promising strengths observed for the first round of CMCs that incorporated scheelite fiber coatings deposited from the ATFI alkoxide based precursor, we initially intended to use similar coatings for this second round of CMC test specimens. A large batch (4 liters) of coating precursor was received from ATFI. The xray diffraction pattern for powder derived from the precursor is shown in **Figure 46**. There is only a very minor peak for  $\text{Ca}_3\text{WO}_6$  present at about  $22.2^\circ 2\theta$  (this is an  $I_{65}$  peak, the  $I_{100}$  peak at  $31.5^\circ 2\theta$  overlaps with a  $\text{CaWO}_4$  peak).

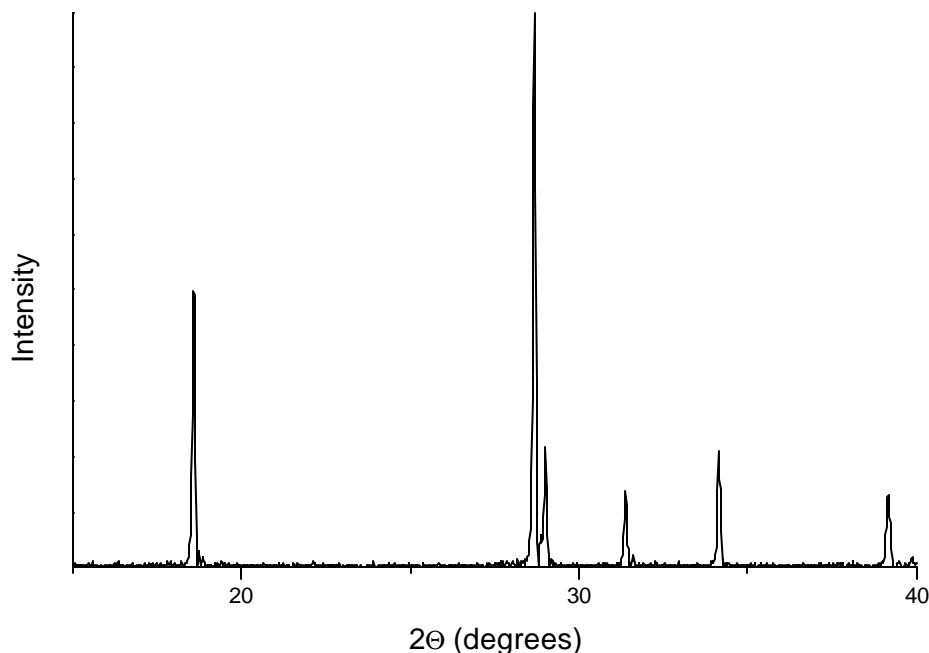


**Figure 46.** X-ray diffraction pattern for powder derived from the ATFI coating precursor

Nextel 610 fiber was coated with the precursor using MTI's continuous fiber coater. The coated fiber was obtained from three different spools of fiber (core numbers 19:54Q, 1:10S and 11:40Q). Coating of the fiber extended over a two day period. The coated fiber was accumulated onto seven spools (labeled A through G) during the coating operation. Following the coating operation, uncoated fiber from the three source spools and coated fiber from each take-up spool was heat-treated at  $1000^\circ\text{C}$  for one hour. The resulting single fiber strengths (measured by ATFI) are provided in **Table 9**.

**Table 9. Strength of coated and uncoated Nextel 610 fiber (tested at ATFI).**

<b>Fiber Condition</b>	<b>Source Spool ID</b>	<b>Avg. Strength (GPa)</b>
Uncoated	Core no. 19:54Q	2.9
Uncoated	Core no. 1:10S	2.97
Uncoated	Core no. 11:40Q	2.46
Coated – spool A	Core no. 19:54Q	1.65
Coated – spool B	Core no. 1:10S	1.87
Coated – spool C	Core no. 1:10S	1.66 (as-coated strength = 3.0)
Coated – spool D	Core no. 1:10S	2.17 as-coated strength = 3.1)
Coated – spool E	Core no. 11:40Q	2.00
Coated – spool F	Core no. 11:40Q	2.16
Coated – spool G	Core no. 11:40Q	2.10

During the coating process, precipitate accumulated in the precursor reservoir. Some precipitate is expected to occur from the breaking of coating bridges as the coated fiber tow repeatedly passes over the rollers of the fiber coater. There seemed to be a larger than expected amount of precipitate accumulating the precursor reservoir. X-ray diffraction analysis was performed on the precipitate following a heat treatment to 1000°C. The powder exhibited a very large amount of WO<sub>3</sub>. This would indicate that the coatings deposited onto the fibers are significantly nonstoichiometric. Based on the x-ray diffraction and single fiber tensile test results, it was decided not to use the fiber coated with the ATFI precursor for composite fabrication.

For this second round of CMCs to be processed and tested, it was decided to use Nextel 610 fibers coated with the MTI scheelite precursor that utilized W-metal and calcium formate in a peroxide solution. That precursor has shown good stability over the time frames required to coat large quantities of fiber. Prior to formulating the scheelite precursors a investigation was performed into the possible source of phosphorous contamination that has been observed on fibers coated from these precursors. Phosphorous analysis was performed at Northwestern University on the calcium formate and tungsten metal raw materials by UV-VIS colorimetry. Tungsten powders were heat-treated at 900°C for 2 hours in a vacuum furnace in the hopes of volatilizing any phosphorous containing species that may be present. The results are shown in **Table 10**.

**Table 10. Results of phosphorous chemical analysis on scheelite precursor raw materials.**

Date	Material	Lot No.	Condition	P as P <sub>2</sub> O <sub>5</sub> (w/o)
May 2000	Ca-formate	Gelest 8A-5535	As-rec'd	0.004
May 2000	Ca-formate	Gelest 97G-4388	As-rec'd	0.001
May 2000	W metal	Aldrich 08320MN	As-rec'd	0.04
Oct. 2000	W metal	Aldrich 08320MN	As-rec'd	<0.001
Oct. 2000	W metal	Aldrich 08320MN	900°C/2 hr/vacuum	0.053
Nov. 2000	W metal	Aldrich 08320MN	As-rec'd	0.058
Nov. 2000	W metal	Aldrich 08320MN	900°C/2 hr/vacuum	0.013
Jan. 2001	W metal	Aldrich 08320MN	As-rec'd	0.013
Jan. 2001	W metal	Aldrich 08320MN	900°C/2 hr/vacuum	0.032

The P-analysis results are quite inconsistent and it is unclear whether this is a result of poor sensitivity in the technique or operator error. The results on the tungsten metal samples in Oct. 2000 and Jan. 2001 show the phosphorous content of the as-received powder to be less than that of the heat-treated powder, whereas the reverse was found for the Nov. 2000 sample submittal. It was decided to proceed with the formulation of scheelite precursors using the heat-treated tungsten metal even though there was inconclusive evidence that it helped to reduce the phosphorous content.

Two batches of scheelite coating precursor (AF293 and AF295) were prepared using tungsten powder that had been heat treated to 900°C for 2 hours in a vacuum furnace. Calcium formate from Gelest lot number 97G-4388 was used. The resulting x-ray diffraction patterns of powder derived from the precursors are shown in **Figures 47 and 48**. The AF293 batch showed good stoichiometry (within the resolution of x-ray diffraction analysis). Batch AF295 appears very slightly calcium rich; peaks for Ca<sub>3</sub>WO<sub>6</sub> are present at 19.4° and 22.2° 2θ. Coatings were deposited from the as-formulated precursors. In addition, alumina powder (TM-DAR) was added to precursor AF293 to act as a buffer to possibly scavenge phosphorous impurities that may have been present and/or to react with any excess calcium. The alumina powder did not stay suspended well in the precursor and likely did not get incorporated into the coating. Coating were also made with the alumina containing AF293 precursor following storage for 6 days (referred to as the “aged” precursor). And finally, an MTI alumina polymer precursor was added to the supernate of the aged precursor (at 5 wt. percent solids loading) to act as a more finally dispersed buffer. The alumina polymer containing precursor was not very stable and only a small amount of fiber was coating using it. Uncoated and coated fibers were heat-treated at 1000°C and 1050°C for one hour in air (a quartz tube furnace was used). The results of single fiber testing of the heat-treated fibers is summarized in **Figure 49**.

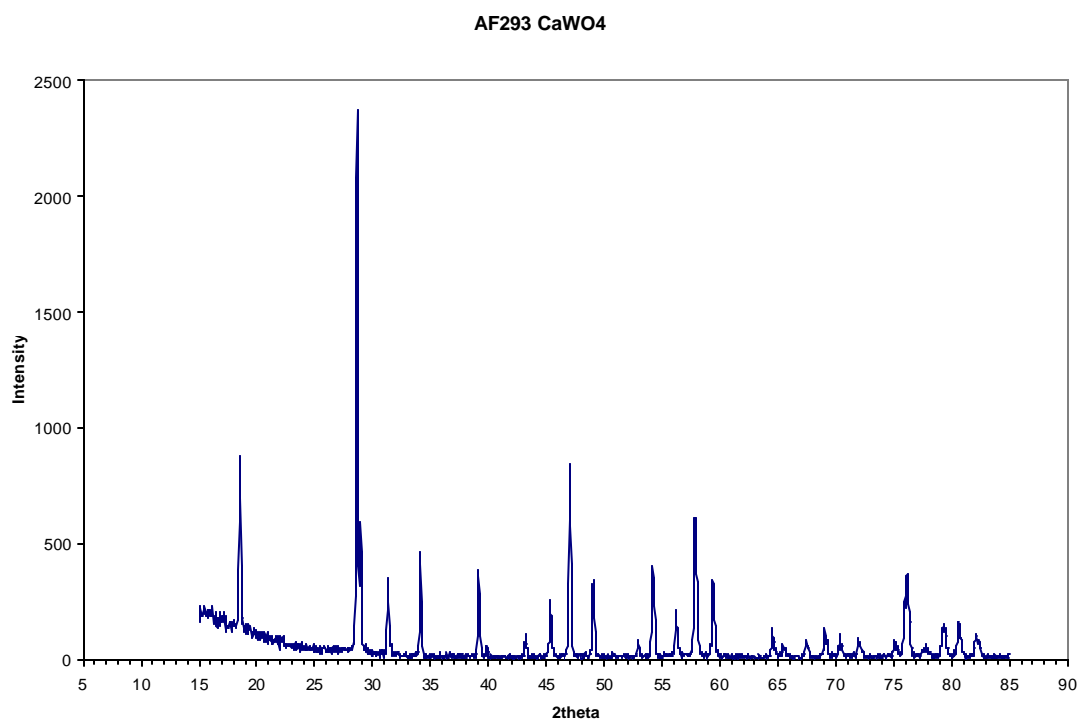


**Figure 47.** XRD result for AF293 scheelite coating from W-metal/calcium formate in peroxide solution.

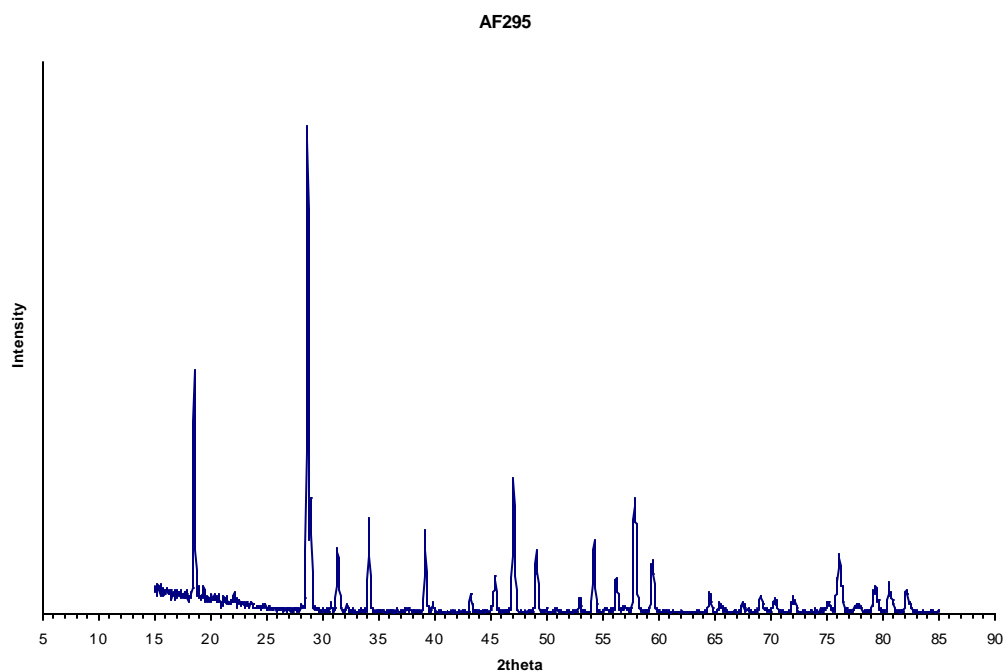


**Figure 48.** XRD result for AF295 scheelite coating from W-metal/calcium formate in peroxide solution.

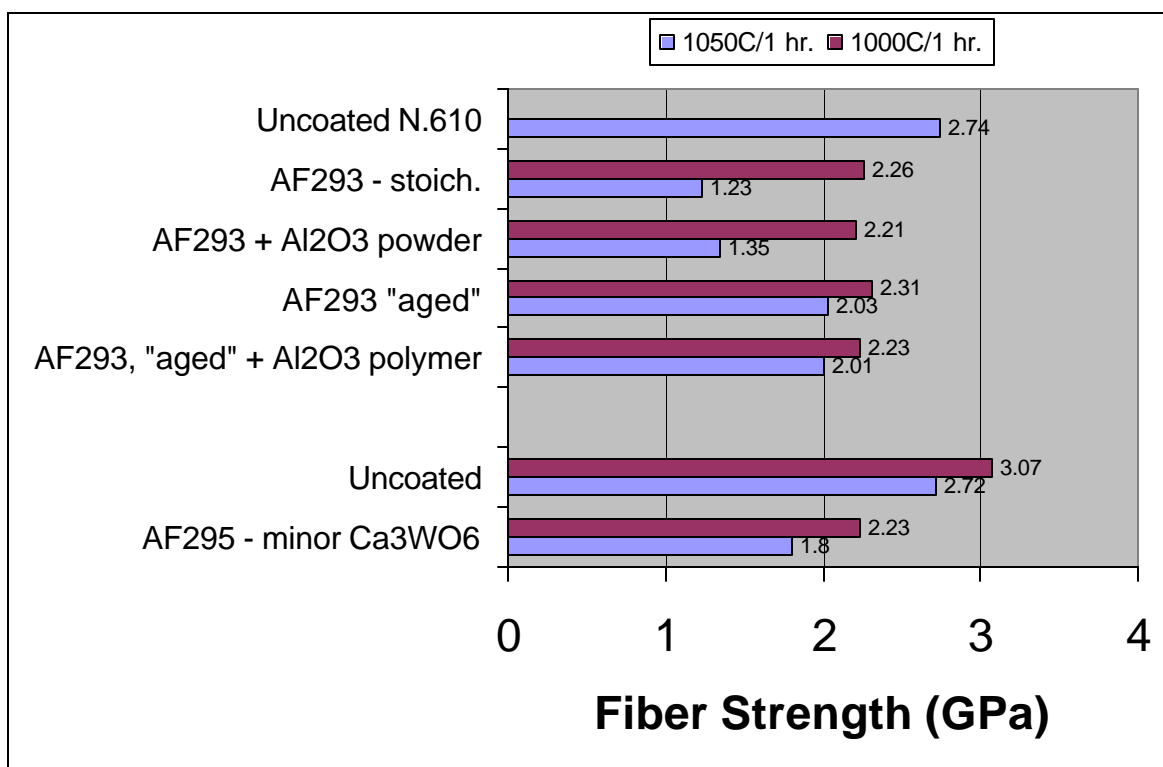


**Figure 49.** Strength of coated and uncoated fibers following heat treatment.

Fibers with coatings derived from AF295 were slightly stronger after 1050°C/1 hour than those with coatings from straight AF293 (1.8 versus 1.23 GPa). This was surprising since the XRD data for AF295 showed some minor Ca<sub>3</sub>WO<sub>6</sub>. No Ca<sub>3</sub>WO<sub>6</sub> peaks were observed for powders from AF293. For the formulation of the AF295 precursor, approximately 50% less hydrogen peroxide was used, compared to AF293. That change in formulation resulted in a significant difference in the nature of the TGA curves for powders derived from the two precursors (see **Figure 50**). Powder from precursor AF295 exhibited a flat weight loss curve above 750°C in contrast to powders from AF293. The near absence of volatiles at high temperatures with the AF295 precursor may be a reason for the lower strength degradation. The overall strength retention of these coated fibers was poor, especially at the higher temperatures. The strength retention after 1000°C was considered sufficient to proceed with fabrication of CMC panels.



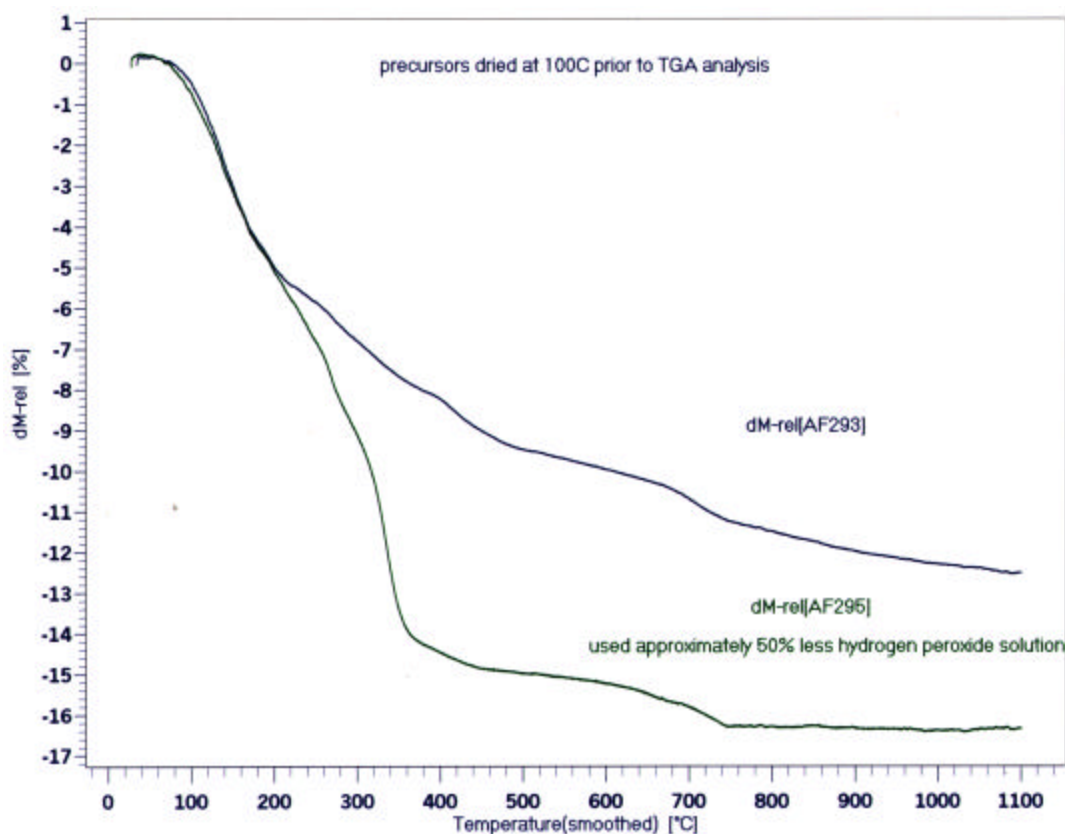


**Figure 50.** Comparison of TGA curves for scheelite precursors AF293 and AF295.

Composites were fabricated using fibers coated with the straight/unaltered AF293 precursor, the “aged” AF293 precursor and with uncoated fibers (baseline condition). An inadequate quantity of fiber coated with the AF295 precursor was available for fabricating composite panels. Unidirectional preforms were pressure cast with an alumina slurry. The panels were fired to 1000°C for one hour to provide some initial sintering of the matrix and to densify the fiber coatings. This initial heat treatment step was 100°C greater than that used for panels fabricated for the first series of CMC panels in which TEM analysis revealed a highly porous coating that was infiltrated with matrix. The heat treatment temperature was limited to 1000°C to prevent strength degradation to the fibers. The panels were then further densified using either an alumina polymer precursor formulated by MTI (used for panels with fiber coatings from “aged” AF293 precursor) or a CeraBlak™ precursor from ATFI (used for panels with fiber coatings from straight/unaltered AF293 precursor). The panels densified with alumina polymer were fired to 850°C between infiltrations and the panels densified with the CeraBlak™ were fired to 900°C between infiltrations. These firing temperatures were kept low to prevent fiber strength degradation. The low firing temperatures caused the panels to have a high residual porosity (18 to 20 percent total porosity for the CMCs); higher than the 10 to 12 percent desired. **Table 11** summarizes the composites that were fabricated in this second round and the resulting tensile strengths. Virginia Tech tested two specimens with uncoated fibers in the alumina-

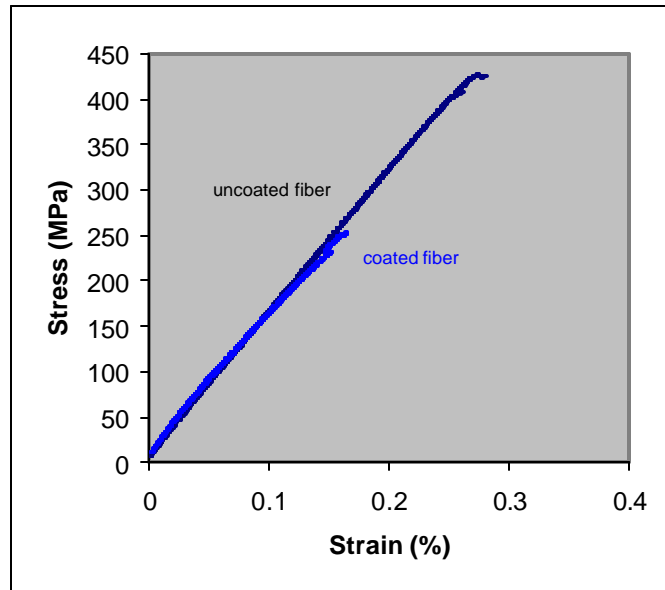
CeraBlak<sup>TM</sup> matrix that were additionally heat treated at 1100°C/1 hr. Tension strengths were similar to that obtained for similar specimens that were only processed to 1000°C.

**Table 11.** Summary of un-notched tensile strengths of second series of CMC samples. Data for individual room temperature tests is shown.

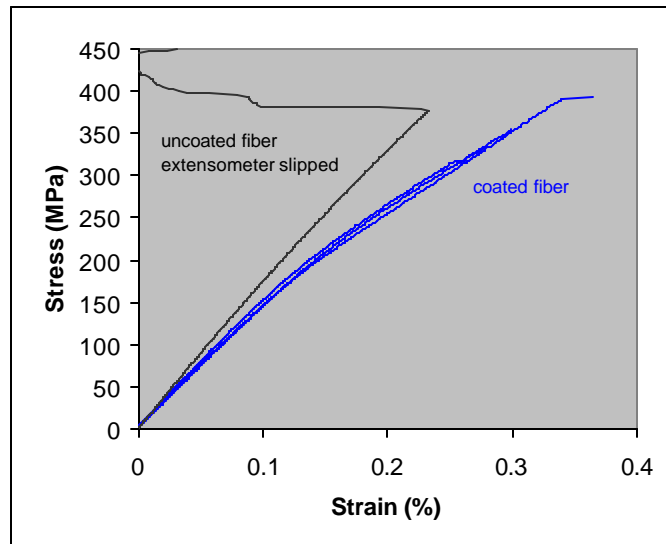
Sample	Coating Precursor	Sol-Gel Matrix	Max. Temp. During Matrix Infiltration	Residual Porosity	MTI Tested Strength/Strain un-notched, MPa	Virginia Tech. Strength/Strain notched, MPa
AF293 (unaltered)	W-metal/Ca-formate peroxide solution	ATFI CeraBlak	900°C	20.3%	239 0.23% 364 0.22% 288 0.19%	380 0.28% 334 0.20%
AF293 - "aged"	W-metal/Ca-formate peroxide solution	alumina	850°C	21.5%	252 0.18% 202 0.19%	337 0.28%
Baseline/Control	uncoated fibers	ATFI CeraBlak	900°C	18.0%	530 0.32% 490 0.28% 540 0.32%	577 na 535 na 503 0.24% *550 0.26% *486 0.26%
		alumina	850°C	18.9%	425 0.28% 363 na	466 0.23% 442 na

\* Specimens additionally heat treated at 1100C/1 hr; a 150C increase from the processing temperature used for alumina-CeraBlak matrix CMC

For both matrix types, the CMC samples containing uncoated fibers exhibited higher strengths than the samples containing scheelite fiber coatings. This lower strength is being attributed to probable degradation of the fiber strength by the scheelite coatings. **Figures 51** compares the stress-strain curves obtained for CMC specimens densified with the MTI alumina polymer precursor. The non-linearity in the stress-strain curve of the scheelite-containing specimen indicates some functioning, such as debonding, of the fiber-matrix interface. **Figure 52** shows the general microstructure of the CMCs containing the scheelite fiber coatings.



Testing performed at AFWL



Testing performed at Virginia Tech

**Figure 51.** Stress-strain curves for unidirectional un-notched CMC in an all alumina matrix (formed using MTI alumina polymer). Coated fiber is lot AF293 – “aged”.

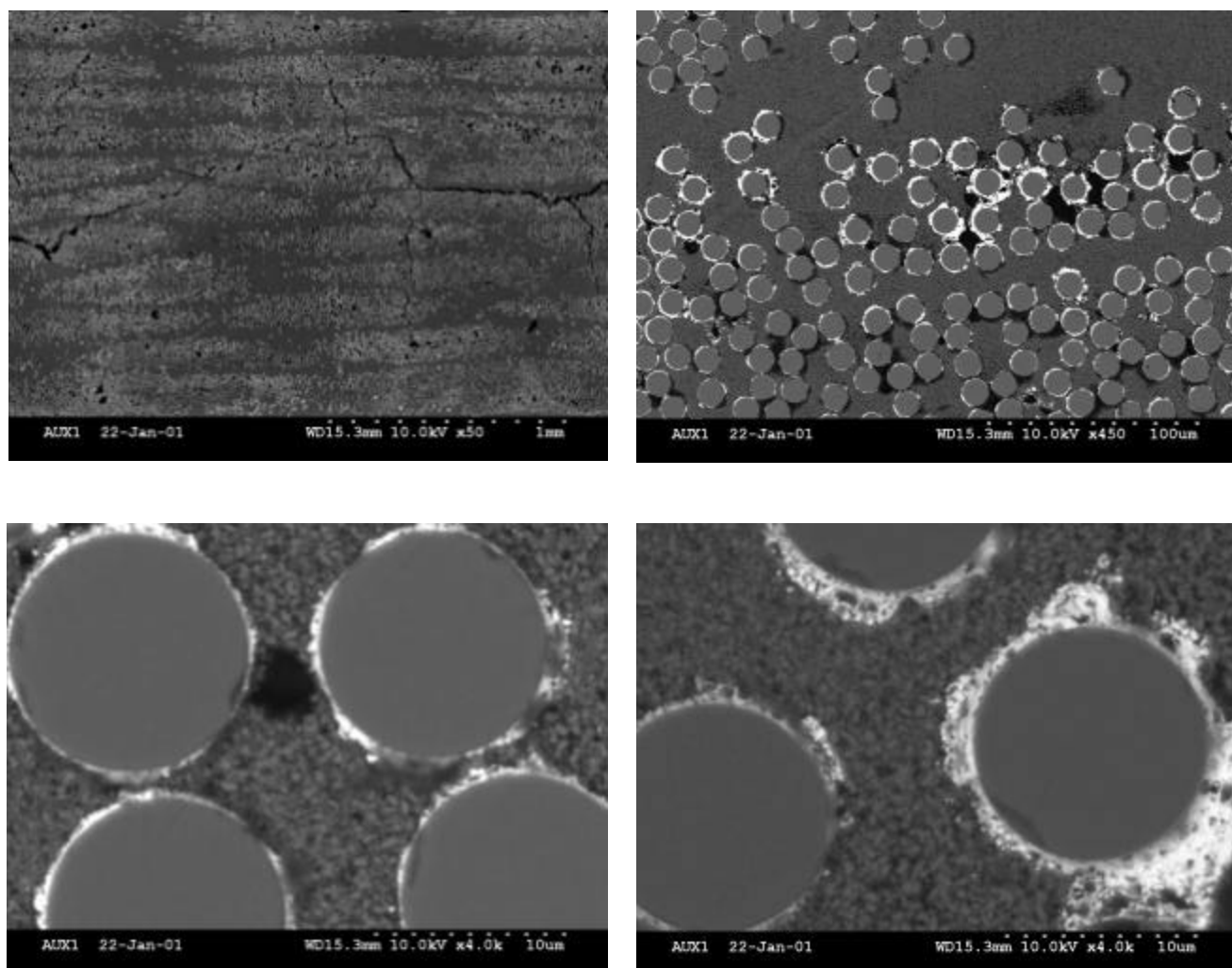
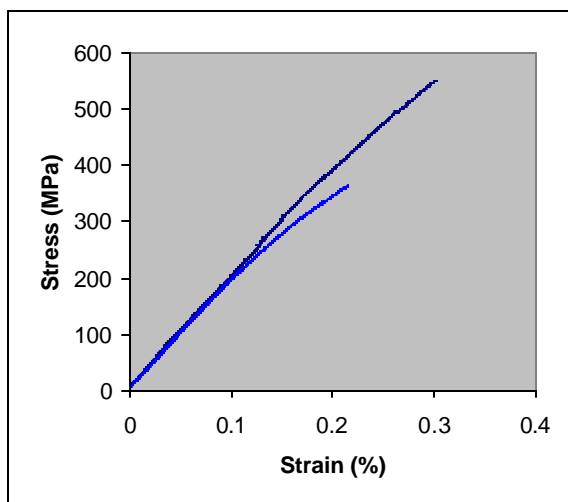
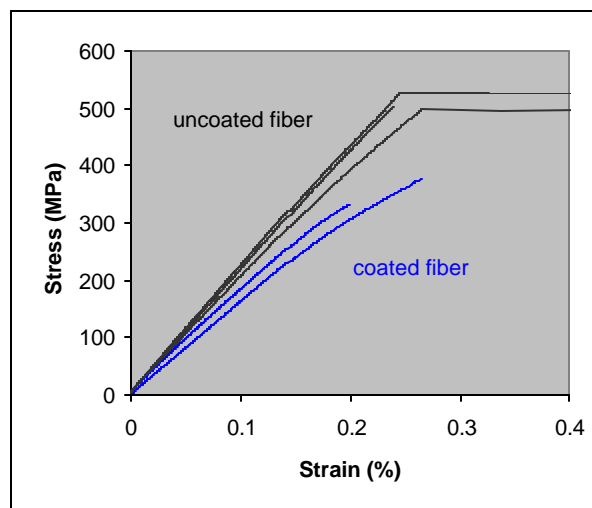


**Figure 52.** Microstructure of CMC containing scheelite precursor in an all alumina matrix.

Typical stress-strain curves obtained for CMCs densified with the CeraBlak<sup>TM</sup> precursor are shown in **Figure 53**. The strengths of CMC densified with the CeraBlak<sup>TM</sup> precursor are higher than that observed for CMC densified with the MTI alumina polymer. This higher strength was observed even though the CeraBlak<sup>TM</sup> matrix CMC panels were processed at a 50°C higher temperature. Both the CeraBlak<sup>TM</sup> and the MTI alumina polymer exhibit low weight loss at high temperatures as shown in the TGA curves of **Figure 54**. The CeraBlak<sup>TM</sup> precursor has an overall lower weight loss.



AFWL Testing



Virginia Tech Testing

**Figure 53.** Stress-strain curves for unidirectional un-notched CMC with an alumina-CeraBlak™ duplex matrix. Coatings were obtained from the unaltered AF293 scheelite precursor.

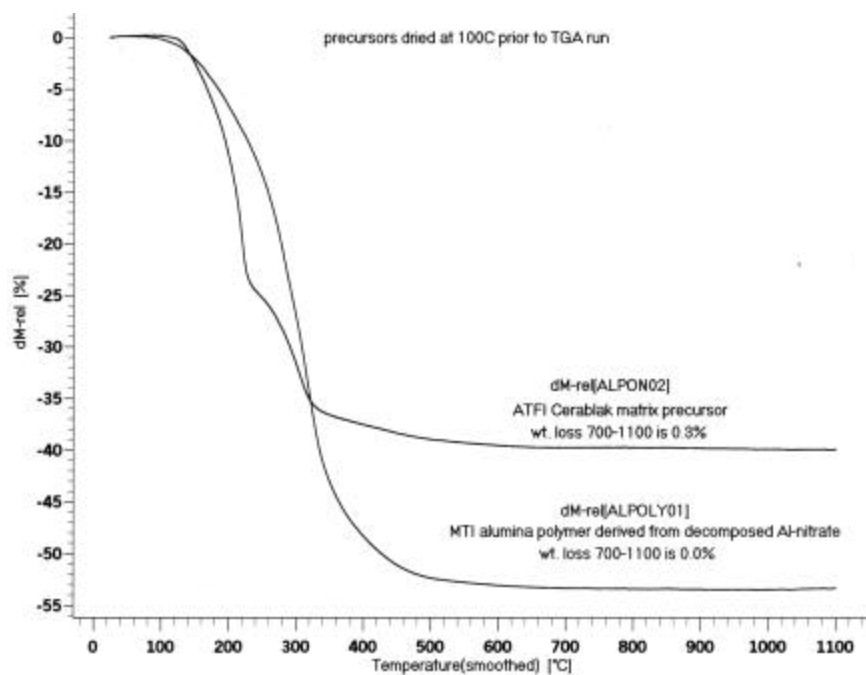


**Figure 54.** TGA comparison of CeraBlak™ and MTI alumina polymer.

Some of the CeraBlak™ containing CMC specimens with uncoated fibers exhibited non-linearity beyond the 350 MPa stress level (its ultimate strength averaging over 500 MPa). This may indicate that the CeraBlak™ phase itself may exhibit some weak bonding to the Nextel 610 fibers. There was a significantly higher degree of non-linearity in the CeraBlak™ CMCs that contained the scheelite fiber coatings supporting the argument that the scheelite coatings are promoting debonding at the fiber-matrix interface. The fracture surface of the CeraBlak™ containing CMC with scheelite fiber coatings is shown in **Figure 55** (secondary electron images) and **Figure 56** (backscattered electron images) and reveals the debonding which has occurred at the scheelite coating.

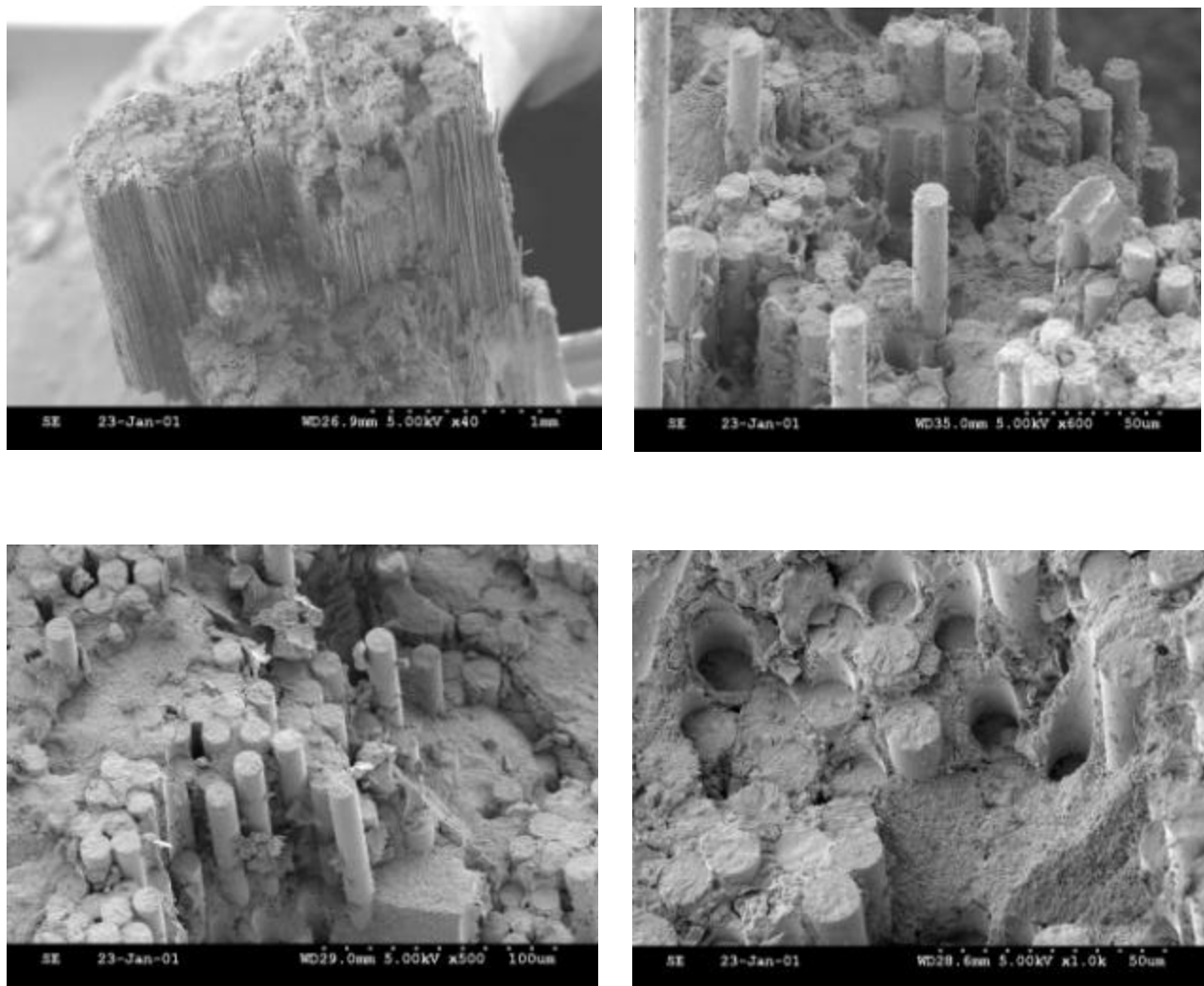


**Figure 55.** Secondary electron images of fracture surface of CMC with scheelite fiber coatings in an alumina-CeraBlak™ duplex matrix.

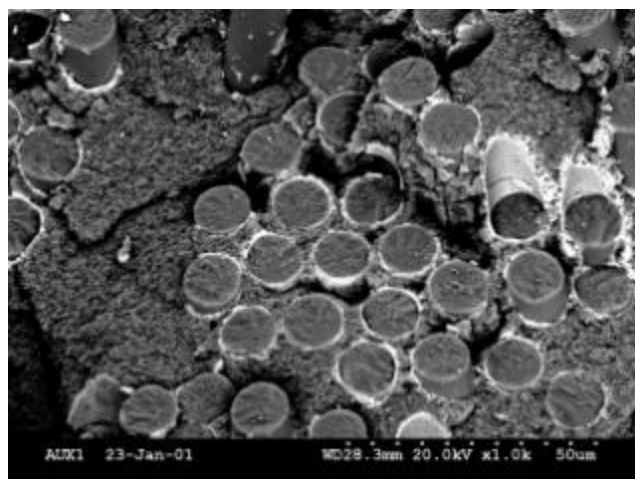
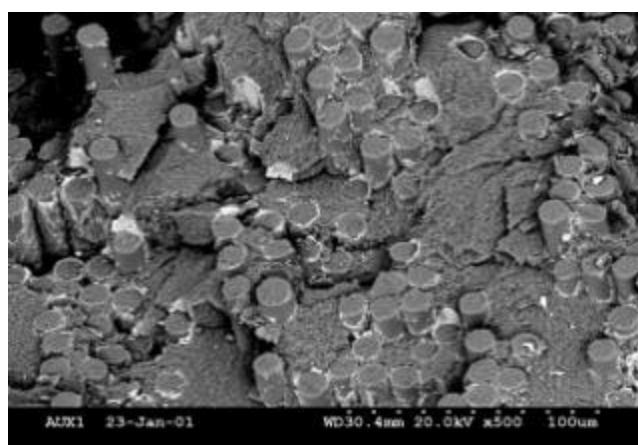
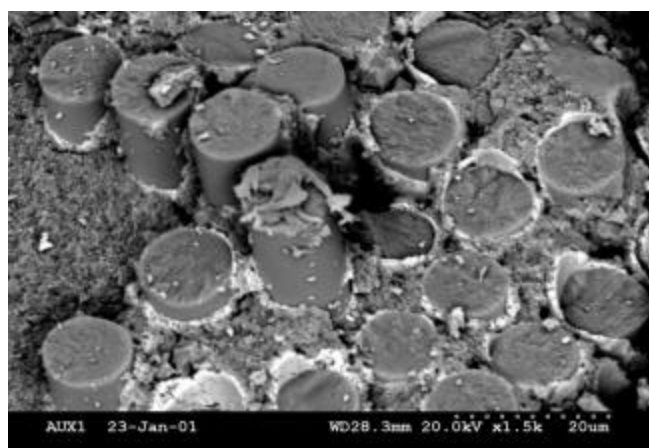


**Figure 56.** Backscattered electron images of fracture surface of CMC with scheelite fiber coatings in an alumina-CeraBlak<sup>TM</sup> duplex matrix.

### **Task 3 – Composite Processing and Properties - Third Series of CMCs**

The focus of the third round of CMCs to be fabricated for use in mechanical property evaluation was the following:

1. Introduce scheelite slurry-derived fiber coatings and compare properties to that obtained using the MTI W-metal/Ca-formate peroxide based coating precursors.
2. Examine only the alumina-CeraBlak duplex matrices given the better composites properties observed in the second series of CMCs.
3. Use higher matrix processing temperatures in order to facilitate achieving a lower residual porosity for the CMCs, and hopefully be able to more fully discriminate the functionality of the scheelite fiber coatings.

### **Solution-Based Precursor**

An additional batch of scheelite precursor was formulated for use in the continuous coating of Nextel 610 fiber for the third series of CMCs. Based on single fiber tensile results from the second series of CMCs, this precursor was formulated with less hydrogen peroxide and was allowed to “age” a few days prior to performing the continuous fiber coating. No rigorous follow up experiments were performed to verify statistically that the lesser amount of hydrogen peroxide and/or the “aging” step actual yields higher strength fibers, however, there seemed to be no significant risk in instituting those features. **Figure 57** shows TGA curves for precursors used in second series of CMCs (AF293 and AF295) and the most recent batch (AF298). All three precursors were formulated from hydrogen peroxide, tungsten metal powder and calcium formate. AF295 and AF298 were formulated with the lesser hydrogen peroxide content. Both powders obtained from precursors formulated with the lesser hydrogen peroxide showed a similar total weight loss of ~16 percent, however, the decomposition profiles are slightly different. Clearly, there are critical parameters to the precursor formulation that are not well understood. We had hoped to duplicate the flat TGA curve at high temperatures that was observed with the AF295 precursor. The TGA line for the recent precursor, AF298, was not quite as flat at the high temperatures. Nextel 610 fibers were coated with AF298 precursor at 40 inch/min and a 650°C furnace temperature.



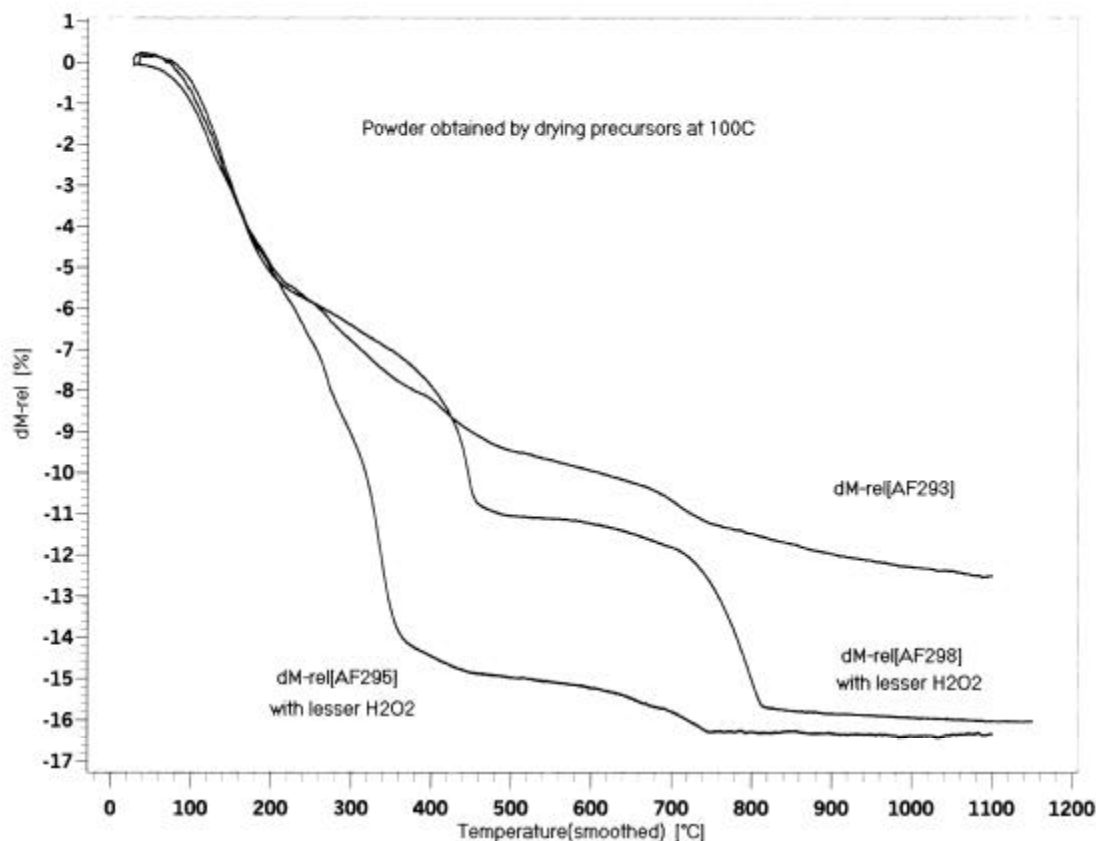


**Figure 57.** TGA curves for scheelite precursors formed from tungsten metal, hydrogen peroxide and calcium formate.

### **Slurry-Based Precursors**

We decided to re-examine the use of scheelite slurries for continuous fiber coatings for this third round of CMCs. We had briefly investigated scheelite slurries earlier in the program and had experienced trouble obtaining fine particle sizes. We wanted to re-examine the use of slurries as a means for producing fiber coatings that would cause less fiber strength degradation. A new batch of slurry was formed using a 99.9%  $\text{CaWO}_4$  powder from Aldrich. The powder was attrition milled using an alumina-lined container and yttria stabilized zirconia shaft and milling media. Throughout the milling process, Darvan C dispersant (ammonium polymethacrylate) was added to reduce the viscosity of the slurry and allow for efficient milling. The slurry was milled for a total of 19 hours during which time the median particle size was reduced from 8.95 to 0.181 microns. Two batches of coated fibers were prepared with the slurry precursor:

1. 5.2 wt. percent slurry, 650°C furnace temperature, ~40 inch/min
2. 9 wt. percent slurry, 815°C furnace temperature, 40 inch/min

Uncoated fiber tows and fiber tows containing the solution and slurry based scheelite coatings were heat treated at 1000°C and 1050°C for one hour. Single fiber filament strengths were measured for the coated and un-coated fibers. The comparison of the fiber strength retention obtained with the slurry coatings and the solution based coatings is shown in **Figure 58**.

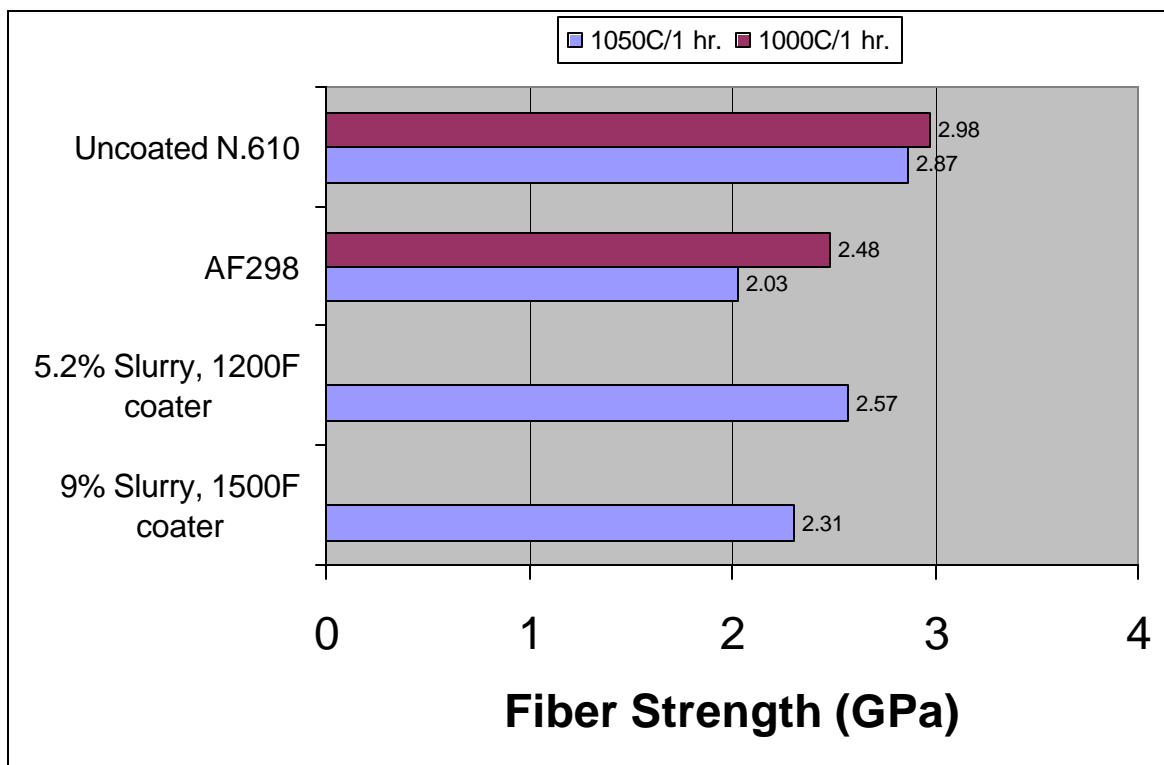


**Figure 58.** Single filament strengths of coated and uncoated Nextel 610 fibers.

The coatings produced from the solution precursor caused greater strength degradation to the fibers than the slurry-derived coatings. The results obtained with the solution-based precursors were very similar to results obtained for the second series of CMCs. As reported in Task 1, the sodium content of Darvan C could possibly contribute to the strength degradation, but so little Darvan C is required to disperse the suspension, plus the minor 70 ppm content of the Darvan C makes this explanation implausible. The cause for the strength degradation associated with the slurry-based coatings is unknown. An additional cause may involve the use of a commercial scheelite powder with a purity level of only 99.9%. In hindsight, a preferred method for formulating the slurry would have been to precipitate a slurry in-house using a calcium salt and a tungstate source. Such a precipitate could have been centrifuge washed to remove impurities similar to what has been shown to be the preferred precursor route for monazite coatings. We also believe that the observed strength degradation may be influenced by the non-uniformity of the coatings. Slightly higher strengths were observed for the slurry

coatings deposited from the 5.2 weight percent precursor than from the 9 weight percent precursor, possibly as a result of stress intensities associated with the larger crusty regions from broken fiber-to-fiber bridges in the case of the higher loaded slurries. Even so, the 9 weight percent slurry was chosen for coating fibers to improve the likelihood of achieving good fiber coverage. **Table 12** provides a summary of the CMC specimens that were prepared during the third round and the resulting tensile properties that were measured.

**Table 12.** Summary on un-notched tensile strengths of the third series of CMC samples. Data for individual room temperature tests is shown.

Sample	Coating Precursor	Sol-Gel Matrix	Max. Temp. During Matrix Infiltration	Residual Porosity	V <sub>r</sub> (%)	Virginia Tech. Strength/Strain un-notched, MPa	E <sub>avg</sub> (GPa)
uncoated	none	ATFI CeraBlak	1000°C	7.9%	~40	647 0.29% 403 0.16% *565 0.27% *619 0.30% avg. = 559 MPa	259
AF298	W-metal/Ca-formate peroxide solution	ATFI CeraBlak	1000°C	10.4%	~30	451 0.31% 371 0.22% 374 0.24% *465 0.33% *467 0.33% avg. = 426 MPa	194
Slurry 1	9% by wt. slurry 815°C coating temp.	ATFI CeraBlak	1000°C	10.4%	~34	503 0.33% 464 0.30% *482 0.31% *498 0.31% avg. = 487 MPa	186
Slurry 2	9% by wt. slurry 1038°C coating temp.	ATFI CeraBlak	1000°C	9.50%	~29	347 0.22% 386 0.22% 394 0.23% *450 0.32% *350 0.21% *413 0.29% *384 0.24% avg. = 389 MPa	180

\* ultimate strengths obtained from hysteresis testing

A higher fiber volume fraction was obtained for the CMC with uncoated fiber as a result of the better packing density obtained with the uncoated fiber preform. The microstructure of the CMC with the uncoated fibers is shown in **Figure 59**. The high packing density of the fibers leads to some matrix-starved regions.

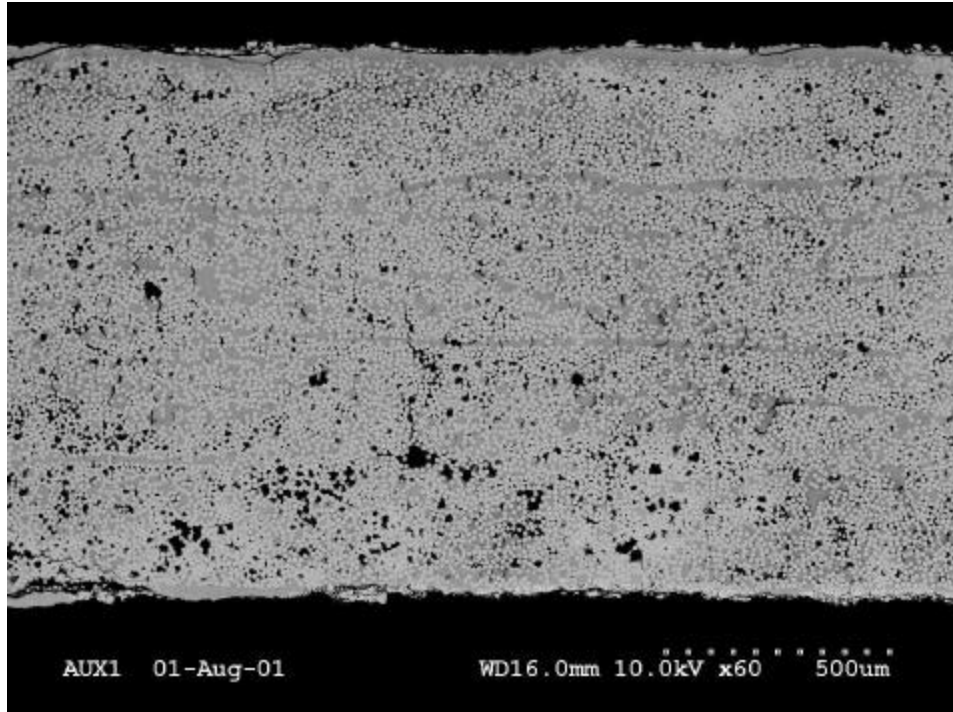


**Figure 59.** Microstructure of a round 3 CMC containing uncoated fiber in an alumina-CeraBlak duplex matrix.

As shown in **Figure 60**, the scheelite coatings obtained from the AF298 solution precursor continue to show inherent porosity that becomes filled with matrix during composite processing. It should be stated that only a minor fraction of the circumference of the fibers appears not to be in contact with scheelite.

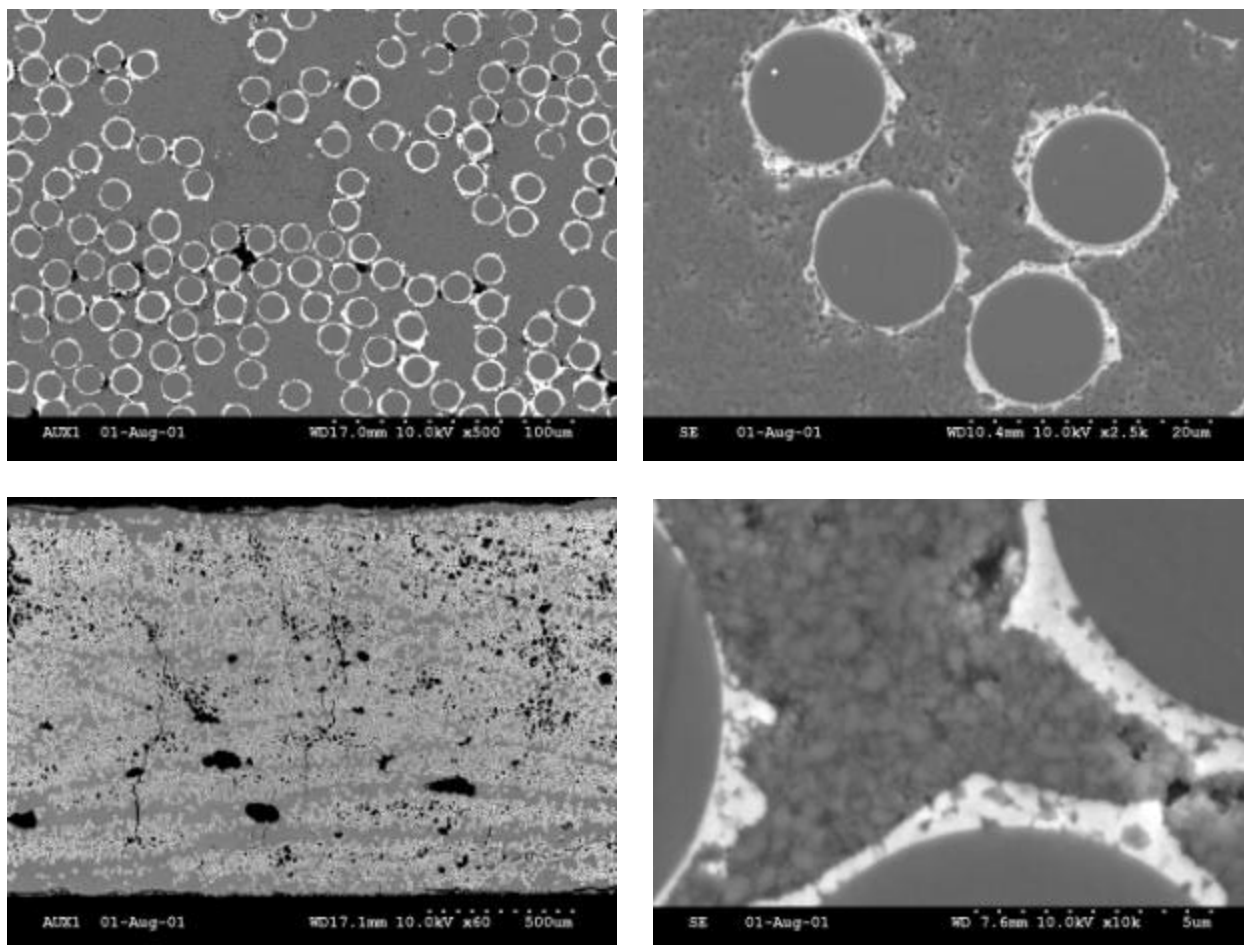


**Figure 60.** Microstructure of third round of CMC made with solution based (AF298) scheelite fiber coatings in an alumina-CeraBlak duplex matrix.

The CMC microstructure and the coating quality obtained using the 9 weight percent scheelite slurry with a coater temperature of 815°C is shown in **Figure 61**. These slurry-derived coatings show much less coverage of the fibers than the solution based coating precursors. The coatings are also much thinner than that obtained with the solution precursors.

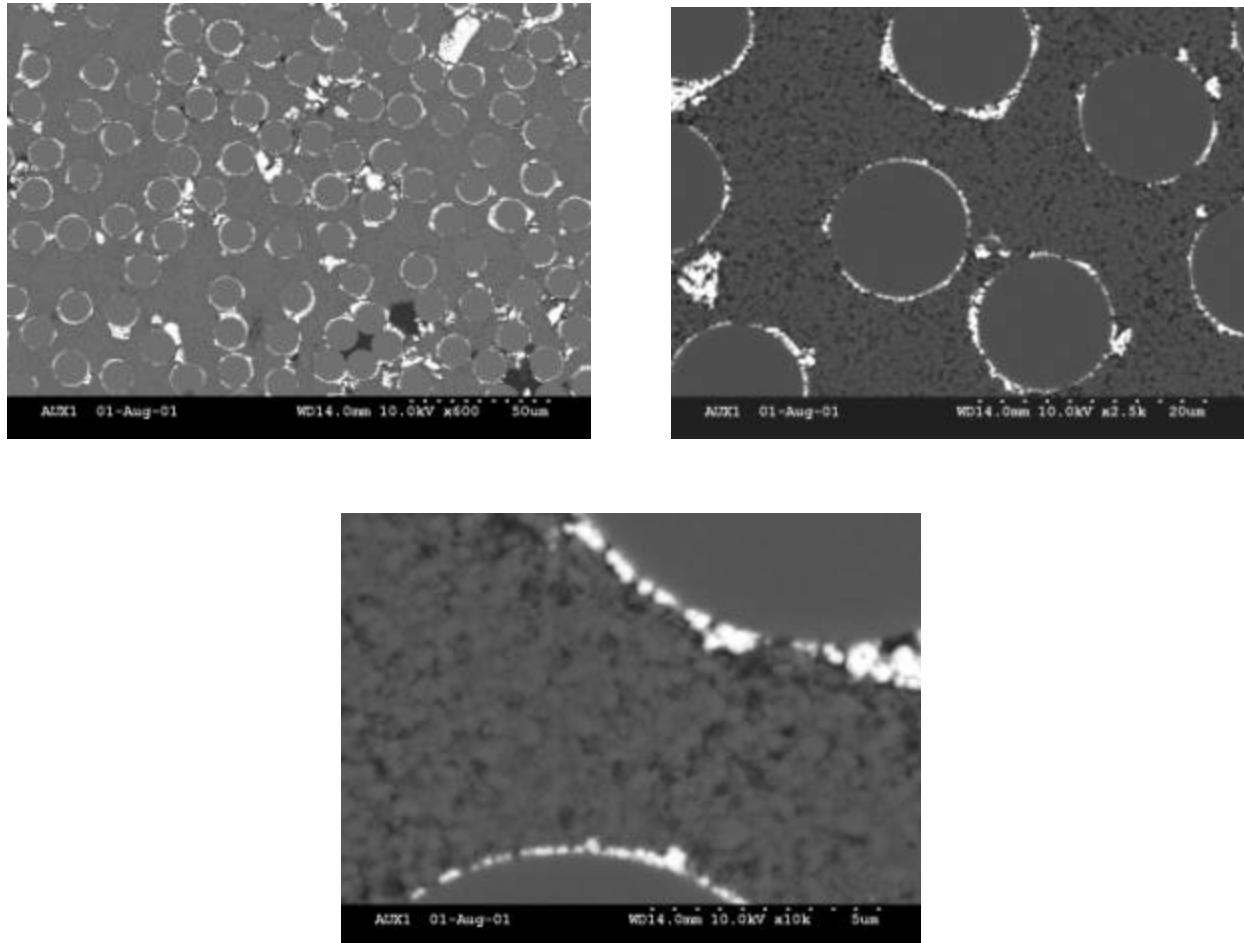


**Figure 61.** CMC with slurry derived fiber coatings processed at 815°C during the coating process.

Some fiber was coated at a higher temperature (1038°C exposure during 6 passes through the fiber coater) in hopes of obtaining a more continuous slurry derived fiber coating. The microstructure of the resulting composite and fiber coatings is shown in **Figure 62**. The resulting scheelite coatings appear somewhat thicker and there is better coverage than was obtained when a fiber coater temperature of only 815°C was used. Porosity within the fiber coating continues to be filled with matrix material.

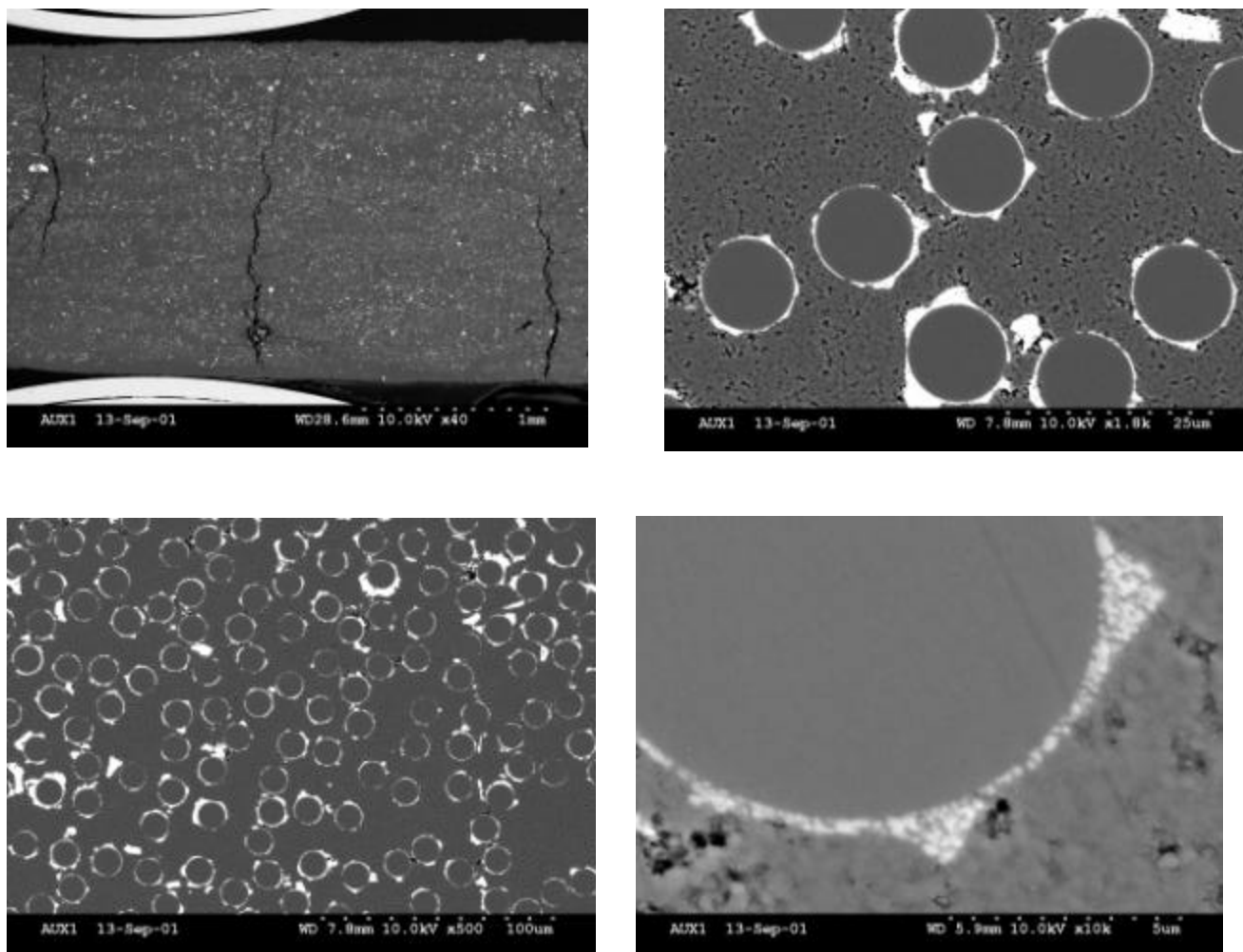


**Figure 62.** CMC fabricated using slurry derived coatings fired to 1038°C during the fiber coating operation.

The room-temperature stress-strain curves for the CMC specimen types described in Table 12 are shown in **Figure 63**. As observed in the previous series of CMC samples, the specimens containing uncoated fiber in an alumina-CeraBlak duplex matrix continue to exhibit the highest strength. Some non-linearity is observed for the CMCs with uncoated fibers above 400 MPa. For the CMCs containing scheelite fiber coatings, the strengths were slightly higher for the slurry coatings (815°C coating temperature) than for CMCs with fiber coatings derived from the AF298 solution based precursor. However, CMCs fabricated with slurry coatings that had been heated at 1038°C during the coating process exhibited ultimate tensile strengths even lower than the strengths obtained with the AF298 solution coatings. Apparently, the higher coating temperature was sufficient to cause additional fiber strength degradation. The stress-strain curves for all the specimens containing scheelite fiber coatings show a higher degree of non-linearity than the control specimens without fiber coatings. These results support the conclusion that the fiber coatings are promoting fiber-matrix interfacial debonding.

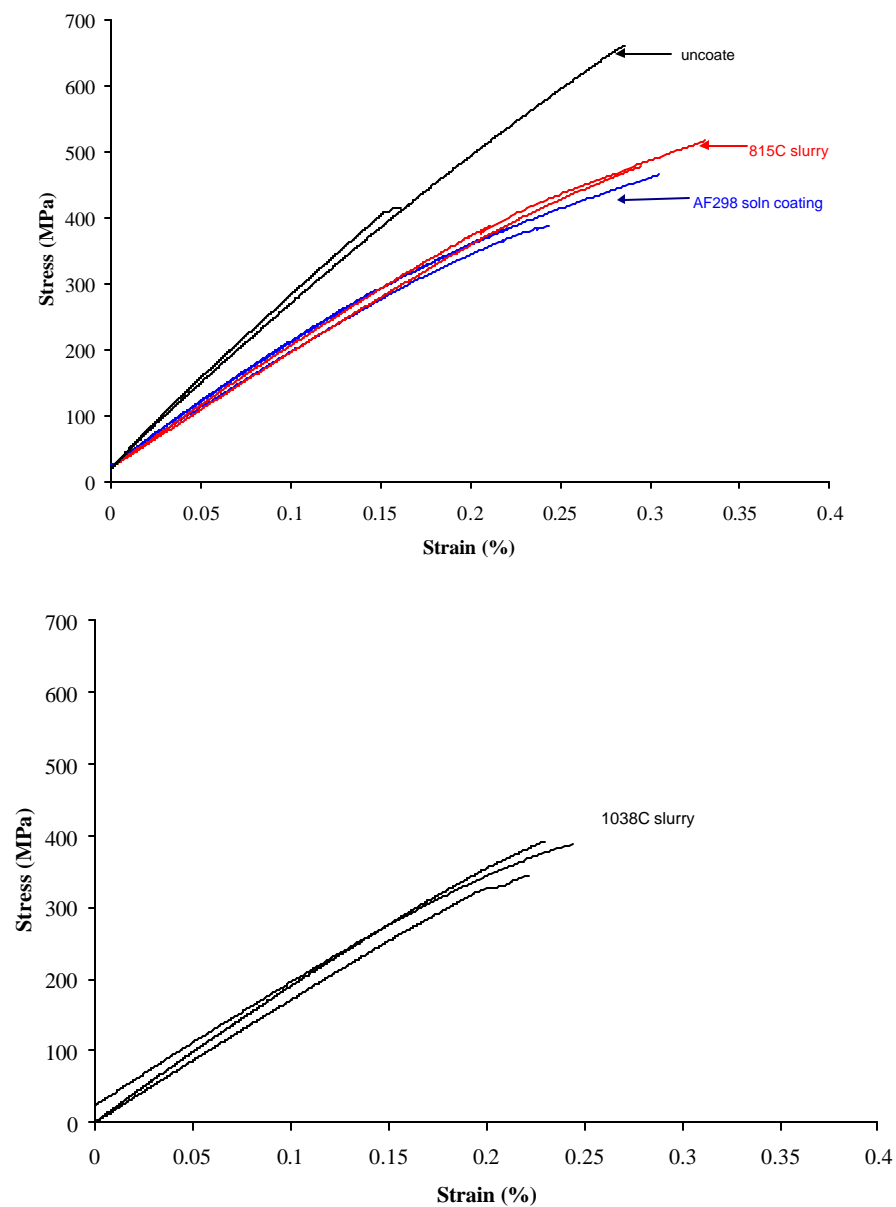


**Figure 63.** Room-temperature stress-strain curves for series 3 CMCs. Testing performed by Virginia Tech.

To further explore the functionality of the scheelite coatings, the fracture surfaces of the tests specimens were examined. The gross fractures of the four specimen types is shown in



**Figure 64-68.** The subsequent Figures show the SEM images of the fracture surfaces. Examination of the fracture surfaces revealed two primary points:

1. The CMC panel with uncoated fibers exhibited some fiber pullout, quite comparable to what was observed for composites with scheelite fiber coatings.
2. Debonding was evident along the scheelite fiber-matrix interface, although a large fraction of fibers showed very limited pullout lengths. Strength degradation of the Nextel 610 fibers by the scheelite coatings would be a factor in limiting the fiber pullout length.
3. There appears to be some inter-tow matrix cracking, that seems more prevalent in the lower fiber volume CMCs which contained the scheelite fiber coatings.

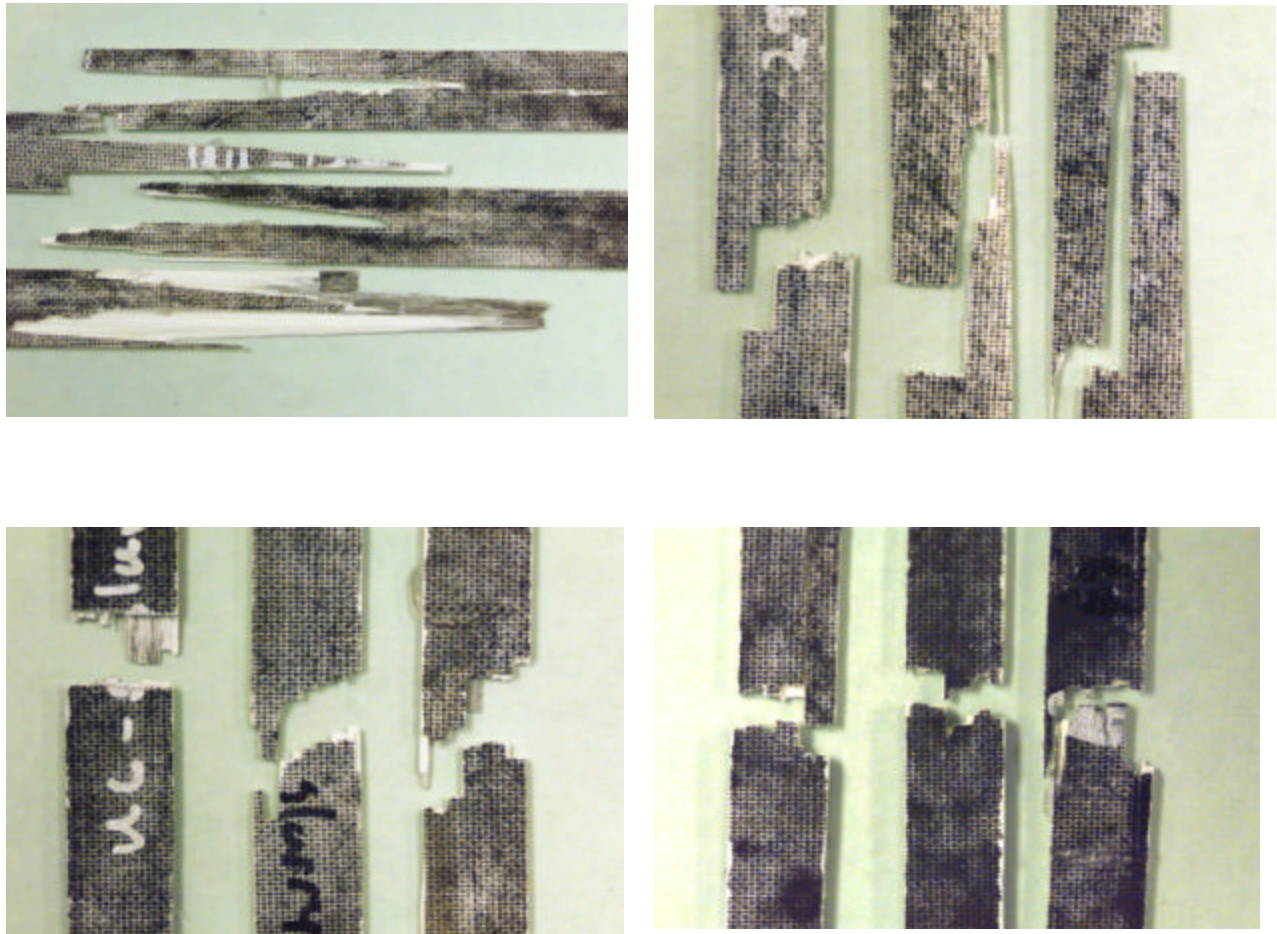


**Figure 64.** Macroscopic views of CMC fractures: (a) uncoated, (b) AF298 solution coatings, (c) 815°C heated slurry coatings and (d) 1038°C heated slurry coatings.

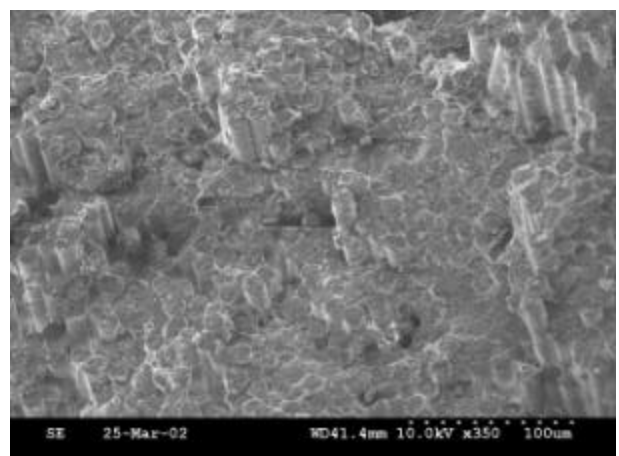
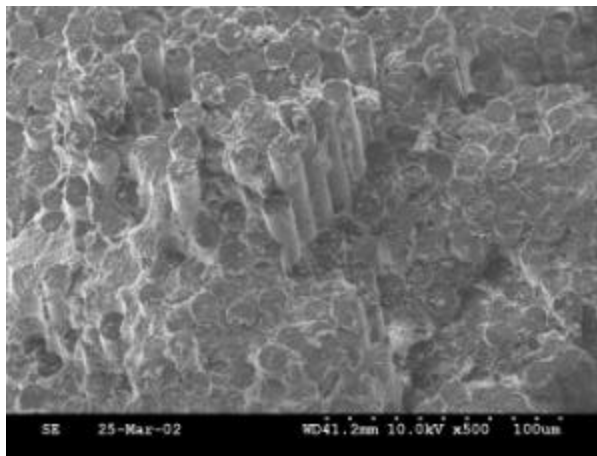
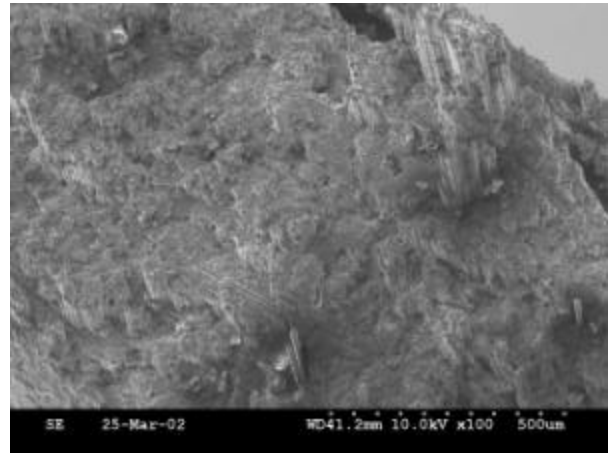
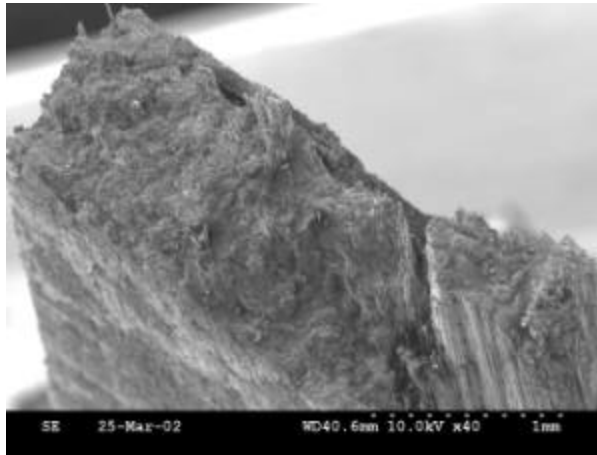


**Figure 65.** SEM images of fracture surface of series 3 CMC with uncoated fiber in an alumina-CeraBlak duplex matrix.

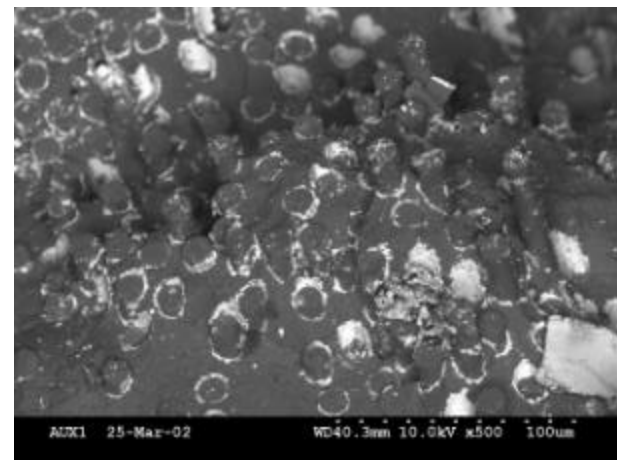
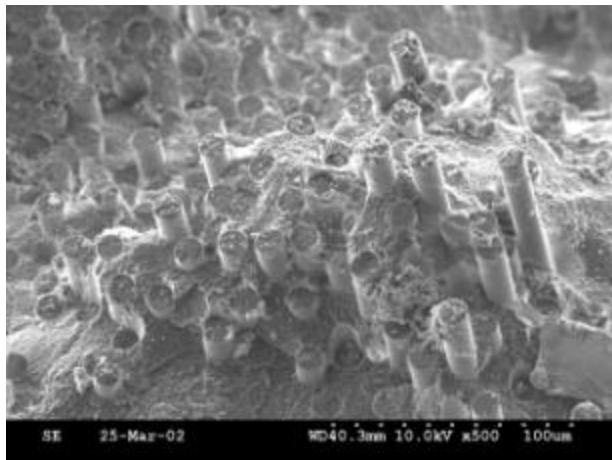
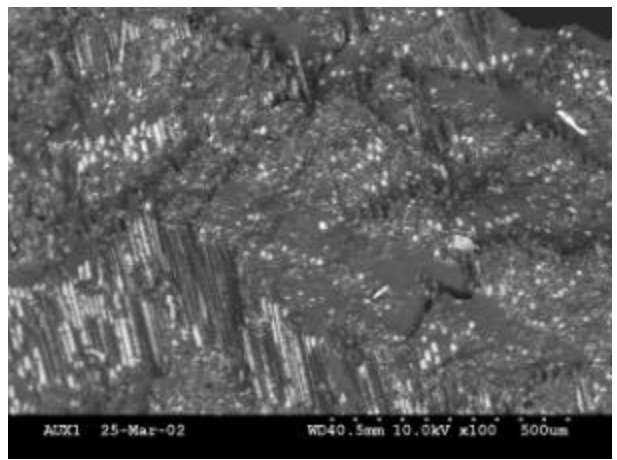
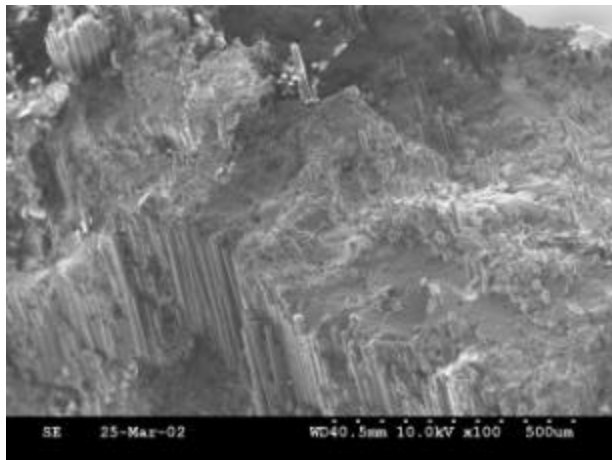
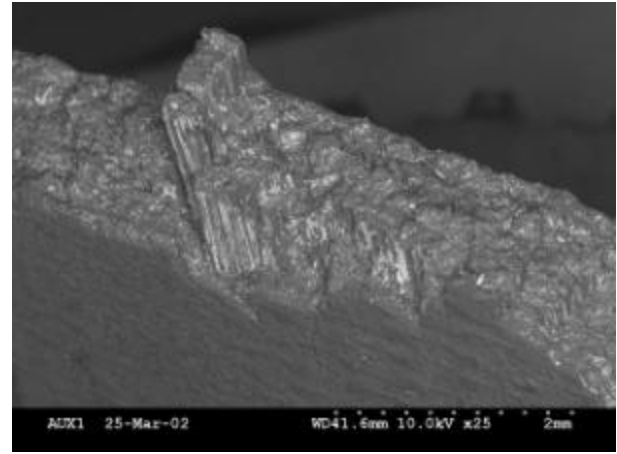
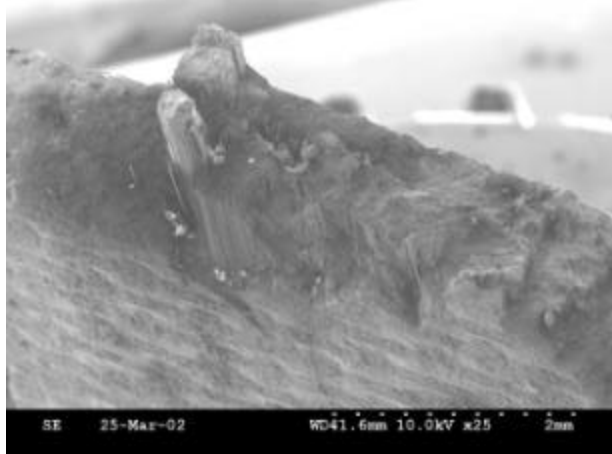


**Figure 66.** SEM images of fracture surface of series 3 CMC with solution-based AF298 scheelite fiber coatings in an alumina-CeraBlak duplex matrix.

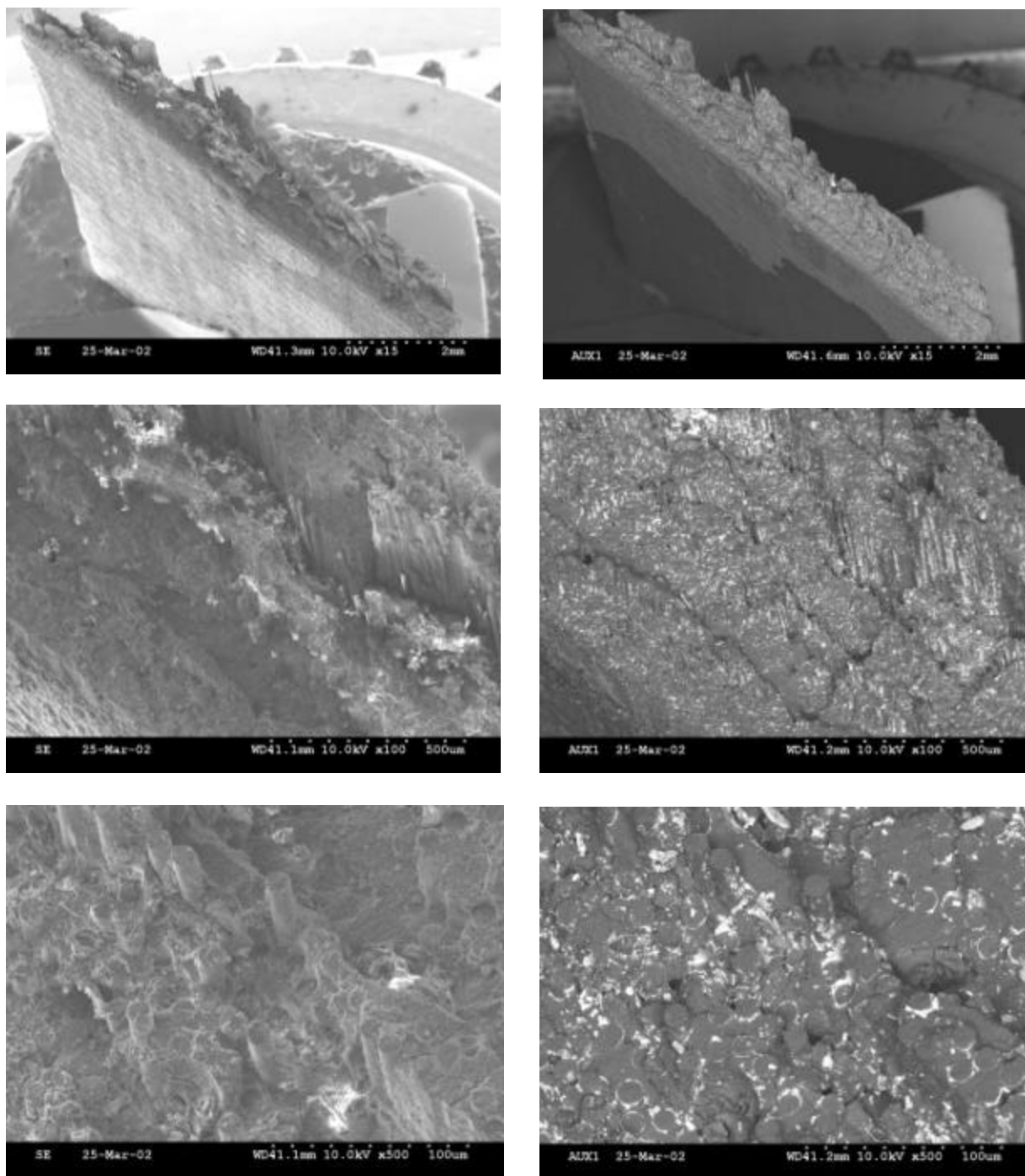


**Figure 67.** SEM images of fracture surface of series 3 CMCs containing slurry-derived scheelite fiber coatings (815°C condition) in an alumina-CeraBlak duplex matrix.

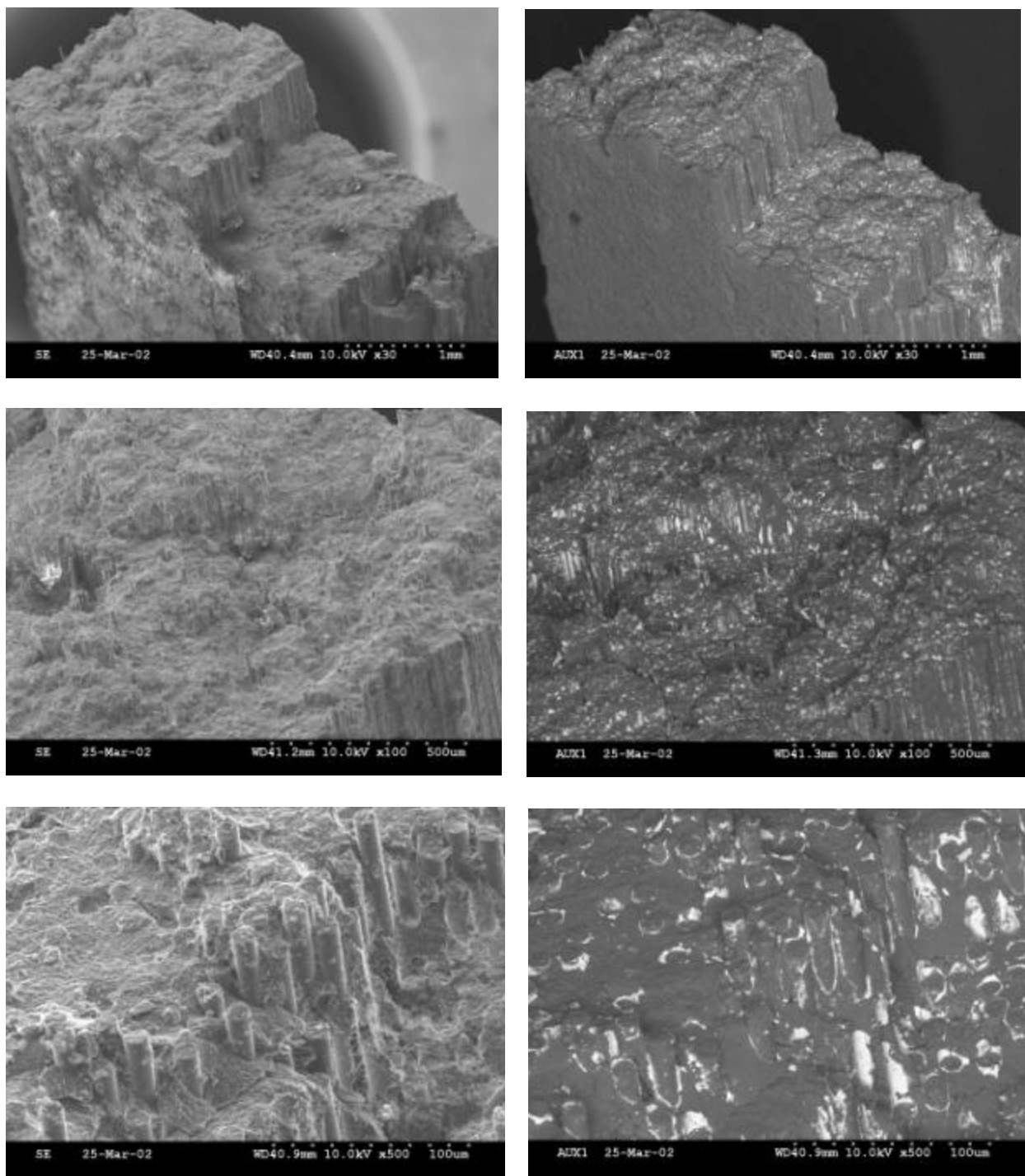


**Figure 68.** SEM images of fracture surface of series 3 CMC containing slurry-derived scheelite coatings (1038°C condition) in an alumina-CeraBlak duplex matrix.



Some stress-strain hysteresis testing was performed in an effort to further explore possible differences in the mechanical behavior of CMCs with and without fiber coatings. Stress-strain hysteresis curves for the four specimen types are shown *Figures 69-72*. Multiple curves for each specimen type are shown to give some indication of the variation in the hysteresis response.

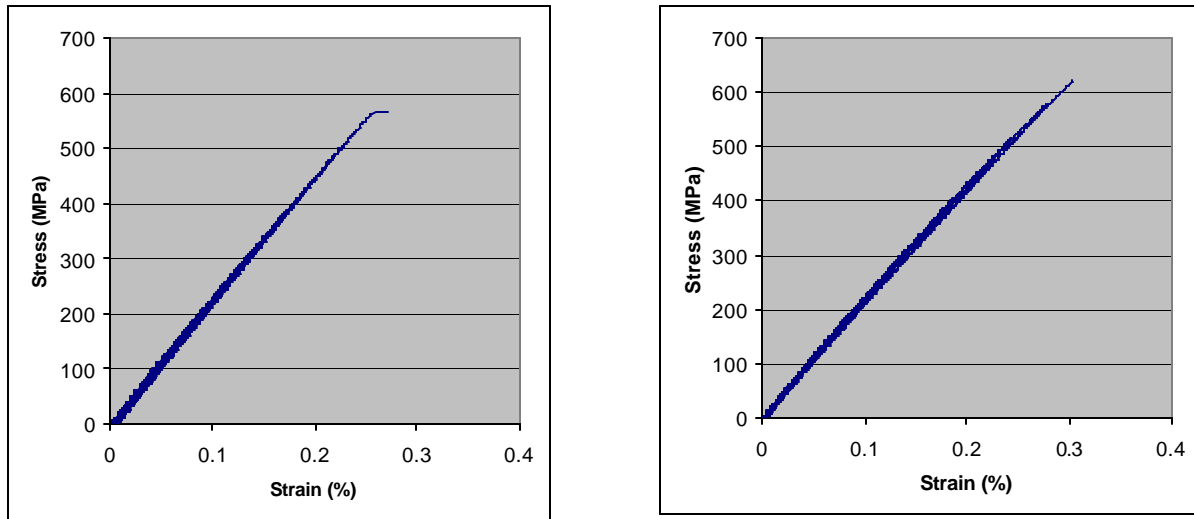


*Figure 69.* Hysteresis curves of CMCs with uncoated fibers.

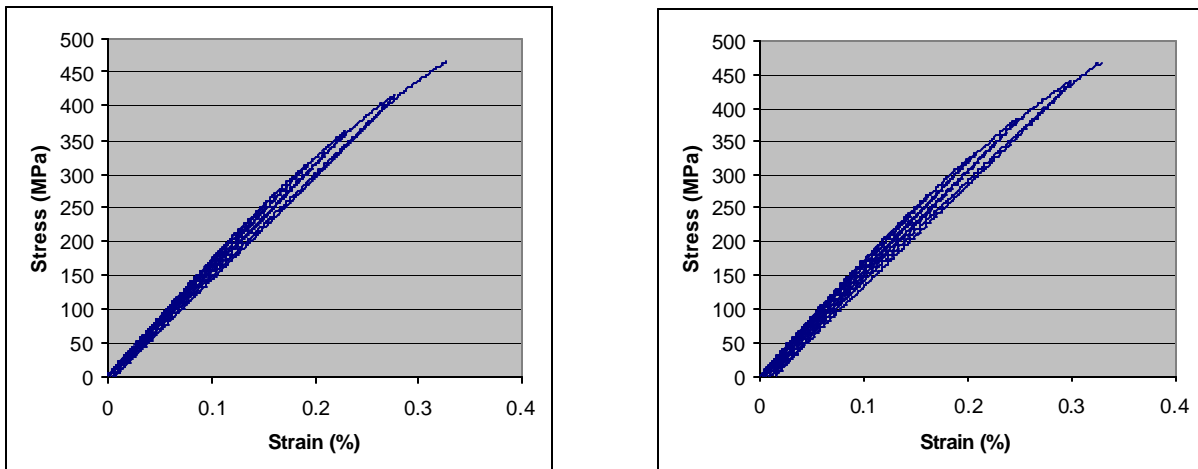


*Figure 70.* Hysteresis curves of CMCs with solution-derived scheelite fiber coatings (AF298).

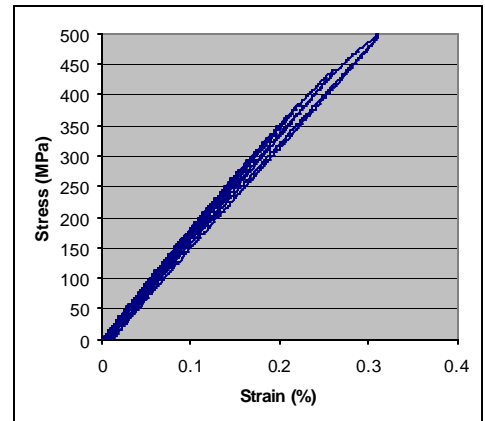
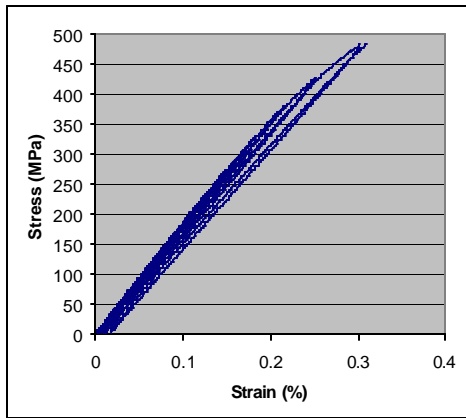


**Figure 71.** Hysteresis curves of CMCs with slurry-derived scheelite fiber coatings (815°C condition)

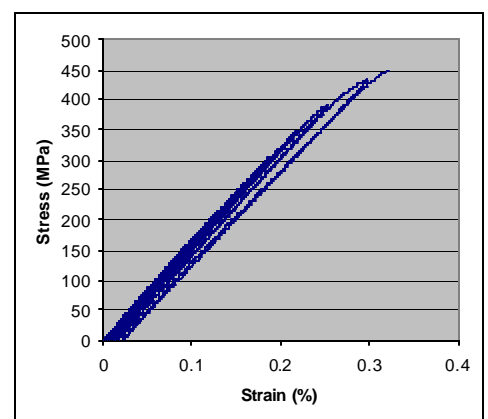
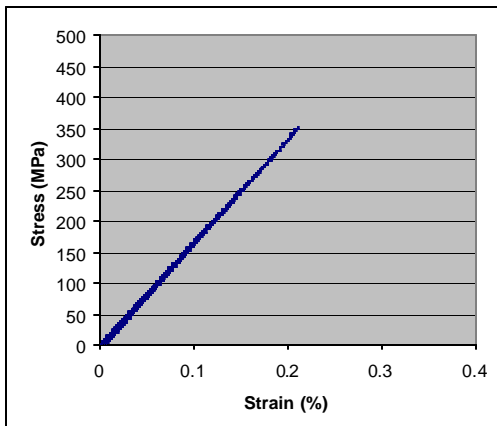
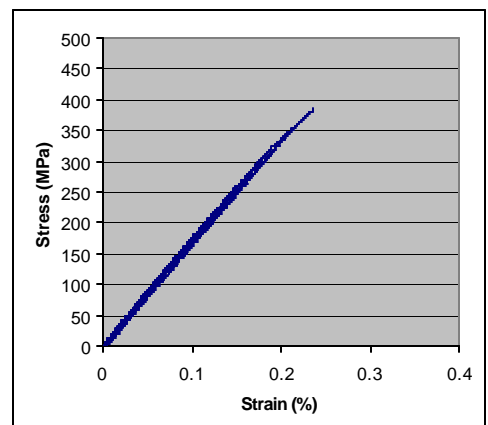
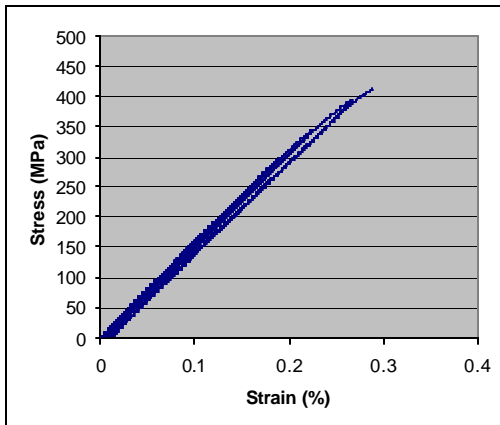


**Figure 72.** Hysteresis curve of CMCs with slurry-derived scheelite fiber coatings (1038°C condition).

## SECTION 5 - CONCLUSIONS

Unidirectional composites were fabricated using uncoated and scheelite coated Nextel 610 fibers. The composite matrix was applied through an initial pressure casting step utilizing an alumina slurry followed by repeated infiltrations and drying/firing of a solution based alumina or CeraBlak precursor or polysiloxane as a silica precursor. Because of difficulty experienced in achieving scheelite coatings and matrix precursors (other than CeraBlak<sup>TM</sup>) that would not degrade the fiber strength upon exposure to temperatures greater than 1000°C, the ultimate processing temperature for the composites was kept at or below 1000°C. Even with this relatively low (for CMCs) processing temperature, some composites were fabricated with residual porosity levels as low as 10 percent using a CeraBlak<sup>TM</sup> precursor. Such a CMC density was considered sufficient to test the functionality of scheelite fiber coatings, versus the damage tolerant fracture behavior that can be experienced in porous matrix CMCs.

The resulting analysis of the stress-strain behavior and fracture surfaces of these “dense” CMCs reveal that the scheelite coatings do contribute to fiber-matrix interfacial debonding and non-linear stress-strain behavior. The functionality of the scheelite coatings is backed up by hysteresis tensile loading curves revealing broader hysteresis loops than CMC containing uncoated fibers and by the abundant debonding and fiber pullout observed in fracture surfaces. The best tensile strengths observed for CMCs containing scheelite coatings were obtained with slurry-derived coatings and were in the 450 MPa range ( $V_f \sim 30\%$ ). Additional work will be required to demonstrate a scheelite coating that does not significantly damage the strength of the fibers before dense CMCs can be fabricated with fully realized strength properties up to the anticipated use temperatures for such a composite of 1100°C to 1200°C. It is suspected that the cause of the strength degradation is related to contamination, most frequently phosphorous, within the precursor, but this needs to be examined further. Slurry based coatings were only examined later in the program, but they seem to offer improved fiber strength retention. Custom precipitated scheelite slurries (rather than using commercial scheelite powders) that could be repeatedly washed to eliminate unwanted impurities would be a recommended approach to attempting to improve the strength retention of coated fibers. Once scheelite coatings are developed that exhibit better fiber strength retention, then higher composite processing temperatures could be used to achieve a denser scheelite coating and a denser matrix.

Promising tensile properties were obtained for a “dense” composite system (8% residual porosity in the CMC) that did not contain any fiber coatings, which was an unexpected outcome of this project. Unidirectional composites ( $V_f \sim 40\%$ ) of Nextel 610 in duplex matrix of alumina plus CeraBlak<sup>TM</sup> exhibited strengths of over 600 MPa, along with some degree of non-linearity in the stress-strain curves. Although once normalized to the  $V_f$ , the strengths are similar to what was observed for CMCs with slurry-derived coatings, they are nonetheless impressive for a coatingless CMC system. Mechanical properties of specimens at temperatures exceeded to 1000°C processing temperature used here are required to verify the potential for CeraBlak<sup>TM</sup> as a matrix candidate for CMC.



## ATTACHMENT 1 – REFERENCES

1. K.L. Luthra, "Oxidation-Resistant Fiber Coatings for Non-oxide Ceramic Composites," *J. Am. Ceram. Soc.*, **80**[12] 3253-57 (1997).
2. P.E.D Morgan and D.B. Marshall, "Ceramic Composites Having a Weak Bond Material Selected from Monazites and Xenotimes," United States Patent No. 5,514,474, May 7, 1996.
3. R.W. Goettler, S. Sambasivan and V. Dravid, "Isotropic Complex Oxides as Fiber Coatings for Oxide-Oxide CFCC," *Ceram. Eng. Sci.*, **18**[3], p 279 (1997).
4. R.S. Hay, "Sol-Gel Coating of Fiber Tows," *Ceram. Eng. Sci. Proc.*, 12[7-8] 1064-1074 (1991).
5. E.E. Boakye, R.S. Hay, M.D. Petry, "Continuous Coating of Oxide Fiber Tows Using Liquid Precursors: Monazite Coatings on Nextel 720 <sup>TM</sup>," *J. Am. Ceram. Soc.*, **82**[9] 2321-31 (1999).
6. R.W. Goettler, "Mechanical Properties of Monazite Containing Oxide-Oxide CFCC," presented at the 21<sup>st</sup> Annual Cocoa Beach Conference and Exposition on Composites, Advanced Ceramics, Materials and Structures, American Ceramic Society, paper no. C-0061-97F, Cocoa Beach, FL, January 12-16, 1997.
7. E.E. Boakye, R.S. Hay, P. Mogilevsky and L.M. Douglas, "Monazite Coatings on Fibers: II, Coating without Strength Degradation," *J. Am. Ceram. Soc.*, 84[12] 2793-2801 (2001).
8. H. Schneider, K. Okada, J. Pask, "Mullite and Mullite Ceramics," John Wiley and Sons, New York, NY, pp 105-140 (1994).
9. J.C. Hulig and G.L. Messing, "Hybrid Gels for Homoepitactic Nucleation of Mullite," *J. Am. Ceram. Soc.*, **72**[9] 1725-1729 (1989).
10. E. Tkalcec, R. Nass, J. Schmauch, H. Schmidt, S. Kurjica, A. Bezjak and H. Ivankovic, "Crystallization Kinetics of Mullite from Single-Phase Gel Determined by Isothermal Differential Scanning Calorimetry," *J. Non-Crystalline Solids*, **223**, 57-72 (1998).
11. I. Jaymes, A. Douy and D. Massiot, "Synthesis of a Mullite Precursors from Aluminum Nitrate and Tetraethoxysilane via Aqueous Homogeneous Precipitation: An <sup>27</sup>Al and <sup>29</sup>Si Liquid- and Solid-State NMR Spectroscopic Study," *J. Am. Ceram. Soc.*, **78**[10] 2648-2654 (1995).